Supplementary Information (SI) for Journal of Materials Chemistry B.

Emissive Triphenylamine Functionalised 1,8-Naphthalimide and Naphthalene Diimide Fluorophores: Aggregation, Computation and Biological Studies

Laura Ramírez Lázaro,‡[a,b] L. Constance Sigurvinsson,‡[a,c] Niamh Curtin,[d] Joanna Ho,[a] Ena T. Luis,[a] Deirdre A. McAdams,[a] Tómas A. Gudmundsson,[a,c] Chris S. Hawes,[e] Denis Jacquemin,[f,g] Donal F. O'Shea,[c,d] Eoin Scanlan,[a,b] Adam F. Henwood,[a,b] and Thorfinnur Gunnlaugsson*[a,b,c]*

[a] School of Chemistry and Trinity Biomedical Sciences Institute (TBSI), Trinity College, Dublin, The University of Dublin, Dublin 2, Ireland

[b] Synthesis and Solid-State Pharmaceutical Centre (SSPC), School of Chemistry, Trinity College Dublin

[c] AMBER (Advanced Materials and Bioengineering Research) Centre, Trinity College Dublin, The University of Dublin, Dublin 2, Dublin, Ireland

[d] Department of Chemistry, Royal College of Surgeons in Ireland (RCSI), 123 St. Stephen's Green, Dublin, Dublin 2, Ireland

[e] School of Chemical and Physical Sciences, Keele University, Keele, ST5 5BG, United Kingdom

[f] Nantes Université, CNRS, CEISAM – UMR 6230, 44000 Nantes, France

[g] Institut Universitaire de France (IUF), 75005 Paris, France

Email: gunnlaut@tcd.ie

SUPPORTING INFORMATION

Table of Contents:

Synthesis and Structural Characterisation

General Synthetic Information

All solvents and chemicals were purchased from commercial sources and used without further purification. Where appropriate, reactions were performed using standard Schlenk techniques under an inert (N_2) atmosphere with reagent grade solvents. Water was purified using a Millipore Milli-Q water purification system. Analytical thin layer chromatography (TLC) was performed using silica plates with aluminium backings (250 mm with indicator F-254). Compounds were visualized under UV light (254 and 365 nm). Centrifugation was performed using a Hettich Zentrifugen Universal 320 (4000 rpm). Flash column chromatography was performed using a Teledyne Isco CombiFlash Rf 200 automated purification system. NMR spectra were recorded on a Bruker Spectrospin DPX-400 spectrometer (400 and 101 MHz for ^{1}H and ^{13}C NMR, respectively) or a Bruker AV-600 spectrometer running (600 MHz and 151 MHz for ^{1}H and ^{13}C NMR, respectively) and were carried out at 293 K. Chemical shifts are reported in ppm using deuterated chloroform ($CDCl_3$) and deuterated DMSO (DMSO-d_6) as the solvents of record and are referenced against the residual solvent peaks. The following abbreviations have been used for multiplicity assignments: “s” for singlet, “d” for doublet, “t” for triplet, and “m” for multiplet. Mass spectrometry was carried out using HPLC grade solvents, using a Bruker micrOTOF-Q III spectrometer interfaced to a Dionex UltiMate 3000 LC. Negative and positive modes were used as required. Masses were recorded over the range 100-2000 *m/z*. Infrared Spectra were recorded with a PerkinElmer Spectrum One FTIR spectrometer fitted with a Universal ATR Sampling Accessory and measured over the range 4000-550 cm^{-1}. Melting points were determined using an Electrothermal IA9000 digital melting point apparatus with 1 °C/min increments.

Compound 5

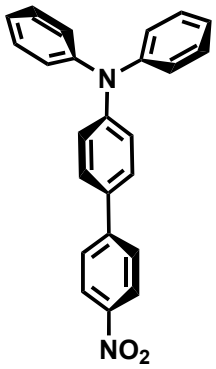

Synthesis of this compound was by a previously reported method.[1] 1-Bromo-4-nitrobenzene (349 mg, 1.73 mmol, 1.0 eq.), 4-(diphenylamino)phenylboronic acid (500 mg, 1.73 mmol, 1.0 eq.) and Na_2CO_3 (366 mg, 3.46 mmol, 2.0 eq.) were added to a 100 mL round bottom flask. Toluene (25 mL) and deionized water (5 mL) were added to the flask. The reaction mixture was degassed through 3 cycles of vacuum and backfilling with argon using a Schlenk line. $Pd(PPh_3)_4$ (40 mg, 0.034 mmol, 0.020 eq.) was added to the flask upon which the mixture turned yellow. The reaction was heated at 78 °C for 18 h. The solvent was removed under reduced pressure. The crude product was purified using column chromatography (silica, 0-60% DCM/Hexane). The product was obtained as a red crystalline solid (509 mg, 1.39 mmol). **Yield:** 80%. **Mp**: 159-160 °C. **Literature value**: 158-160 °C.[1] **^{1}H NMR (400 MHz, DMSO-d_6) δ_H (ppm):** 8.27 (d, J = 8.9 Hz, 2H, H_1), 7.92 (d, J = 8.9 Hz, 2H, H_2), 7.73 (d, J = 8.7 Hz, 2H, H_3), 7.40-7.31 (m, 4H, H_6), 7.15-7.08 (m, 6H, $H_{4,5}$), 7.03 (d, J = 8.7 Hz, 2H, H_7). **^{13}C {^{1}H} NMR (101 MHz, DMSO-d_6) δ_C (ppm):** 148.3, 146.6, 146.1, 146.0, 130.7, 129.8, 128.3, 126.9, 124.9, 124.2, 124.0, 122.0. **APCI-HRMS (*m/z*) calculated for** $C_{24}H_{18}N_2O_2$ 366.1368, found $[M+H]^+$ 367.1440. **ν_{max} (ATR) cm^{-1}:** 1708, 1670, 1587 (Ar C=C stretch), 1511 (N-O stretch), 1485 (Ar C=C stretch), 1339 (C-N stretch), 1275 (C-N stretch) cm^{-1}.

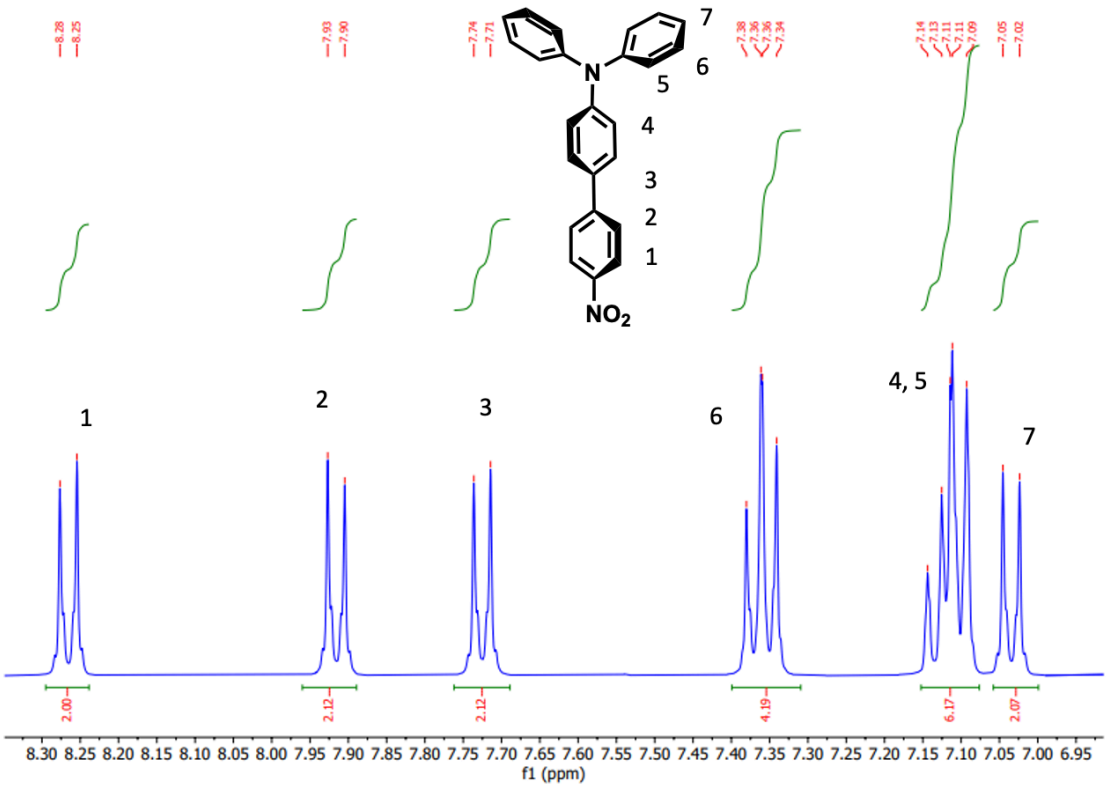

Figure **S1**. ^{1}H NMR spectrum of the aromatic region of **5** in DMSO-d_6.

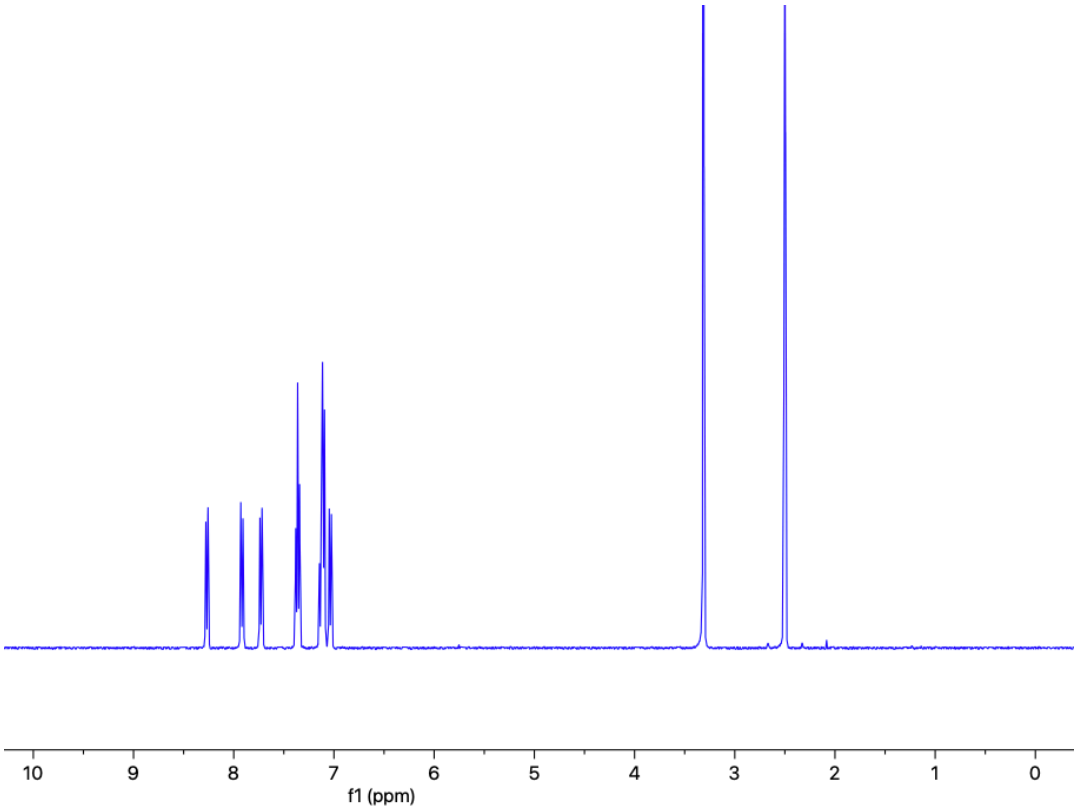

Figure **S2**. ^{1}H NMR spectrum of **5** in DMSO-d_6.

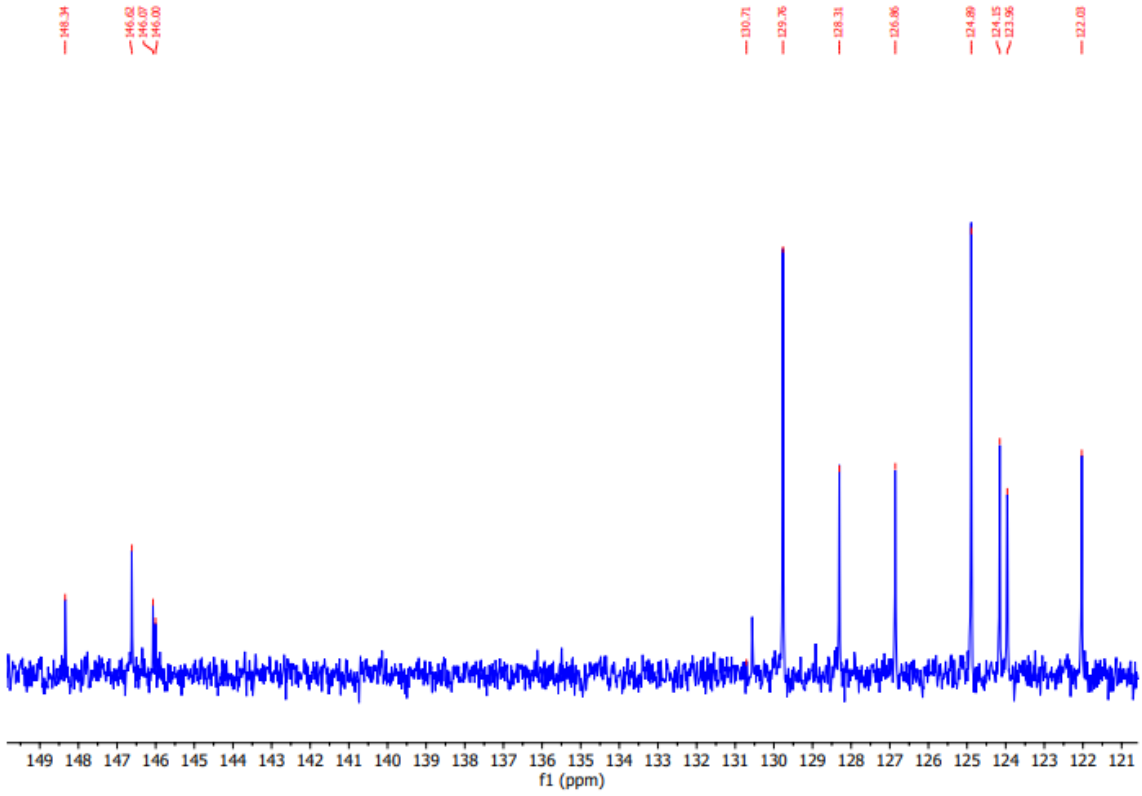

Figure **S3**. ^{13}C NMR spectrum of **5** in DMSO-d_6.

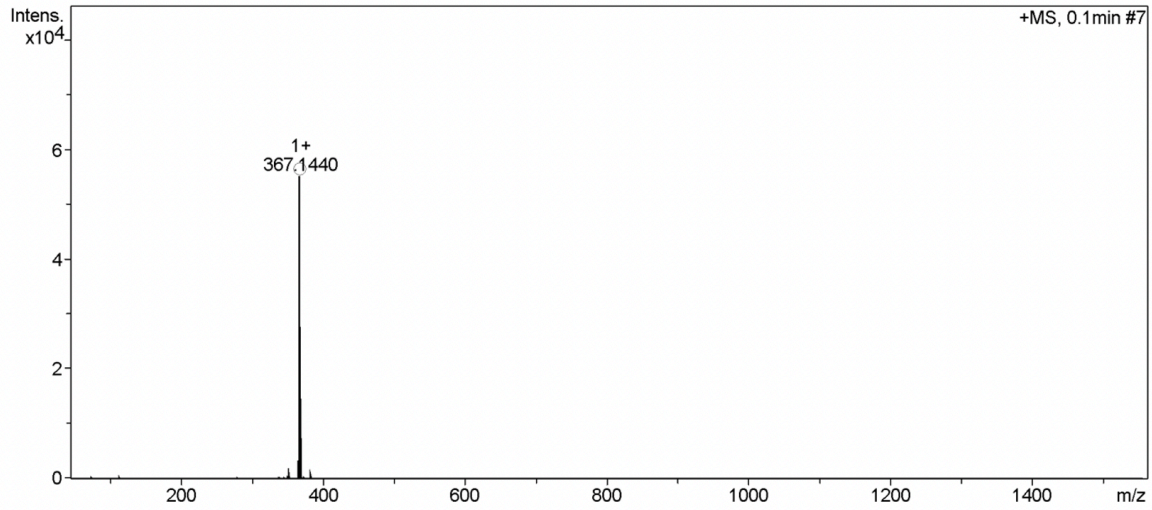

Figure **S4**. APCI-HRMS (*m/z*) of **5**.

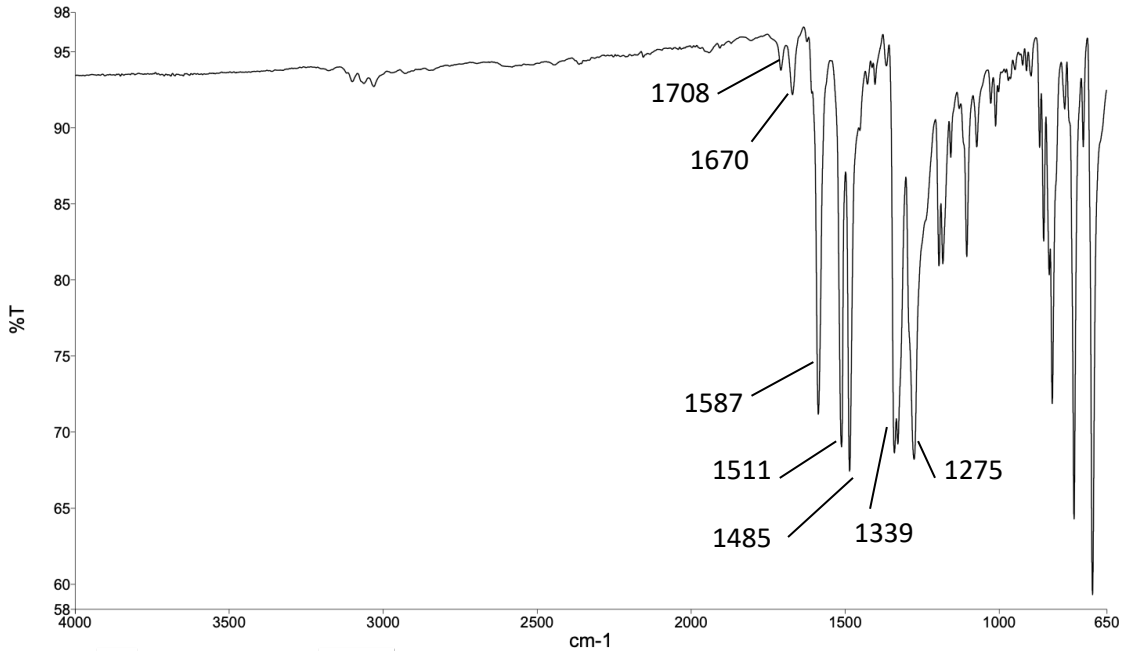

Figure **S5:** FTIR of compound **5**.

Compound 6

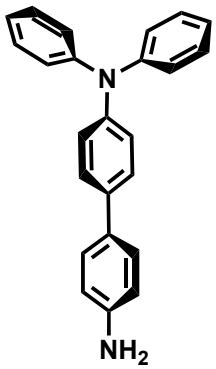

Compound **6** has been previously reported but was synthesised by a method different to that outlined here.[2] Compound **5** (600 mg, 1.64 mmol, 1.0 eq.) was added to a round bottom flask. MeOH (200 mL) was added to the flask, followed by Pd/C (60 mg, 10%wt), and then the reaction vessel was placed under a flow of H_2 at 3 atm in a Parr shaker and left to react for 3 h. The resultant colourless reaction mixture was then filtered through Celite® and washed with MeOH, before the solvent was removed under reduced pressure, to give a brown crystalline solid (541 mg, 1.61 mmol). **Yield:** 98%. **Mp**: 172-173 °C. **Literature value:** to the best of our knowledge, this value has not been previously reported. **^{1}H NMR (400 MHz, DMSO-d_6) δ_H (ppm):** 7.47 (d, J = 8.6 Hz, 2H, H_3), 7.36-7.25 (m, 6H, $H_{2,6}$), 7.06-6.96 (m, 8H, $H_{4,5,7}$), 6.62 (d, J = 8.5 Hz, 2H, H_1), 5.17 (s, 2H, NH_2). **^{13}C {^{1}H} NMR (101 MHz, DMSO) δ_C (ppm):** 148.1, 147.3, 145.1, 135.6, 129.5, 126.9, 126.8, 126.3, 124.4, 123.5, 122.7, 114.3. **ESI-HRMS calculated for** $C_{24}H_{20}N_2$ 336.1626, found $[M+H]^+$ 337.1697. **ν_{max} (ATR) cm^{-1}:** 3466 (N-H stretch), 3376 (N-H stretch), 3028 (Ar C-H stretch), 1622, 1584 (Ar C=C stretch), 1486 (Ar C=C stretch), 1323 (C-N stretch), 1274 (C-N stretch) cm^{-1}.

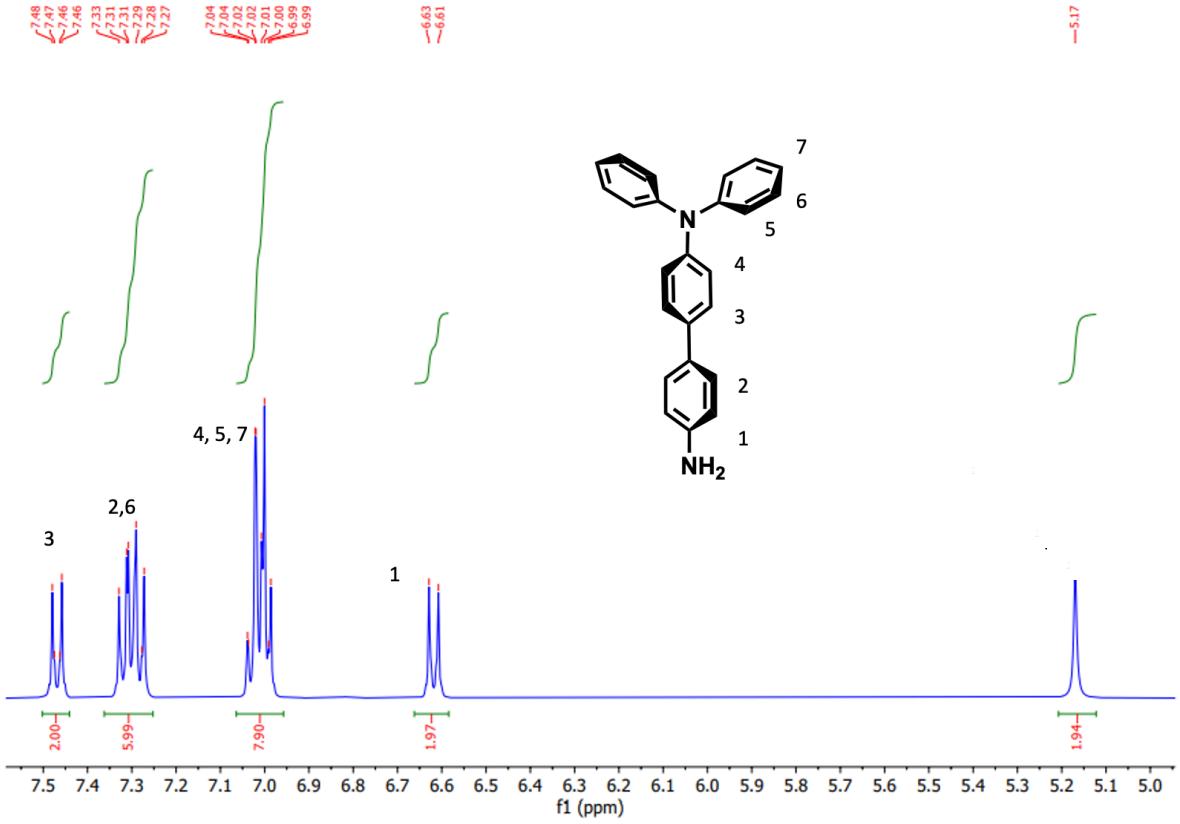

Figure **S6**. ^{1}H NMR spectrum of **6** between 7.5 and 5.0 ppm in DMSO-d_6.

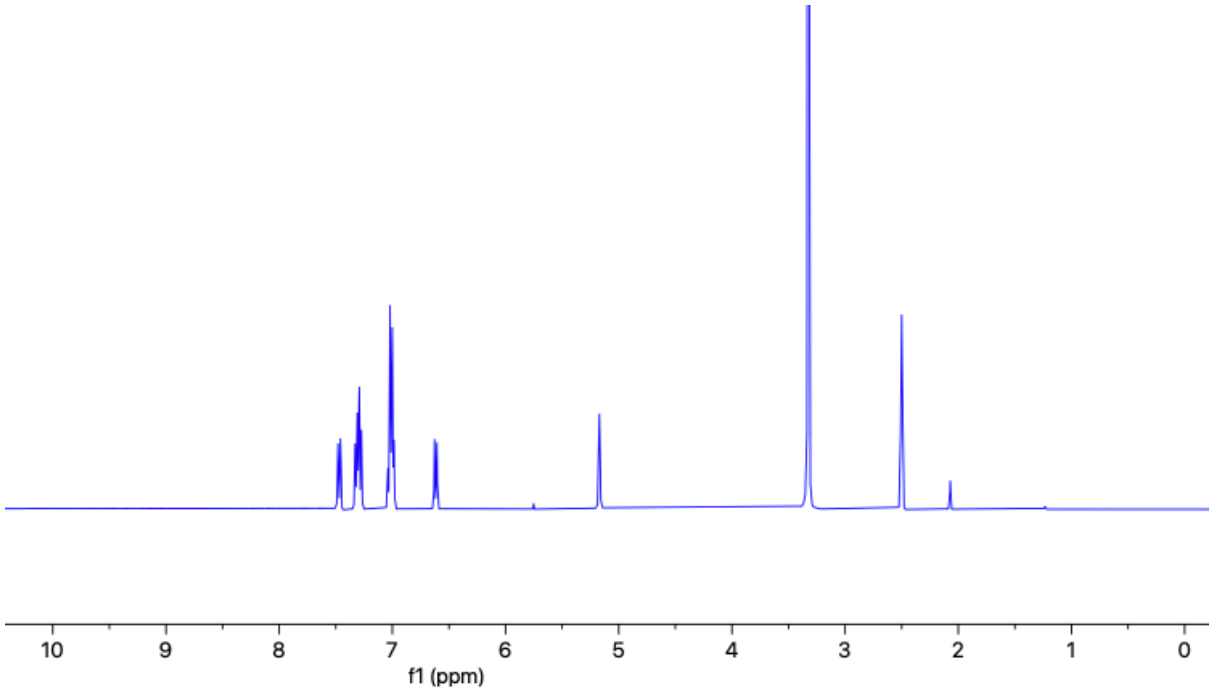

Figure **S7**. ^{1}H NMR spectrum of **6** in DMSO-d_6.

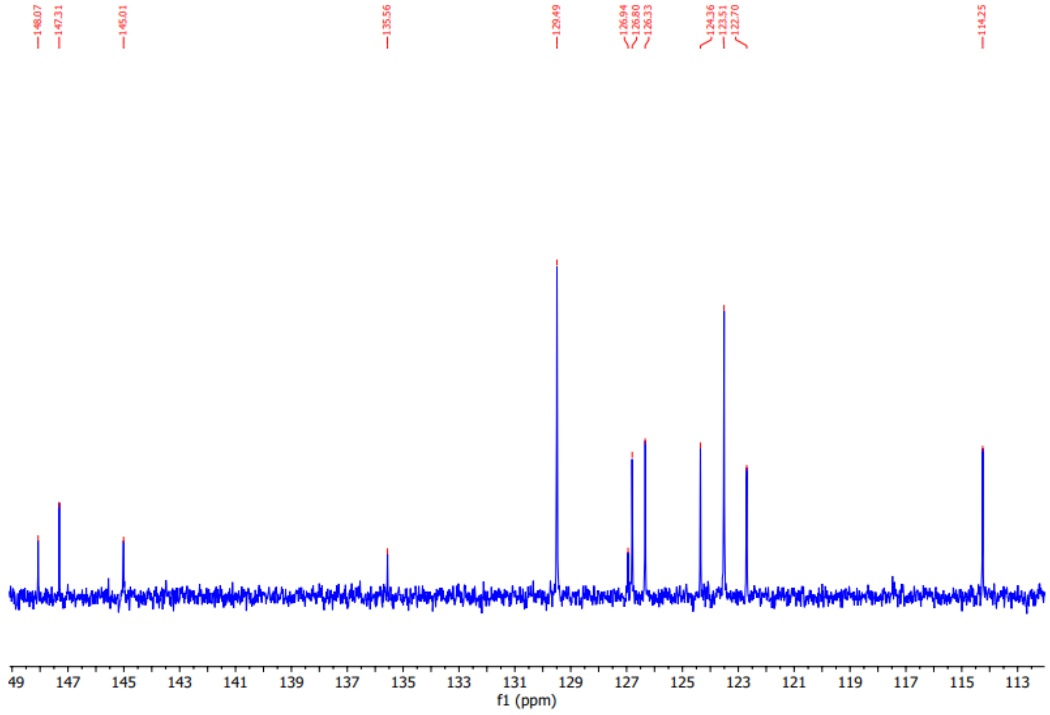

Figure **S8**. ^{13}C NMR spectrum of **6** in DMSO-d_6.

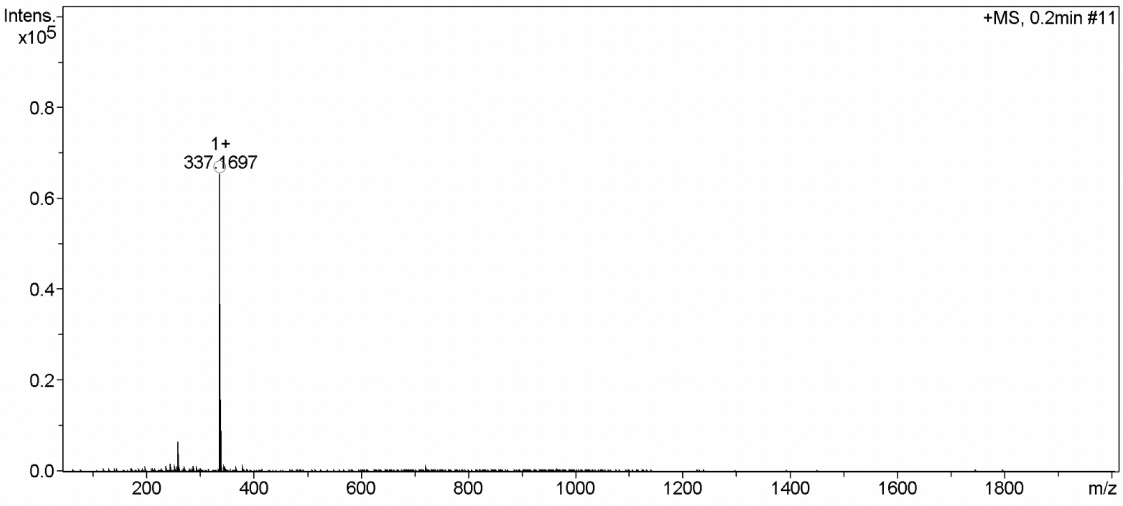

Figure **S9**. ESI-HRMS of **6**.

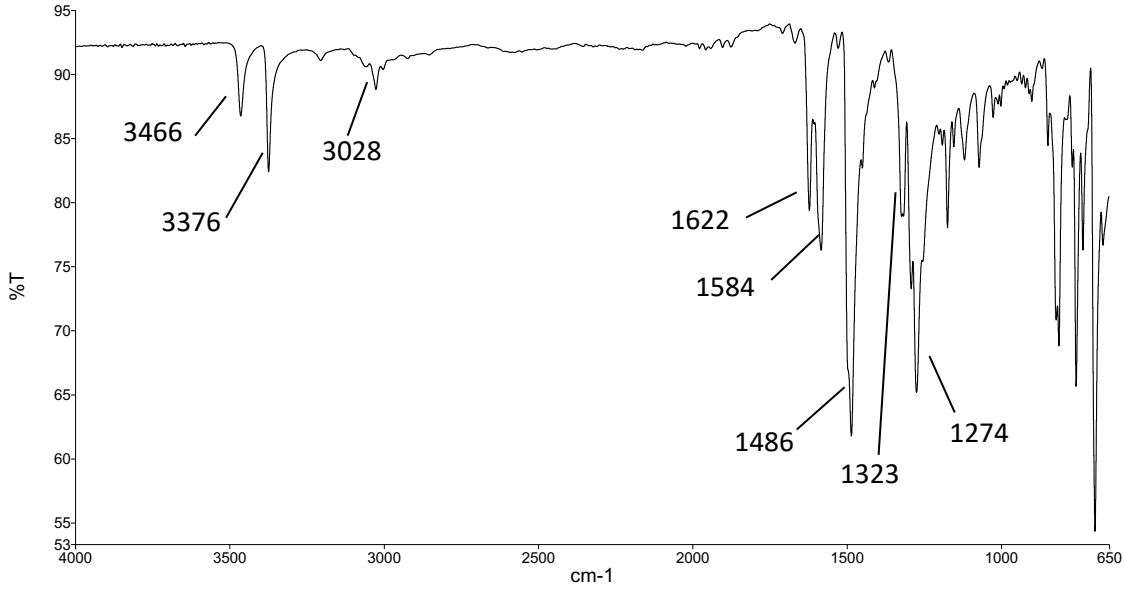

Figure **S10.** FTIR of **6**.

Compound 1

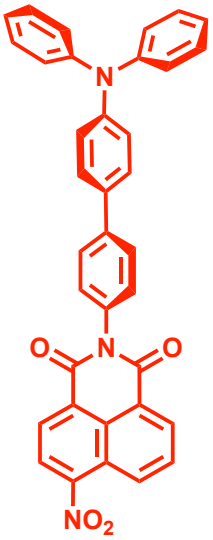

4-Nitro-1,8-naphthalic anhydride (256 mg, 1.06 mmol, 1.0 eq.) and compound **6** (355 mg, 1.06 mmol, 1.0 eq.) were added to a microwave vial along with a magnetic stirrer bar, and then EtOH (15 mL) was added. The reaction mixture reacted for 3 h at 110 ºC. The mixture was left to cool to room temperature and then cooled to 0 °C in an ice bath to encourage precipitation of the product. The precipitate was then filtered and washed with cold EtOH. The product was dried and a pink solid was obtained (435 mg, 0.776 mmol). **Yield:** 74%. **Mp:** 273-275 ºC. **^{1}H NMR (400 MHz, DMSO-*d*$_6$) δ_H (ppm):** 8.78 (d, *J* = 9.0 Hz, 1H, H_3), 8.63 (m, 3H, $H_{1,2,5}$), 8.15 (t, *J* = *8.52,* 1H, H_4), 7.79 (d, *J* = 8.4 Hz, 2H, H_6), 7.69 (d, *J* = 8.6 Hz, 2H, H_8), 7.47 (d, *J* = 8.4 Hz, 2H, H_7), 7.35 (t, *J* = 7.8 Hz, 4H, H_{11}), 7.09 (m, 8H, $H_{9,10,12}$). **^{13}C {^{1}H} NMR (151 MHz, DMSO-*d*$_6$) δ_C (ppm):** 207.0, 163.8, 163.0, 149.8, 147.5, 147.4, 140.2, 134.9, 133.7, 132.2, 130.6, 130.1, 129.9, 129.4, 129.3, 128.3, 127.8, 127.1, 124.8, 124.7, 123.9, 123.8, 123.6, 123.4. **APCI-HRMS calculated for** $C_{36}H_{23}N_3O_4$ 561.1689, found $[M+H]^+$ 562.1759. **ν_{max} (ATR) cm^{-1}:** 3036 (Ar C-H stretch), 1720, 1669, 1588 (Ar C=C stretch), 1524 (N-O stretch), 1488 (Ar C=C stretch) cm^{-1}.

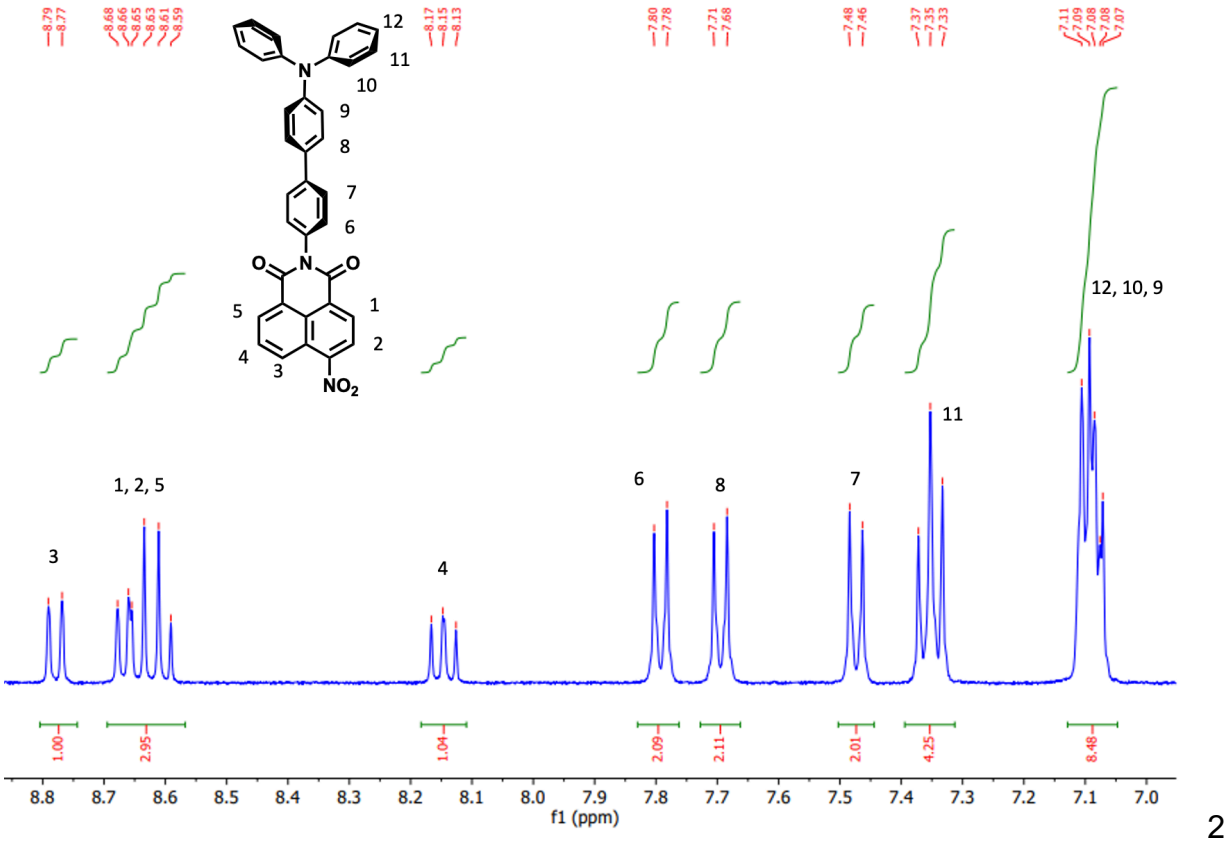

2

Figure **S11**. ^{1}H NMR spectrum of **1** between 8.8 and 7.0 ppm in DMSO-d_6.

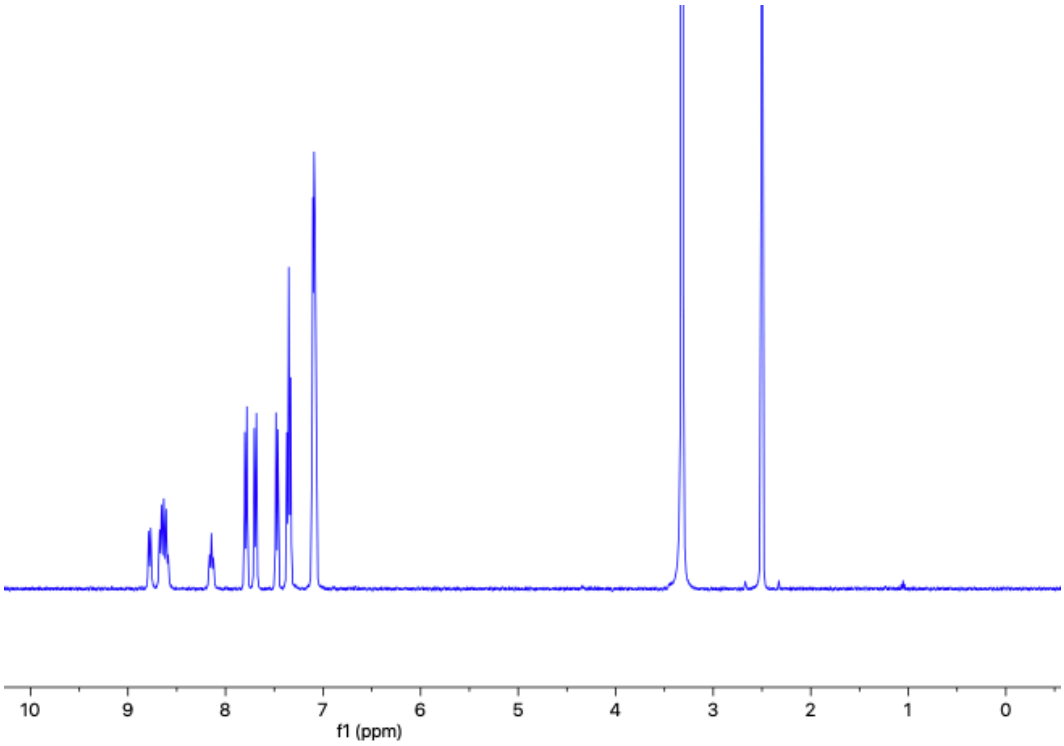

Figure **S12**. ^{1}H NMR spectrum of **1** in DMSO-d_6.

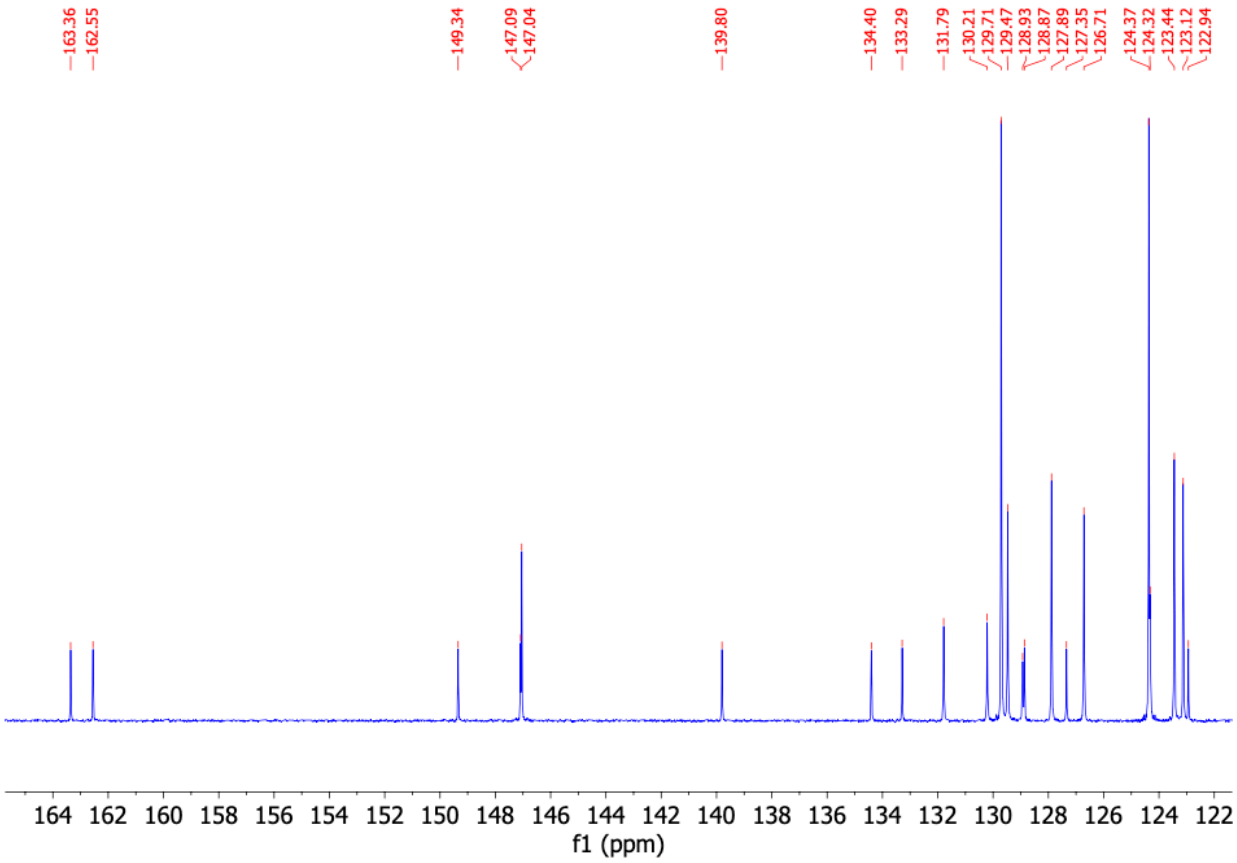

Figure **S13**. ^{13}C NMR spectrum of **1** in DMSO-d_6.

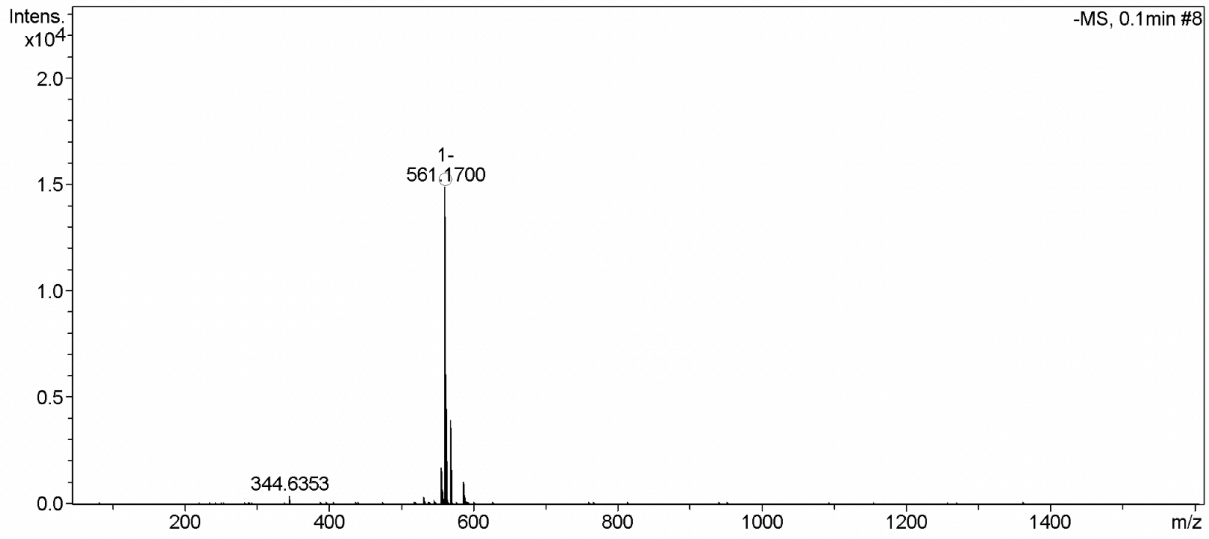

Figure **S14**. APCI-HRMS of **1.**

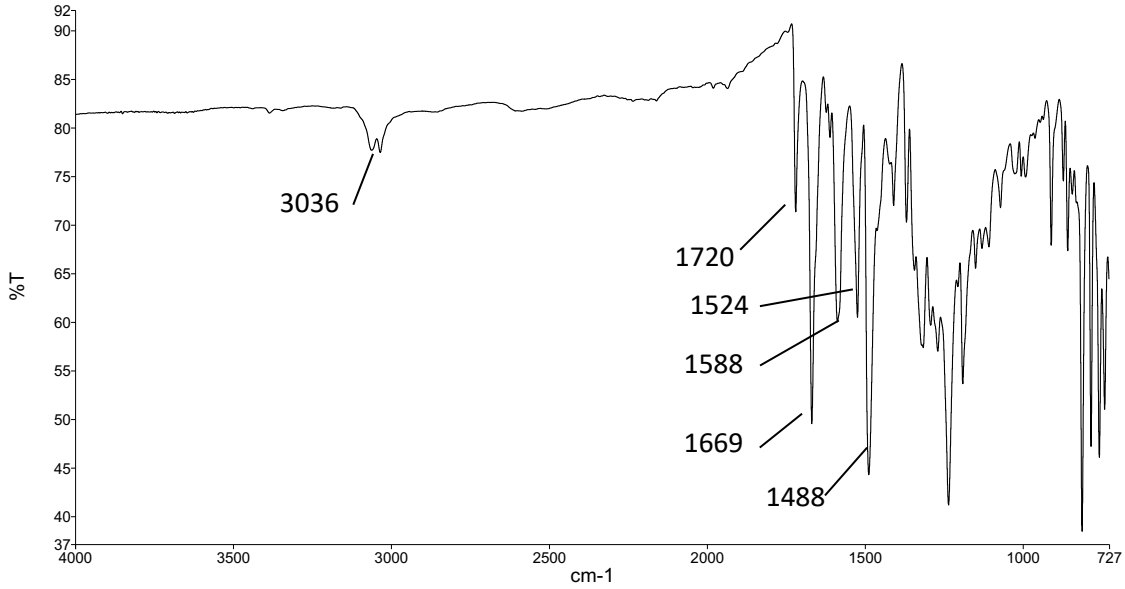

Figure **S15:** FTIR spectrum of **1.**

Compound 2

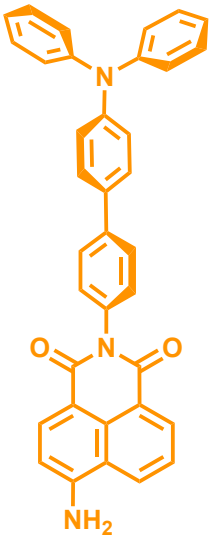

Compound **1** (256 mg, 0.455 mmol, 1.0 eq.) in 100 mL of a solvent mixture of EtOH:MeOH (1:1) was added to a reaction flask. Pd/C (21 mg, 10%wt) was added to the flask and the reaction mixture was placed under a flow of H_2 at 3 atm in a Parr shaker apparatus and left for 9 h. The solvent was then evaporated and Celite was added, before redissolving the reaction mixture in DCM and filtering. The solvent was removed under reduced pressure to give an orange solid was obtained (223 mg, 0.419 mmol). **Yield:** 92%. **Mp**: 215 ºC (degraded). **^{1}H NMR (600 MHz, DMSO-d_6) δ_H (ppm):** 8.67 (dd, *J* = 8.5, 0.9 Hz, 1H, H-3), 8.47-8.43 (m, 1H, H_1), 8.21 (d, *J* = 8.3 Hz, 1H, H_5), 7.76-7.72 (m, 2H, H_6), 7.71-7.65 (m, 3H, H_4, H_7), 7.50 (s, 2H, NH_2), 7.38-7.32 (m, 6H, $H_{11,12}$), 7.12-7.05 (m, 8H, $H_{8,9,10}$), 6.88 (d, *J* = 8.3 Hz, 1H, H_2). **^{13}C {^{1}H} NMR (151 MHz, DMSO-d_6) δ_C (ppm):** 164.1, 163.3, 152.9, 147.1, 147.0, 139.2, 135.5, 134.0, 133.5, 131.2, 130.3, 129.7, 129.7, 129.6, 127.8, 126.5, 124.3, 124.1, 123.4, 123.2, 122.3, 119.6, 108.3, 107.9, 55.0. **ESI-HRMS (*m/z*) calculated for** $C_{36}H_{25}N_3O_2$ 531.1947, found $[M+Na]^+$ 554.1821. **ν_{max} (ATR) cm^{-1}:** 3476 and 3339 (N-H stretch) 3241 (Ar C-H stretch), 1650, (C=O stretch), 1669, 1576 (Ar C=C stretch), 1488 (Ar C=C stretch) 1366 (C-N stretch) cm^{-1}.

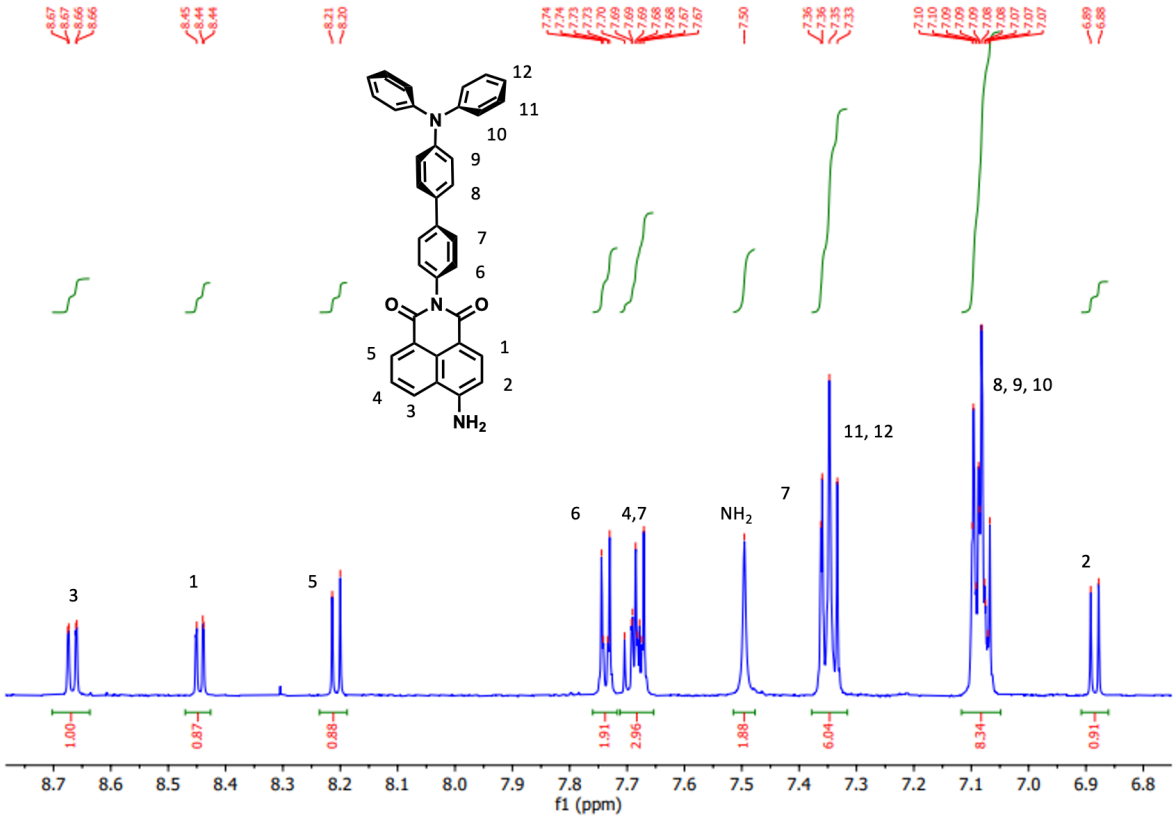

Figure **S16**. ^{1}H NMR spectrum of **2** between 8.7 and 6.8 ppm in DMSO-d_6.

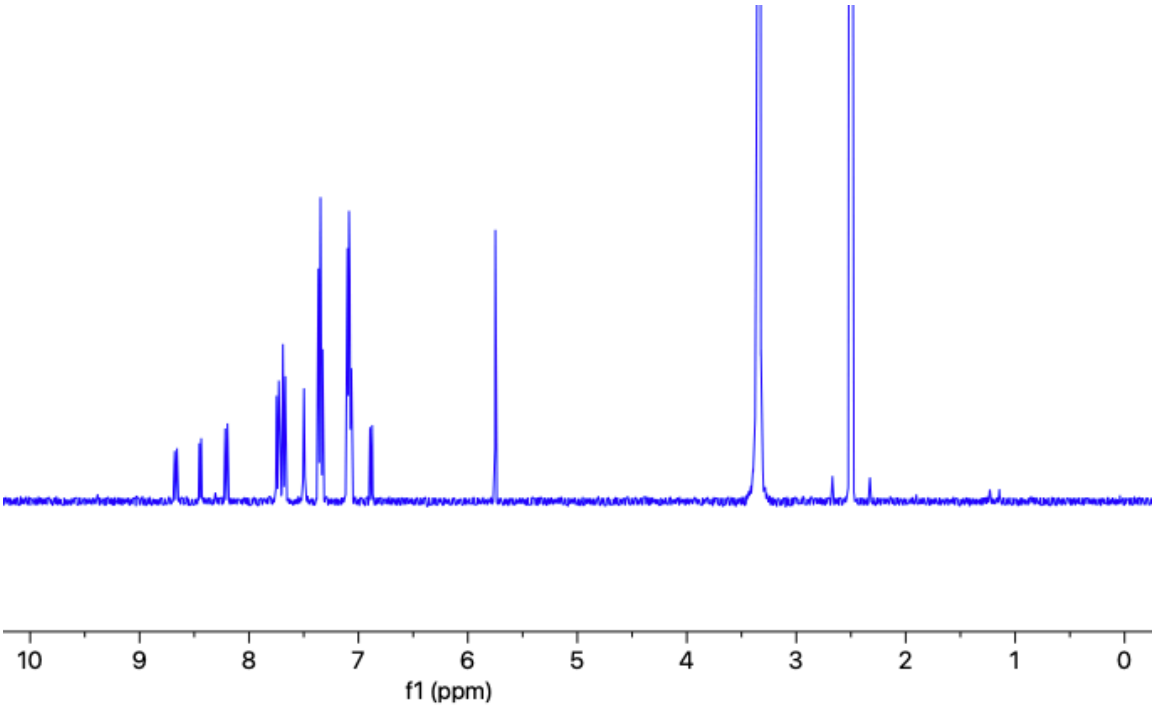

Figure **S17**. ^{1}H NMR full spectrum of **2** in DMSO-d_6.

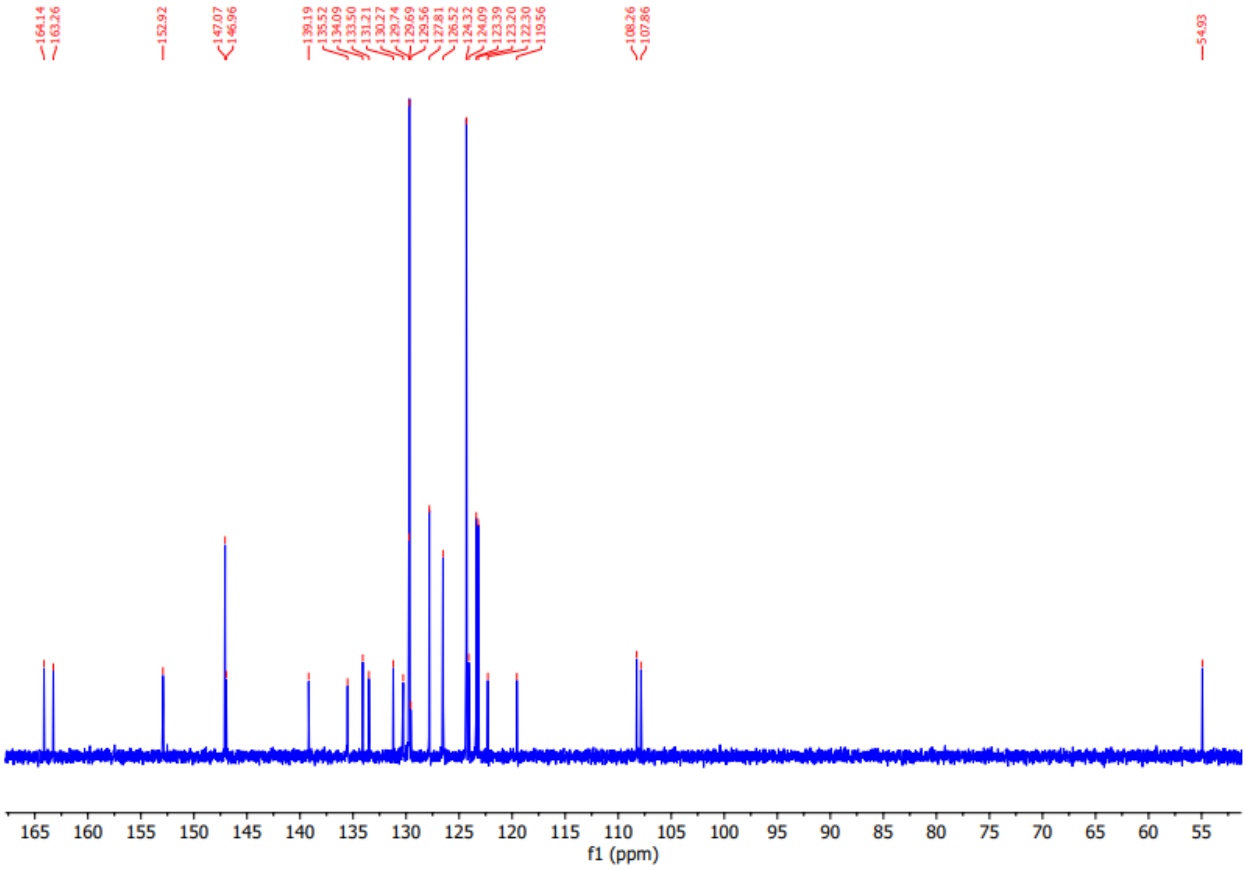

Figure **S18**. ^{13}C NMR spectrum of **2** in DMSO-d_6.

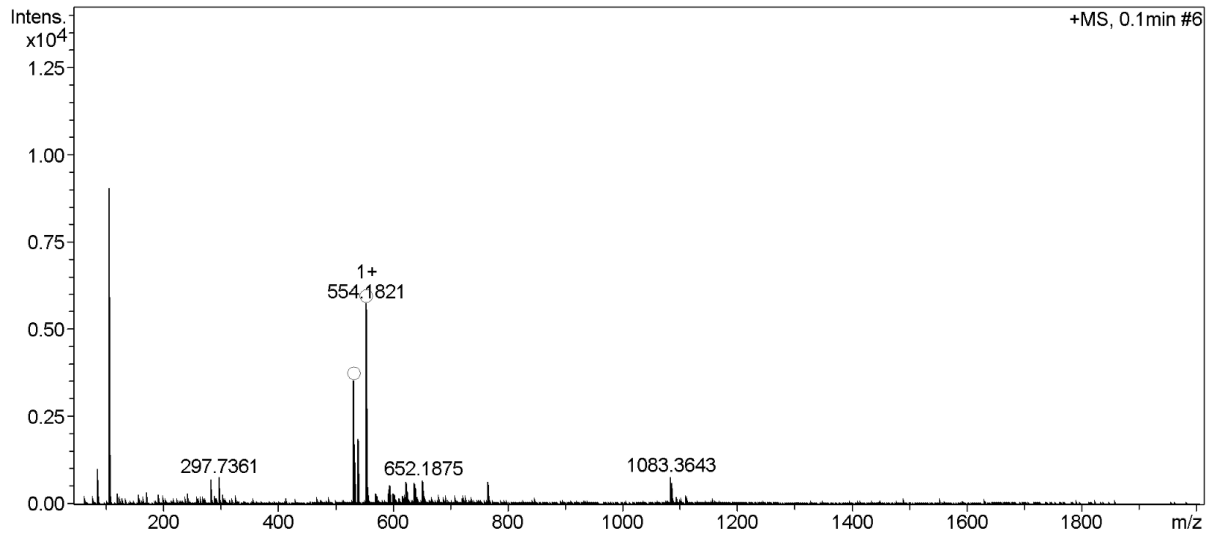

Figure **S19**. ESI-HRMS of **2**.

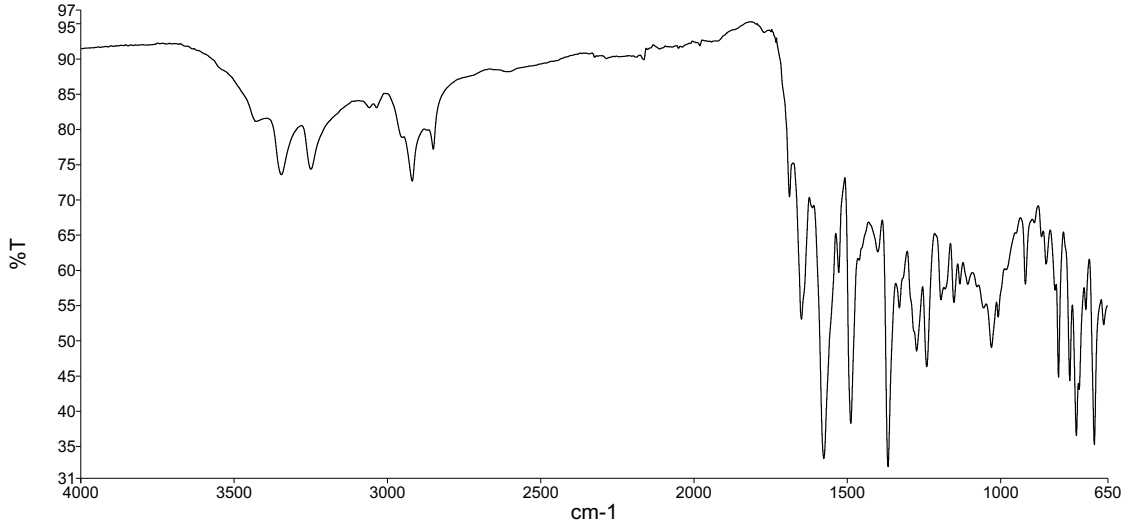

Figure **S20:** FTIR spectrum of **2**.

Compound 4

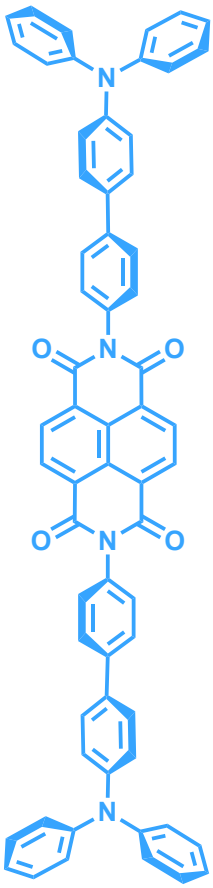

1,4,5,8-Naphthalenetetracarboxylic dianhydride (25 mg, 0.093 mmol, 1.0 eq.) was dissolved in 10 mL of DMF in a round bottom flask and compound **6** was added (125 mg, 0.372 mmol, 2.0 eq.). The reaction mixture was refluxed for 96 h. The reaction mixture was cooled to room temperature and the solid product was isolated by filtration, washed with diethyl ether, and dried under vacuum to yield a purple solid (40 mg, 0.044 mmol) **Yield:** 47%. **Mp**: 250 ºC (degraded). **^{1}H NMR (400 MHz, $CDCl_3$) δ_H (ppm):** 8.88 (s, 4H, H_1), 7.80-7.72 (m, 4H, H_3), 7.57-7.49 (m, 4H, $H_{1,2}$), 7.45-7.36 (m, 4H, H_4), 7.33-7.27 (m, 8H, H_7), 7.20-7.13 (m, 12H, $H_{5,6}$), 7.10-7.03 (m, 4H, H_8). **^{13}C {^{1}H} NMR (101 MHz, $CDCl_3$) δ_C (ppm):** 163.2, 147.8, 147.7, 141.9, 134.0, 133.2, 131.7, 129.5, 128.9, 128.2, 128.0, 127.4, 127.2, 124.8, 123.7, 123.3. **APCI-HRMS (*m/z*) calculated for** $C_{62}H_{40}N_4O_4$ 904.3050, found $[M+H]^+$ 905.3110. **ν_{max} (ATR) cm^{-1}:** 3000 (C-H stretch), 1343 (C-N stretch), 1673 (Ar C=C), 1485 (Ar C=C) cm^{-1}.

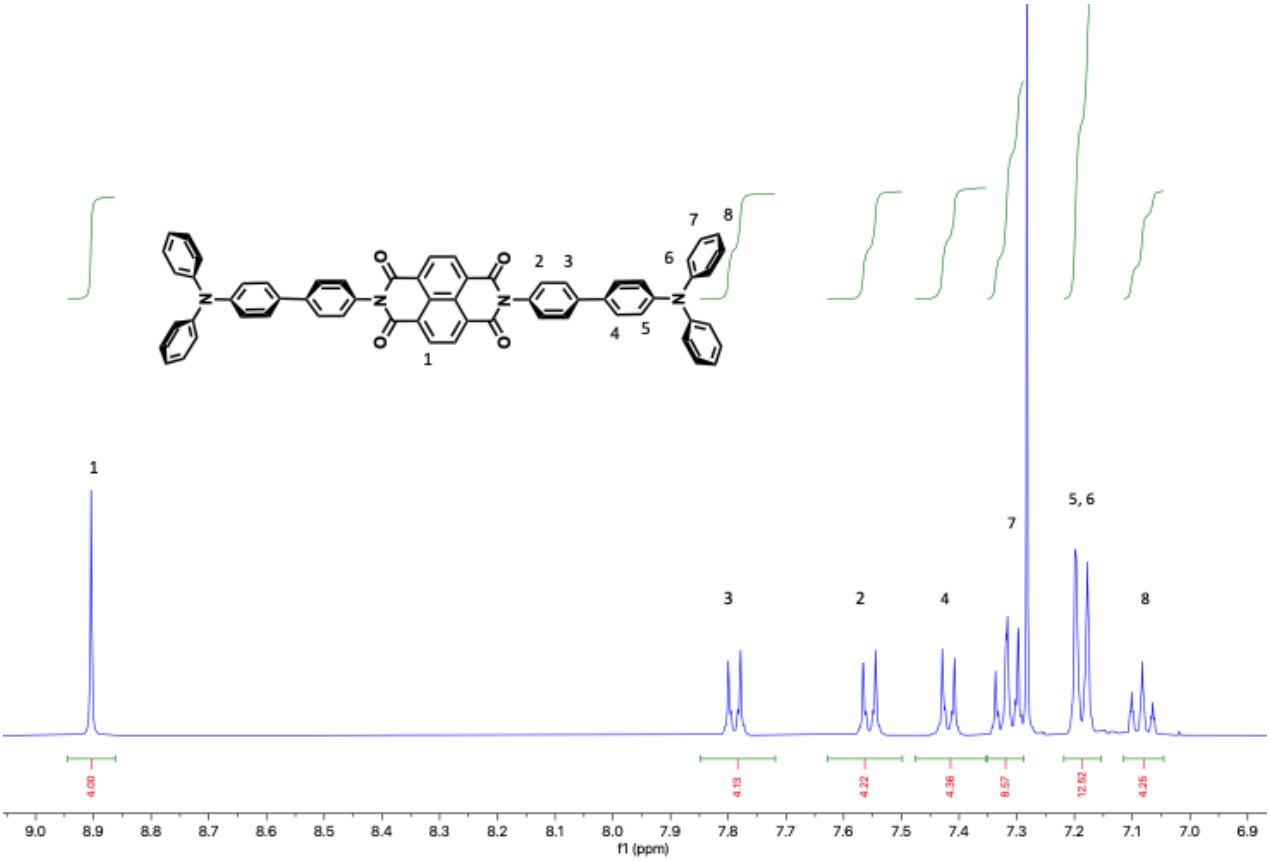

Figure **S21**. ^{1}H NMR spectrum of **4** between 9.0 and 6.9 ppm in $CDCl_3$.

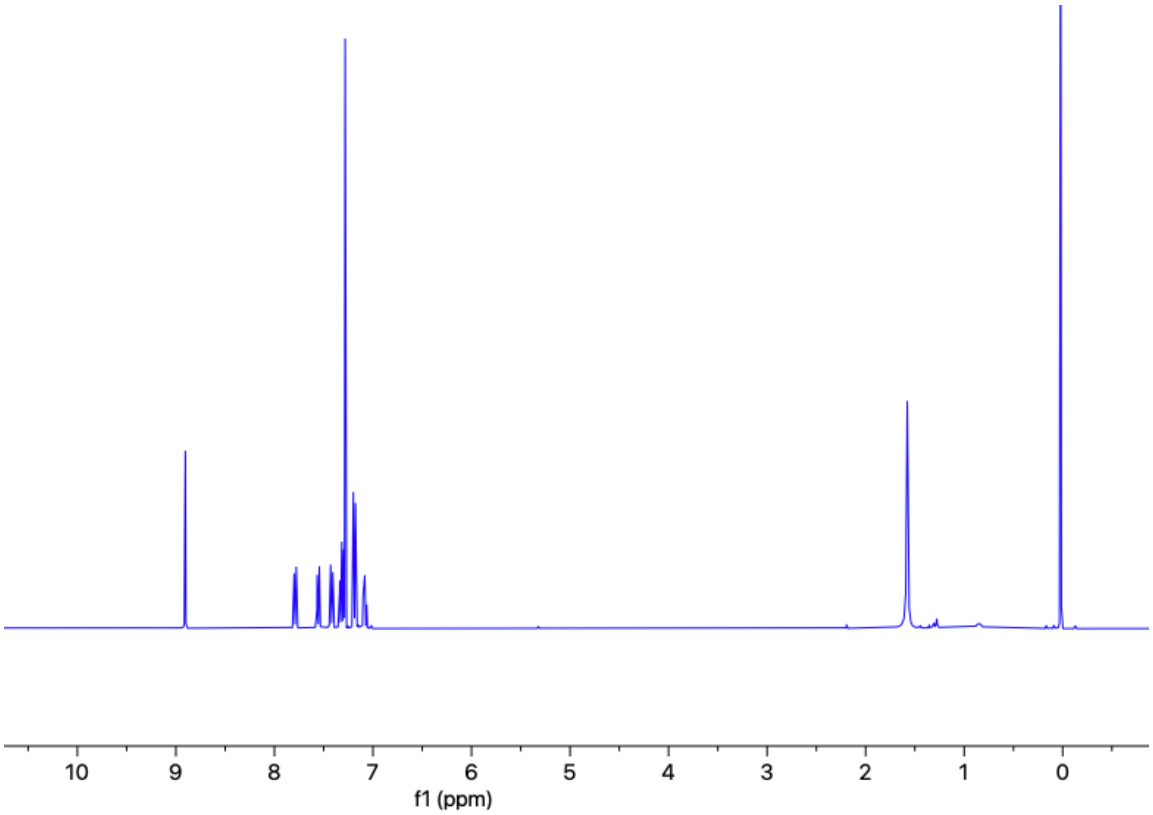

Figure **S22**. ^{1}H NMR full spectrum of **4** in $CDCl_3$.

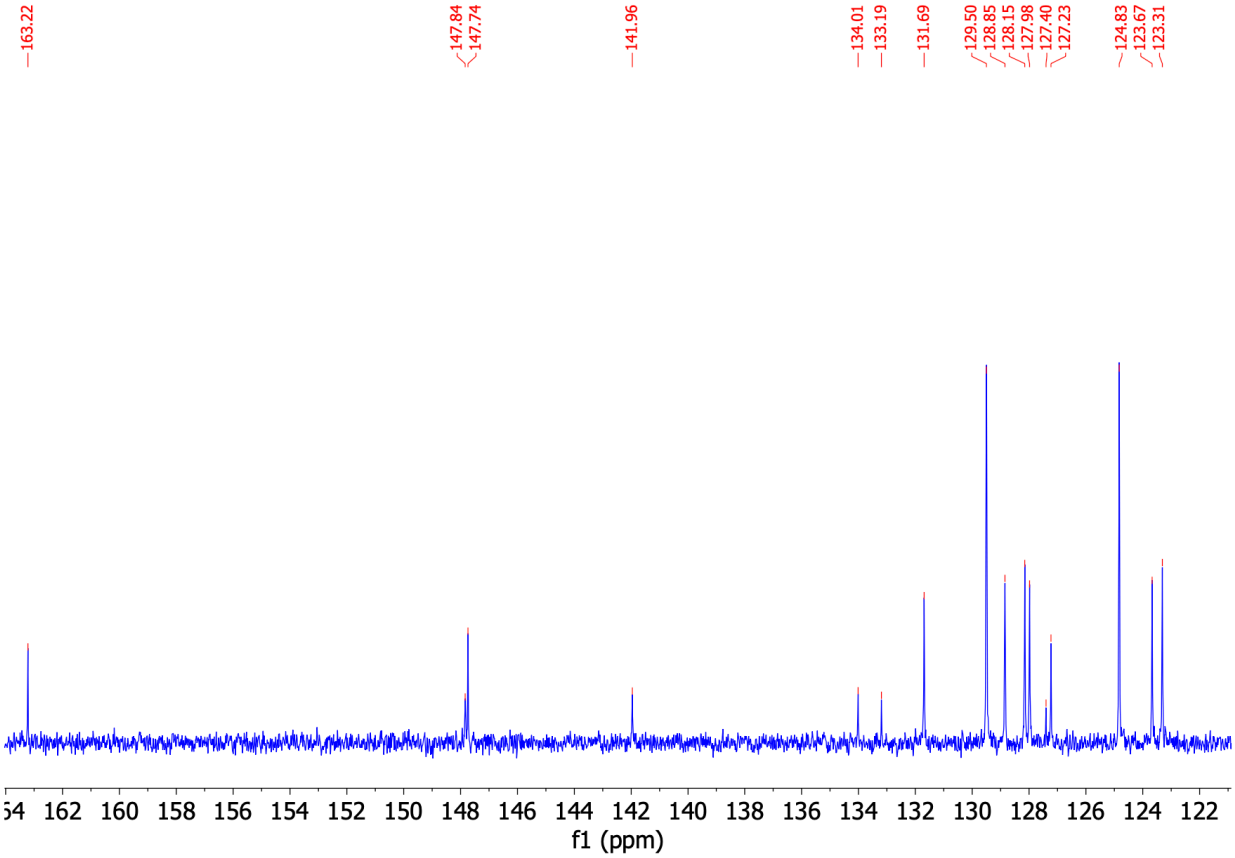

Figure **S23**. ^{13}C NMR spectrum of **4** in $CDCl_3$.

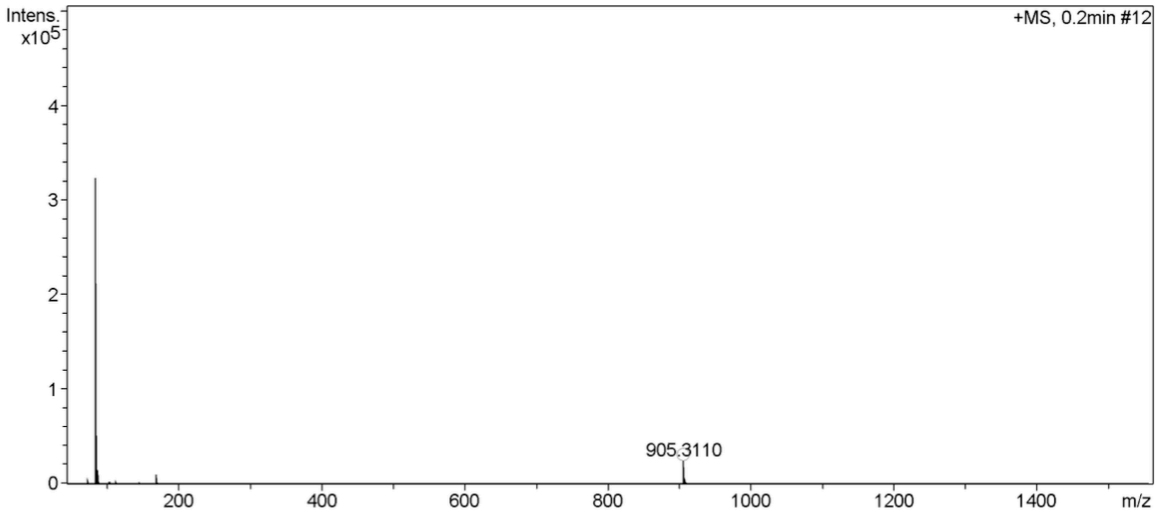

Figure **S24**. APCI-HRMS of **4**.

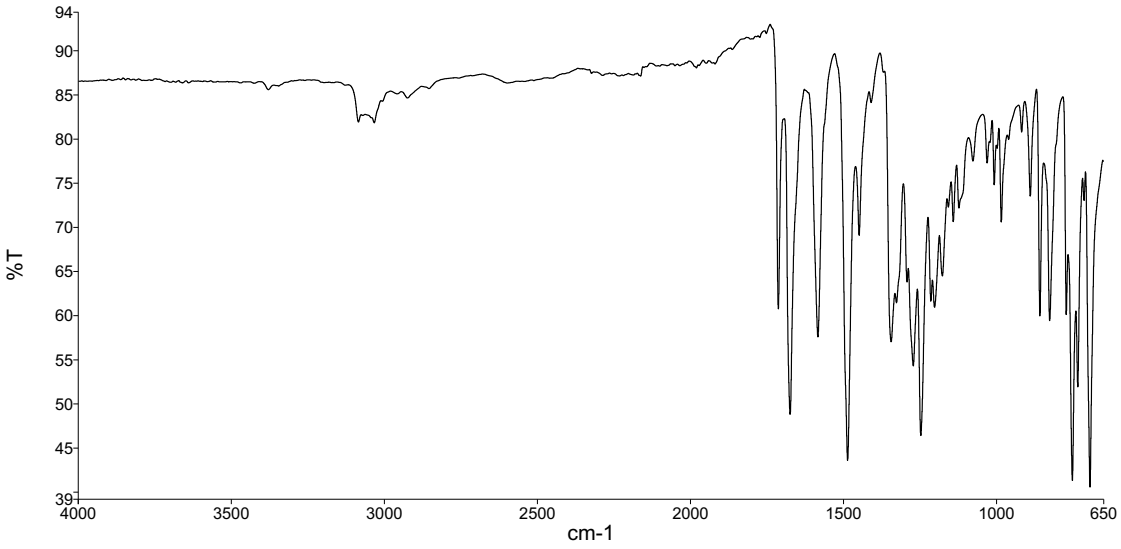

Figure **S25:** FTIR spectrum of **4**.

Compound 7

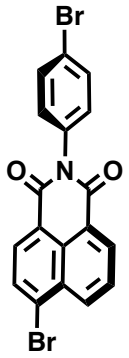

4-Bromoaniline (621 mg, 3.6 mmol, 2.0 equiv.) and 4-bromo-1,8-naphthalic anhydride (500 mg, 1.8 mmol, 1.0 equiv.) were added to a round bottom flask and ethanol was added (20 mL). The reaction mixture was stirred under reflux for 24 h. The reaction was cooled to room temperature. Water (20 mL) was added to the reaction mixture and it was left for 1 h to allow the product to precipitate. The product was isolated by filtration, washed with acetone and water, and dried under vacuum to yield a grey/white solid was obtained (491 mg, 1.14 mmol). **Yield:** 98%. **Mp:** 282-284 °C. **^{1}H NMR (400 MHz, $CDCl_3$) δ_H (ppm):** 8.71 (dd, *J* = 7.3, 1.0 Hz, 1H, H_1), 8.66 (dd, *J* = 8.5, 1.0 Hz, 1H, H_3), 8.46 (d, *J* = 7.9 Hz, 1H, H_5), 8.1 (d, *J* = 7.9 Hz, 1H, H_4), 7.9 (dd, *J* = 8.5, 7.4 Hz, 1H, H_2), 7.68 (d, *J* = 8.5 Hz, 2H, H_6), 7.2 (d, *J* = 8.5 Hz, 2H, H_7). **^{13}C {^{1}H} NMR (101 MHz, $CDCl_3$) δ_C (ppm):** 163.8, 163.7, 134.2, 134.0, 132.8, 132.7, 131.9, 131.4, 131.1, 131.0, 130.5, 129.5, 128.4, 123.2, 123.1, 122.3. **ESI-HRMS (*m/z*) calculated for** $C_{18}H_{10}Br_2NO_2$ 429.9073 found $[M+H]^+$ 429.9066. **ν_{max} (ATR) cm^{-1}:** 1703 (C=O stretch), 1667, 1562, 1484 (aromatic C=C stretch), 1346 (C-N stretch), 1231. **Anal. Calc.: ($C_{18}H_9BrNO_2$):** C, 50.15; H, 2.10; N, 3.25; Br, 37.07. **Found:** C, 50.10; H, 1.82; N, 2.68; Br, 36.18.

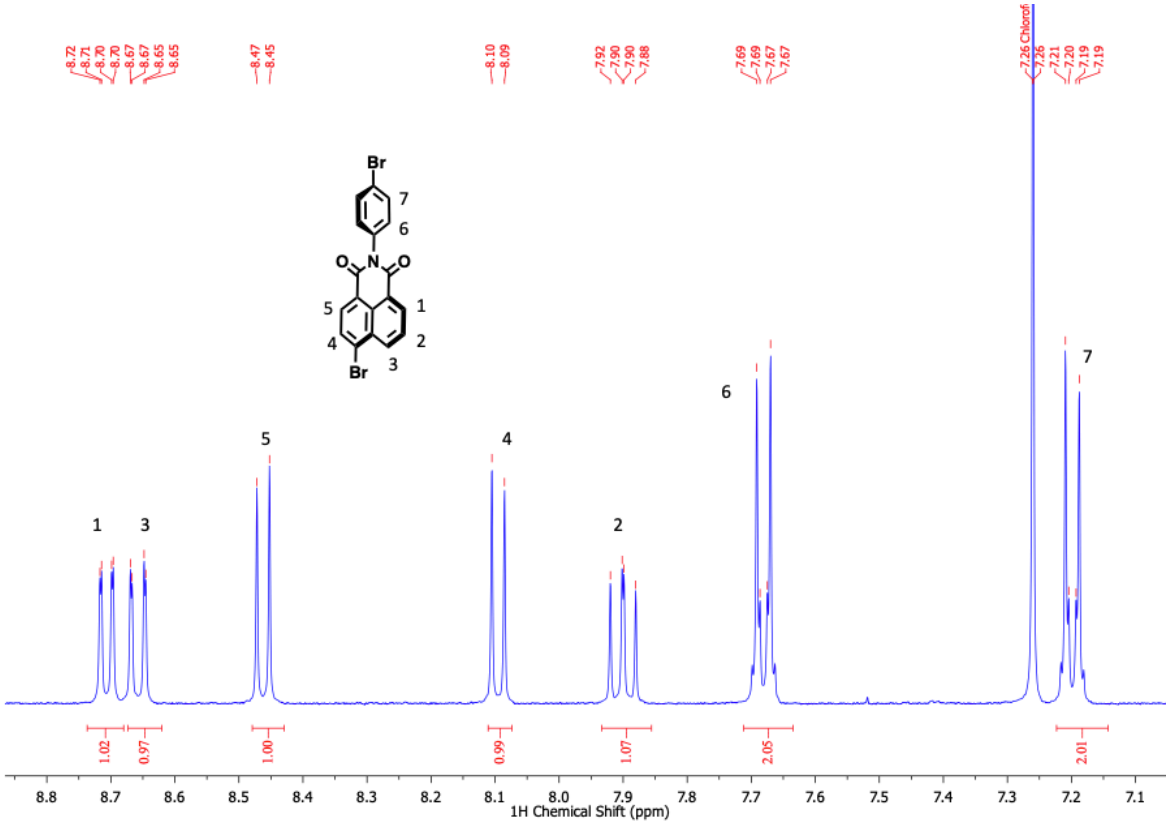

Figure **S26**. ^{1}H NMR spectrum of **7** between 8.8 and 7.1 ppm in $CDCl_3$.

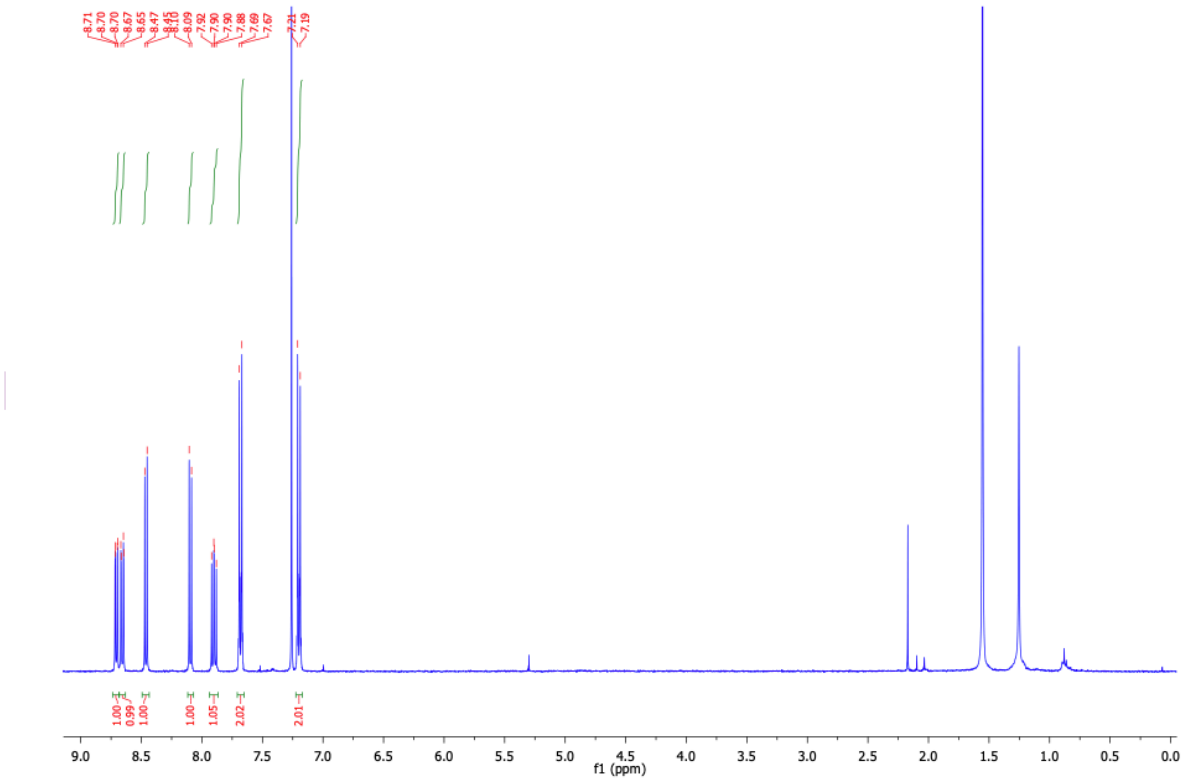

Figure **S27**. ^{1}H NMR full spectrum of **7** in $CDCl_3$.

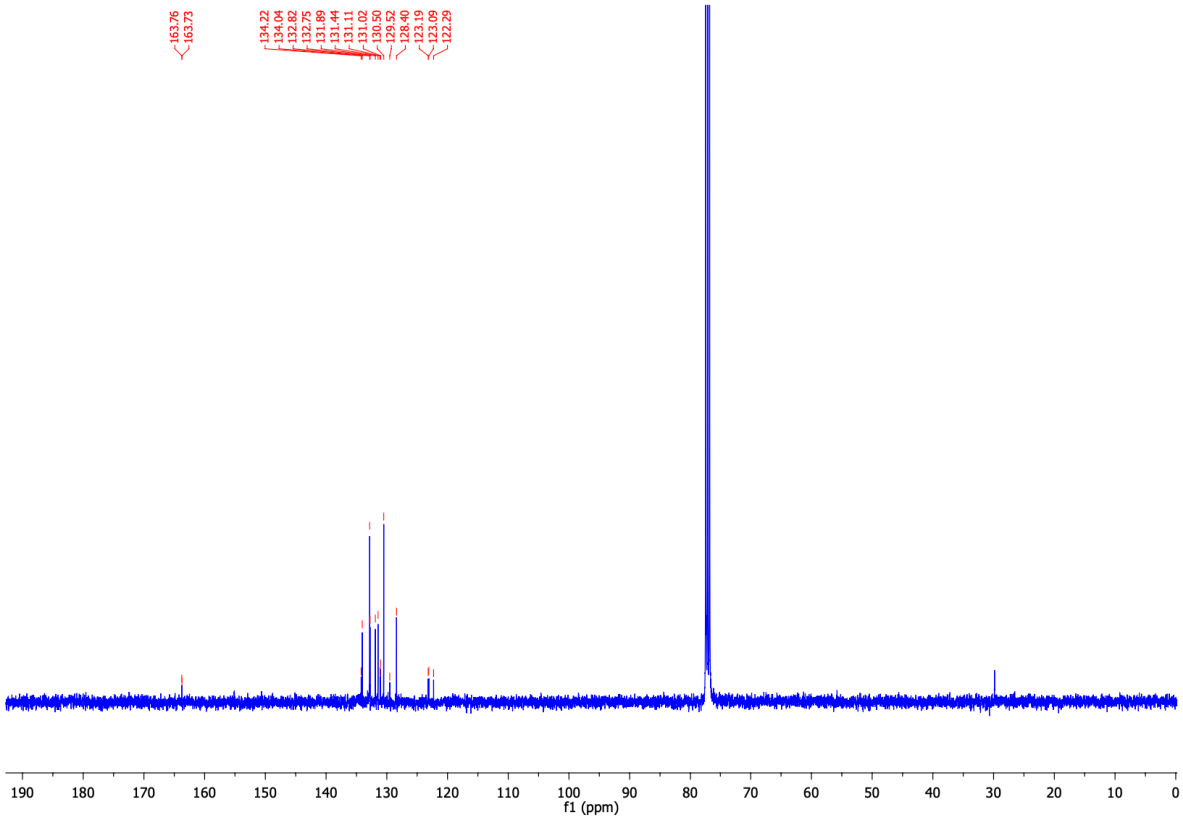

Figure **S28**. ^{13}C NMR spectrum of **7** in $CDCl_3$.

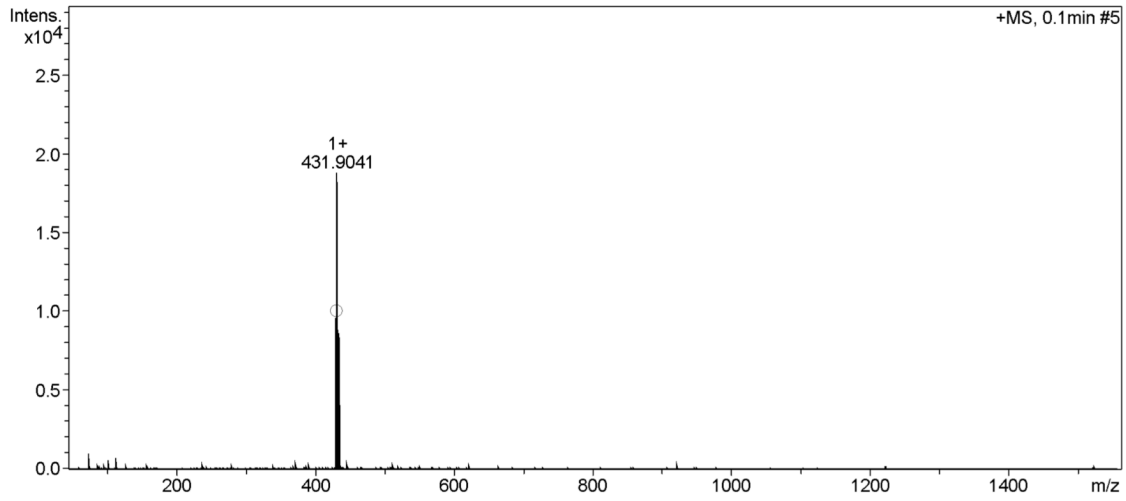

Meas. m/z	#	Ion Formula	m/z	err [mDa]	err [ppm]	rdb	N-Rule	e⁻ Conf	mSigma
429.906621	1	C18H10Br2NO2	429.907279	0.7	1.5	13.5	ok	even	17.0

Figure **S29**. ESI-HRMS of **7**.

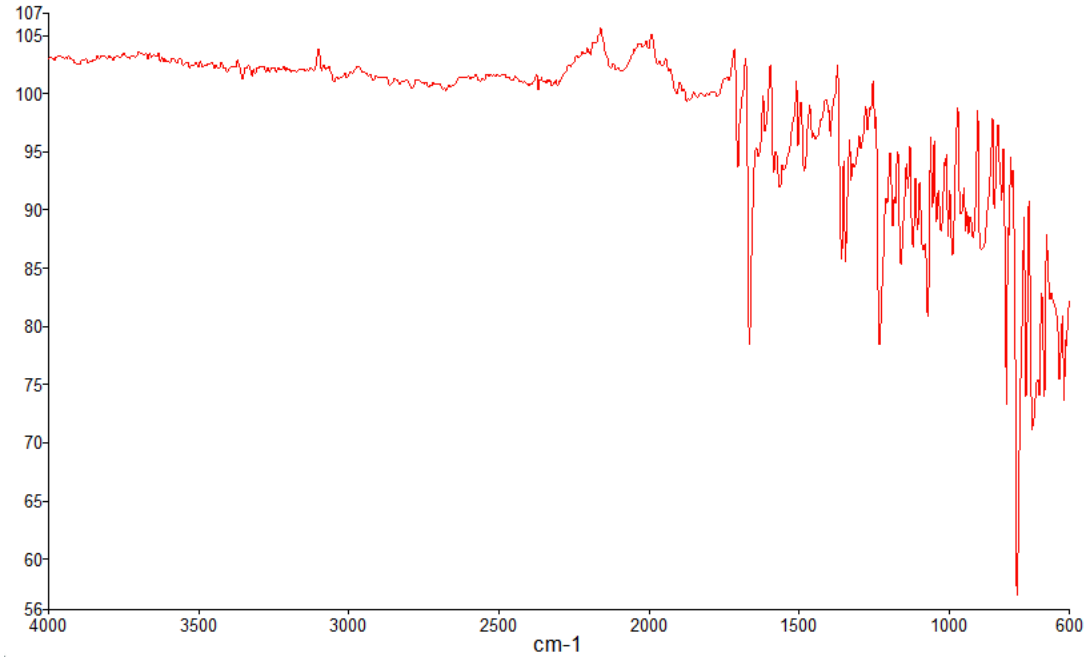

Figure **S30**. FTIR spectrum of **7**.

Compound 3

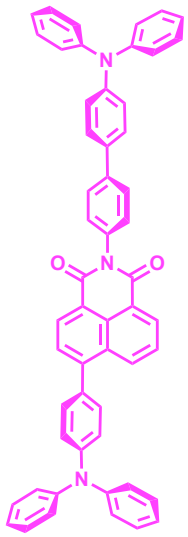

A solution of THF (25 mL) and water (5 mL) was degassed by three cycles of vacuum and backfilling with argon *via* the Schlenk line. Compound **7** (200 mg, 0.72 mmol, 1.0 equiv.), SPhos (60 mg, 0.14 mmol, 0.2 equiv.), $Pd(OAc)_2$ (16 mg, 0.072 mmol, 0.1 equiv.), K_3PO_4 (461 mg, 2.2 mmol, 3.0 equiv.) and 4-(diphenylamino)phenylboronic acid (439 mg, 1.5 mmol, 2.1 equiv.) were added to the flask upon which the solution turned dark orange. The reaction mixture was heated at 66 °C for 72 h. After heating, the product was cooled to room temperature and the solvent was then evaporated under reduced pressure. DCM (100 mL) and deionized water (100 mL) were then added, and the phases were separated. The aqueous phase was extracted with DCM four times, and the organic extracts were combined. The organic layer was then washed with deionized water (100 mL) and saturated aqueous K_2CO_3 solution (100 mL). The organic layer was dried over $MgSO_4$, filtered, and the solvent was evaporated under reduced pressure. The crude product was purified using column chromatography (silica, hexane/ethyl acetate, 4:1). Ethanol (20 mL) was added to the product and sonicated for 10 mins. The mixture was centrifuged for 10 mins and the supernatant was disposed of (repeated twice). Diethyl ether was added to the solid and centrifuged again for 10 mins (repeated twice). The supernatant was removed and the solid was dried for 24 h under vaccum. A yellow solid product was obtained (183 mg, 0.24 mmol). **Yield:** 52%. **Mp:** 300 °C. **^{1}H NMR (600 MHz, $CDCl_3$) δ_H (ppm)**: 8.70 (d, *J* = 6.7 Hz, 1H, H_1), 8.69 (d, *J* = 7.5 Hz, 1H, H_5), 8.48 (d, *J* = 8.4 Hz, 1H, H_3), 7.78 (dd, *J* = 8.4 Hz, 1H, H_2), 7.77 (d, *J* = 7.5 Hz, 1H, H_4), 7.74 (d, *J* = 8.4 Hz, 2H, H_7), 7.52 (d, *J* = 8.5 Hz, 2H, H_8), 7.40 (dd, *J* = 13.1, 8.4 Hz, 4H, $H_{6,13}$), 7.33 (t, *J* = 7.9 Hz, 4H, H_{16}), 7.29 (m, 4H, H_{11}), 7.23 (dd, *J* = 8.0, 4.9 Hz, 6H, $H_{14,15}$), 7.16 (dd, *J* = 8.2, 3.0 Hz, 6H, $H_{9,10}$), 7.11 (t, *J* = 7.4 Hz, 2H, H_{17}), 7.05 (t, *J* = 7.3 Hz, 2H, H_{12}). **^{13}C NMR (151 MHz, $CDCl_3$) δ_C (ppm)**: 164.8, 164.6, 148.6, 147.8, 147.6, 147.5, 147.4, 141.4, 134.5, 134.3, 133.4, 132.0, 131.8, 131.5, 131.0, 130.4, 129.7, 129.5, 129.0, 128.2, 127.9, 127.8, 126.9, 125.2, 124.7, 123.8, 123.8, 123.2, 122.6, 121.5. **ESI-HRMS calculated for** $C_{54}H_{38}N_3O_2$ 760.2959, found $[M+H]^+$ 760.2950. **ν_{max} (ATR) cm^{-1}:** 1702 (C=O

stretch), 1666, 1582, 1481 (aromatic C=C stretch), 1364, 1330 (C-N stretch), 1236. **Anal. Calc.: ($C_{54}H_{37}N_3O_2$):** C, 85.35; H, 4.91; N, 5.53. **Found:** C, 84.39; H, 4.89; N, 5.32.

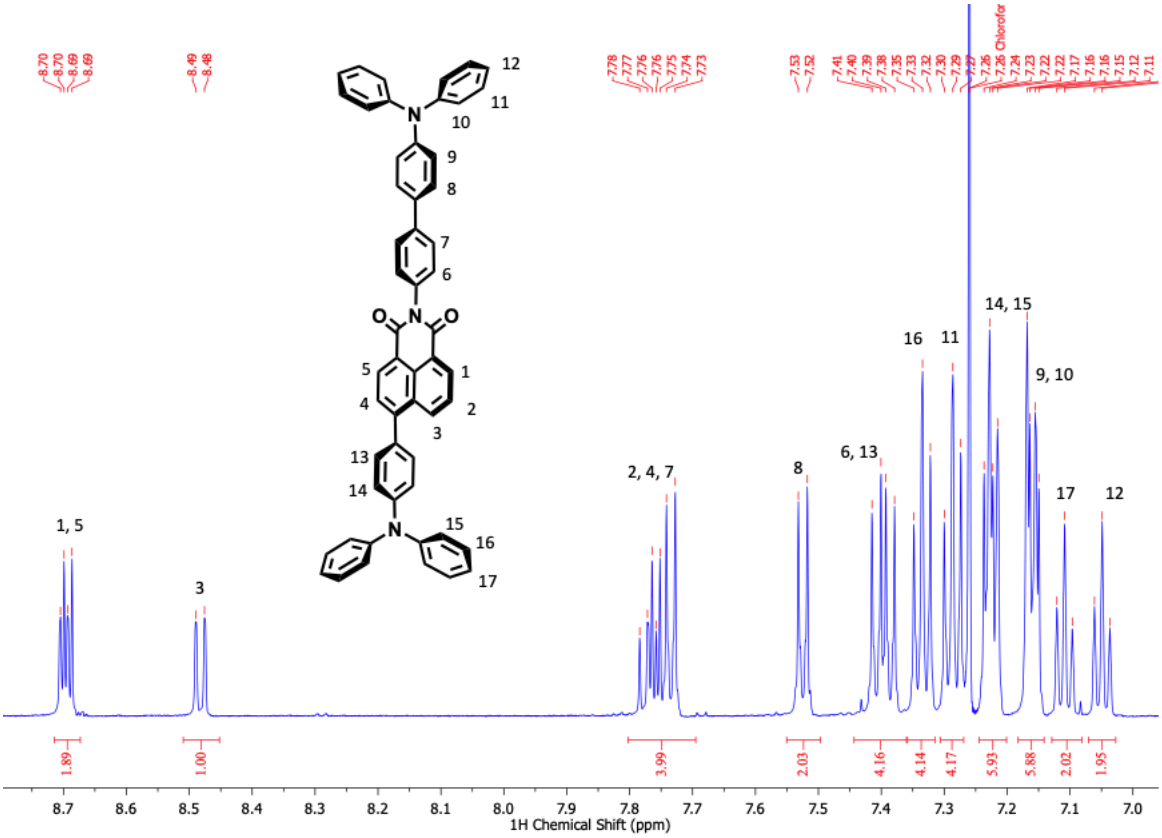

Figure **S31**. ^{1}H NMR spectrum of **3** between 8.7 and 7.0 ppm in $CDCl_3$.

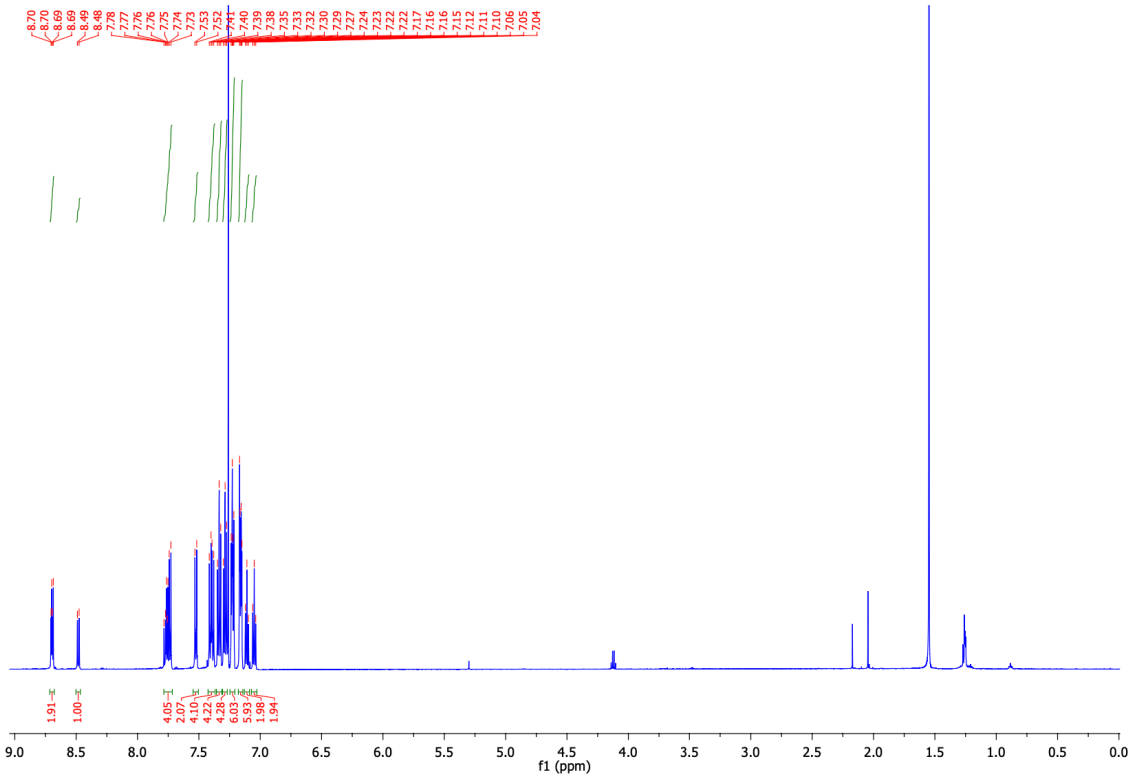

Figure **S32**. ^{1}H NMR full spectrum of **3** in $CDCl_3$.

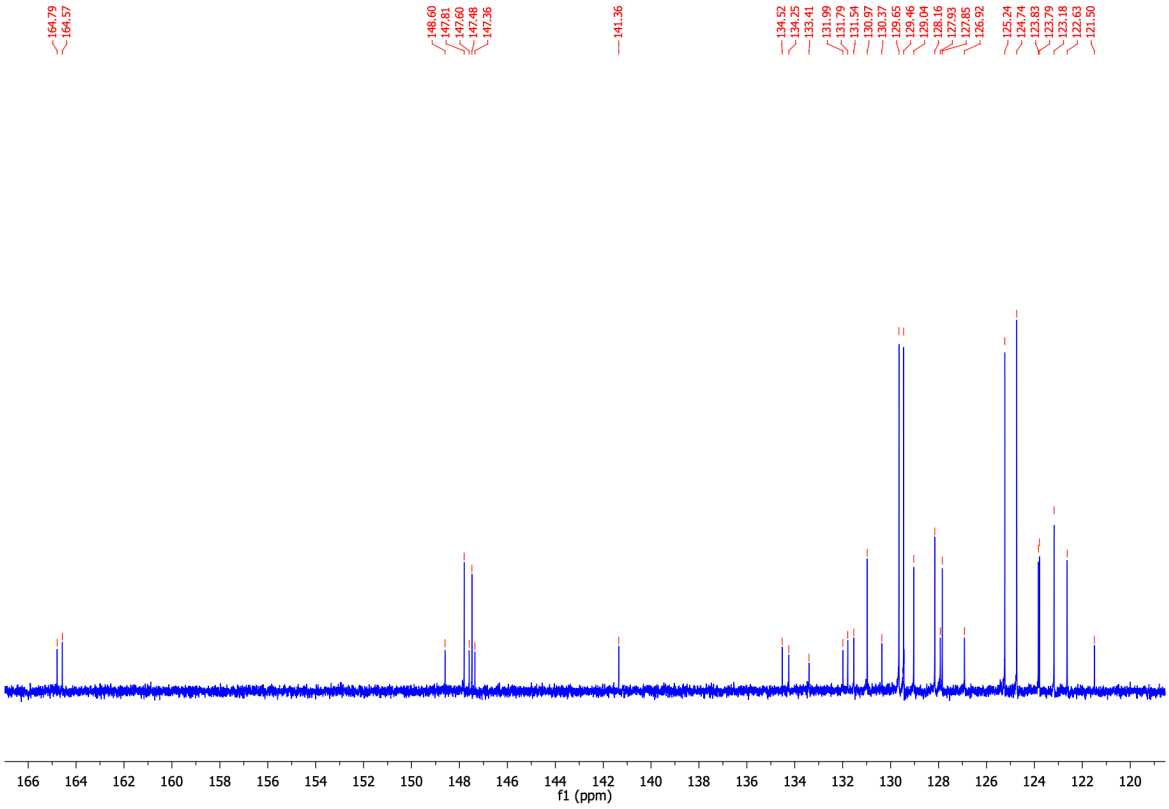

Figure **S33**. ^{13}C NMR spectrum of **3** in $CDCl_3$.

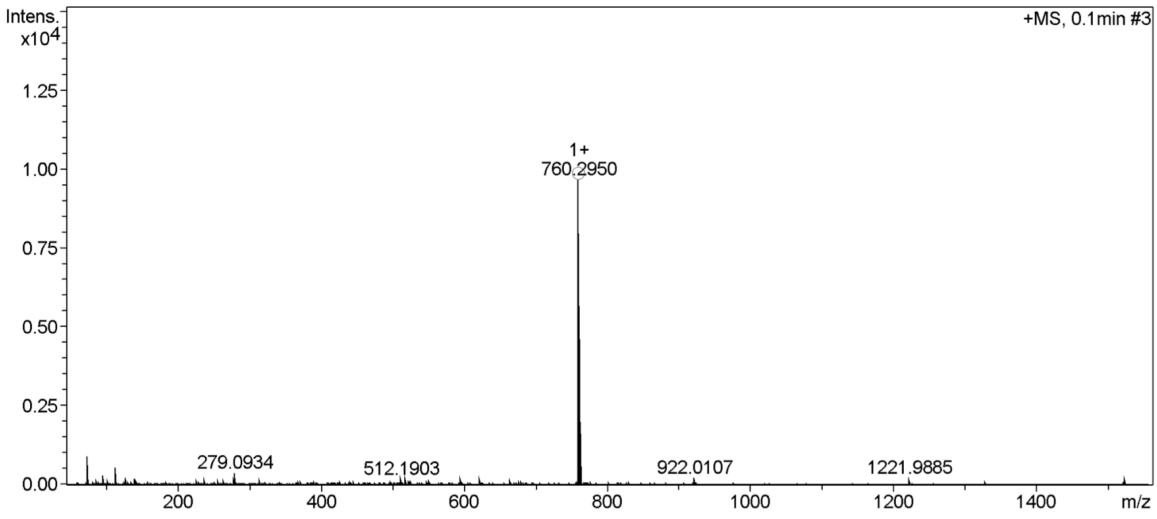

Figure **S34**. ESI-HRMS of **3**.

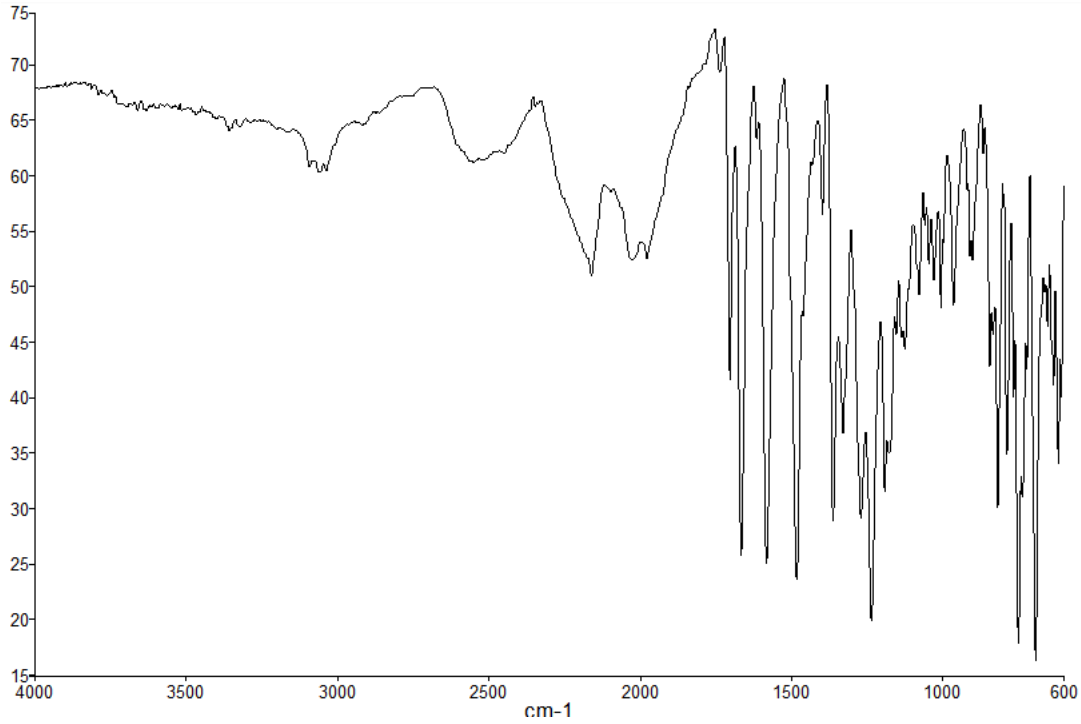

Figure **S35**. FTIR spectrum of **3**.

X-Ray Crystallography

General Information

Structural and refinement parameters are presented in Table S1. Crystallographic data for the structures reported here have been deposited with the Cambridge Crystallographic Data Centre.[3] CCDC [CCDC 2365261-2365266] contain the supplementary crystallographic data for this paper. These data can be obtained free of charge from The Cambridge Crystallographic Data Centre via www.ccdc.cam.ac.uk/structures.

Compound 1

Dark red needles of [$C_{36}H_{23}N_3O_4 \cdot 0.5(C_7H_8)$] were grown by vapour diffusion of hexane into a solution of **1** in toluene. The crystal with dimensions of 0.343 × 0.127 × 0.086 mm was coated in NVH immersion oil, mounted on a MicroMount (MiTeGen, USA) and maintained at a constant temperature of 100 K using a Cobra cryostream. Diffraction data were collected on a Bruker APEX-II Duo dual-source instrument using graphite-monochromated Cu Kα (λ = 1.5418 Å) radiation. Datasets were collected using ω and φ scans. The data were reduced and processed using the Bruker APEX-3[4] suite of programs. Multi-scan absorption corrections were applied using SADABS.[5] The diffraction data were solved using SHELXT[6] and refined by full-matrix least squares procedures using SHELXL-2019[7] within the Olex2[8] GUI. All non-hydrogen atoms were refined with anisotropic displacement parameters. All carbon-bound hydrogen atoms were placed in calculated positions and refined with a riding model, with isotropic displacement parameters equal to either 1.2 or 1.5 times the isotropic equivalent of their carrier atoms. One molecule of toluene was found at the edge of the unit cell along the *a* axis and was modelled with half occupancy in part -1.

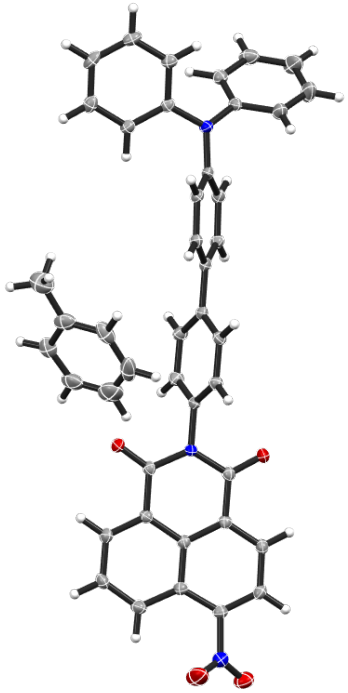

Figure S36. Thermal ellipsoid representation of the X-ray crystal structure of [**1**·0.5(C_7H_8)]. Thermal ellipsoids are shown at 50% probability. Positional disorder in the solvent is omitted for clarity.

Compound 2

Yellow needles of [$C_{36}H_{25}N_3O_2$] were grown from a $CHCl_3$/Et_2O mixture, from which a needle fragment with dimensions of 0.159 × 0.084 × 0.038 was isolated, coated with NVH immersion oil, and mounted on a MiTeGen micromount. Data were collected from a shock-cooled single crystal at 100(2) K on a Bruker APEX2 Kappa Duo diffractometer with a microfocus sealed X-ray tube using mirror optics as a monochromator and an APEX2 detector. The diffractometer was equipped with an Oxford Cobra low temperature device and used Cu *K*α radiation (λ = 1.54178 Å). All data were integrated with SAINT[9] and a multi-scan absorption correction using SADABS[5] was applied. The structure was solved by dual methods using SHELXT[6] and refined by full-matrix least-squares methods against F^2 by SHELXL[7] using Olex2.[8] All non-hydrogen atoms were refined with anisotropic displacement parameters. All hydrogen atoms were refined with isotropic displacement parameters. Some were refined freely and some on calculated positions using a riding model with their U_{iso} values constrained to 1.5 times the U_{eq} of their pivot atoms for terminal sp^3 carbon atoms and 1.2 times for all other carbon atoms. This report was generated using FinalCif.[10]

Donor N-H hydrogen atoms located on the difference map and refined using restraints (DFIX, DANG). During the refinement of **2** an unknown but well-ordered guest molecule was detected within the lattice. After attempting to model diethyl ether and various other common solvent molecules to account for these Fourier residuals, we established the best crystallographic and chemical fit to be diethyl ether hydroperoxide. To our knowledge, although this species is well known as an oxidation product and impurity in unstabilised diethyl ether,[11] this species has not been previously observed crystallographically.

This assignment was primarily made on the basis of the best fit of electron density to the relevant sites, as well as molecular geometry, bond lengths, and hydrogen bonding characteristics. Modelling the unknown species as carbon only, the oxygen sites were clearly evident by their anomalously small U_{eq} values (0.43-0.46) compared to the carbon sites (0.071-0.136). Modelling these three sites as oxygen provided better residuals than any other 2*p* elements. Considering the relevant bond lengths, the most instructive is the peroxide O-O single bond O42-O43 [1.470(5) Å], which is identical within error to that observed in the low temperature structure of 1,4-dioxane-2-hydroperoxide reported by Lindberg [1.481 Å].[12] The other bond lengths (Figure S38) are also consistent with this assignment, likewise the bond angles (all falling in the range 104.6(4) – 115.2(5)° for all refined atoms) also point to a consistent sp^3 hybridisation. As described in the main text, the hydrogen bonding character of the hydroperoxide residue is also fully consistent with a protonated ROOH functional group (Figure S39).

The origin of this species is serendipitous; it is unclear whether this originated as an impurity in the crystallisation solvent or whether small quantities were generated *in situ* by a photosensitization process initiated by compound **2**. All attempts to crystallise compound **2** from other solvents failed. We present the structure of compound **2** here purely as an instructive model of the molecular structure of the main residue, as described in the main text.

Warning: many alkyl peroxides are notoriously unpredictable contact explosives. While we encountered no problems handling the crystals of compound **2** on a milligram scale, the shock sensitivity of this material was not examined, and we made no attempts to produce the hydroperoxide adduct on any significant scale. We recommend extreme caution when handling any peroxide-forming species, especially where crystallisation methods (e.g., vapour diffusion) may remove inhibitors in combination with exposure to sunlight and/or potential photosensitizers.

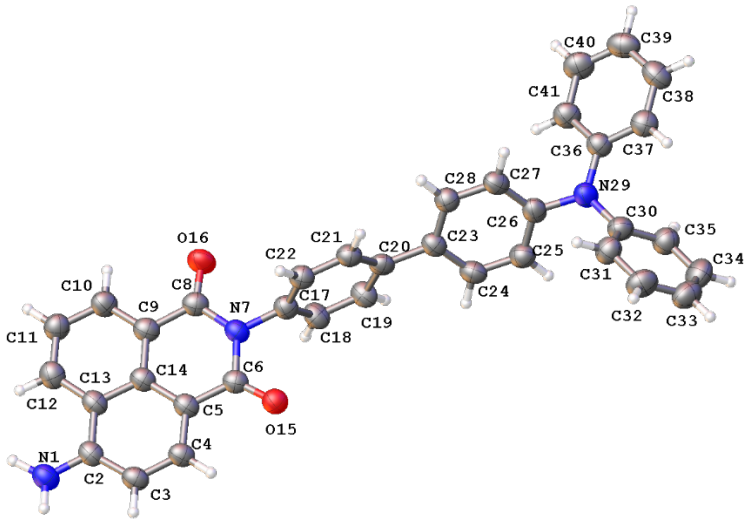

Figure S37. Thermal ellipsoid representation of the X-ray crystal structure of the main residue of **2**. Thermal ellipsoids are shown at 50% probability.

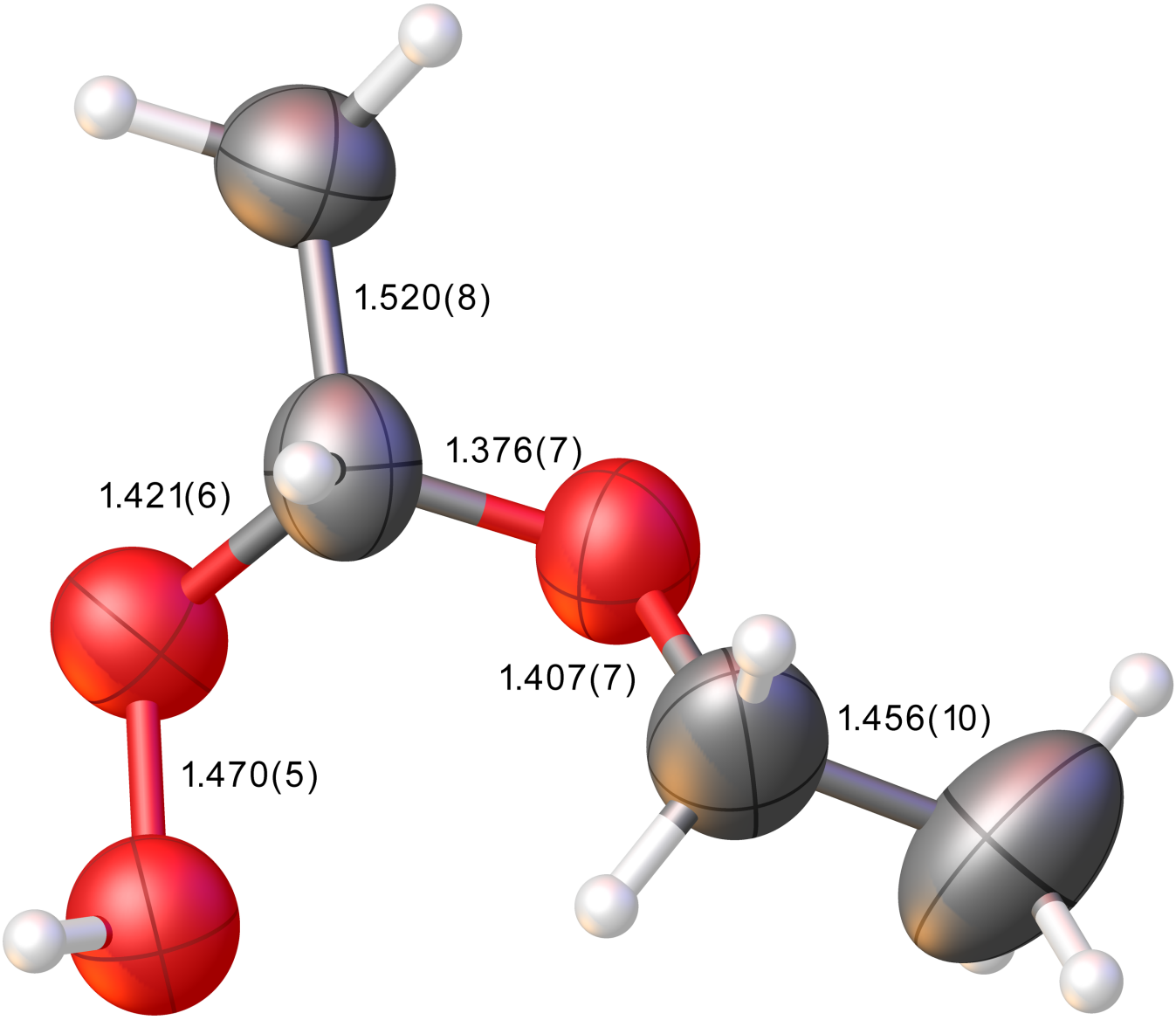

Figure S38. Relevant bond lengths and standard uncertainties for the diethyl ether hydroperoxide guest molecule in the structure of **2**. Ellipsoids are rendered at the 50% probability level.

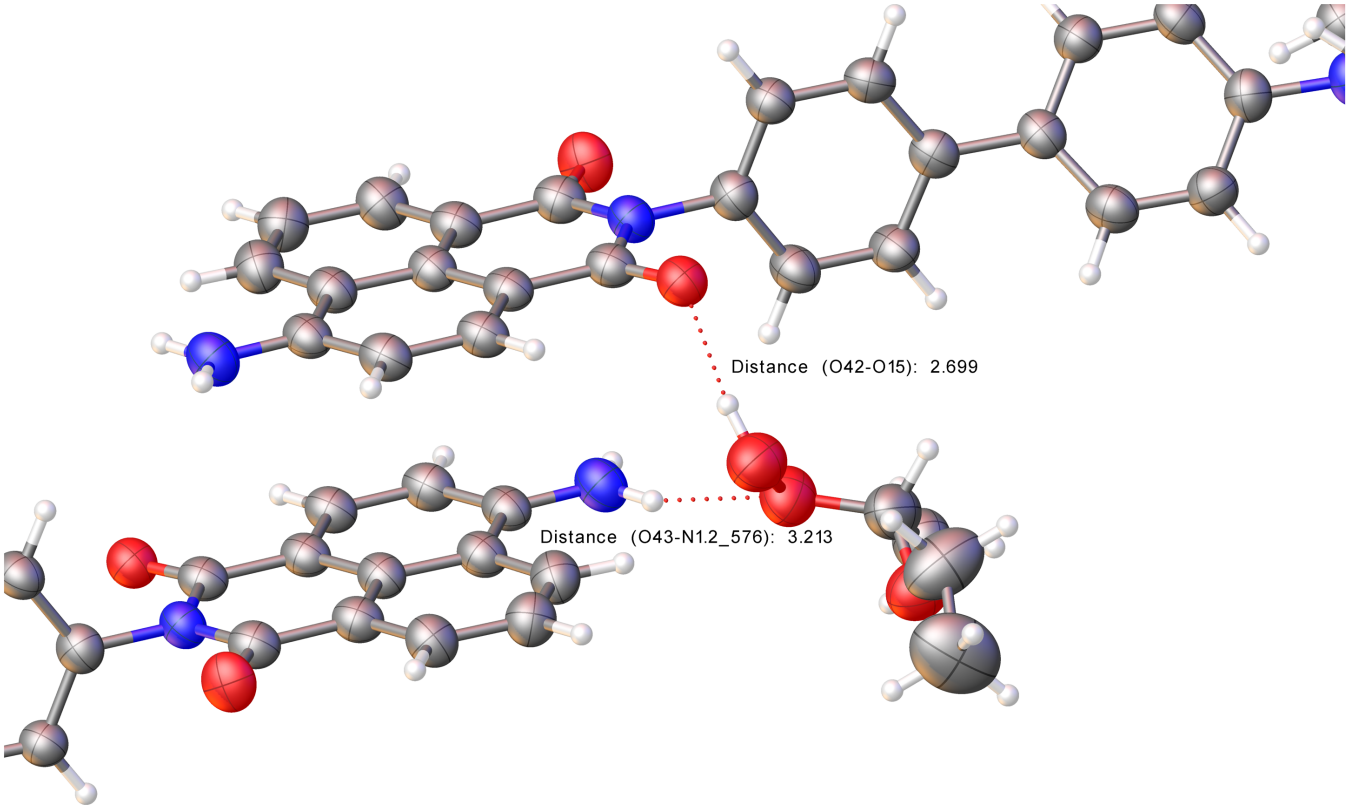

Figure S39: The hydrogen bonding behaviour of the peroxide species in the structure of **2** showing both donor and acceptor character in its interaction with two symmetry-related naphthalimide units.

Compound 3

Crystals of [$C_{54}H_{37}N_3O_2$] were grown by vapour diffusion of hexane into a DCM solution of **3**. The crystal with dimensions of 0.150 × 0.080 × 0.020 mm was coated in NVH immersion oil, mounted on a MicroMount (MiTeGen, USA) and maintained at a constant temperature of 100 K using a Cobra cryostream. Diffraction data were collected on a Bruker APEX-II Duo dual-source instrument using graphite-monochromated Cu Kα (λ = 1.5418 Å) radiation. Datasets were collected using ω and φ scans. The data were reduced and processed using the Bruker APEX-3[4] suite of programs. All data were integrated with SAINT[9] and a multi-scan absorption correction using SADABS[5] was applied. The diffraction data were solved using SHELXT[6] and refined by full-matrix least squares procedures using SHELXL-2019[7] within the Olex2[8] GUI. All non-hydrogen atoms were refined with anisotropic displacement parameters. All carbon-bound hydrogen atoms were placed in calculated positions and refined with a riding model, with isotropic displacement parameters equal to either 1.2 or 1.5 times the isotropic equivalent of their carrier atoms.

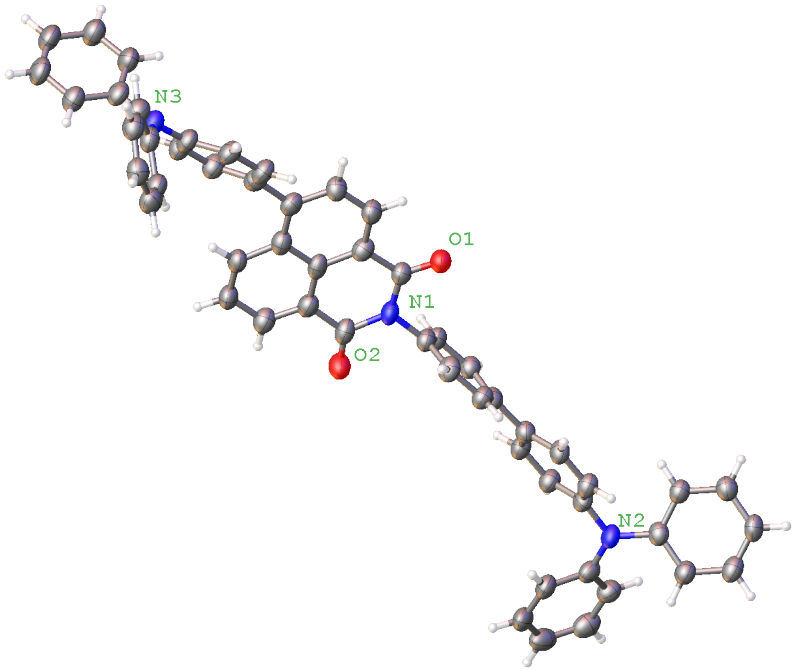

Figure S40. Thermal ellipsoid representation of the X-ray crystal structure of **3**. Thermal ellipsoids are shown at 50% probability. Heteroatoms labelled only.

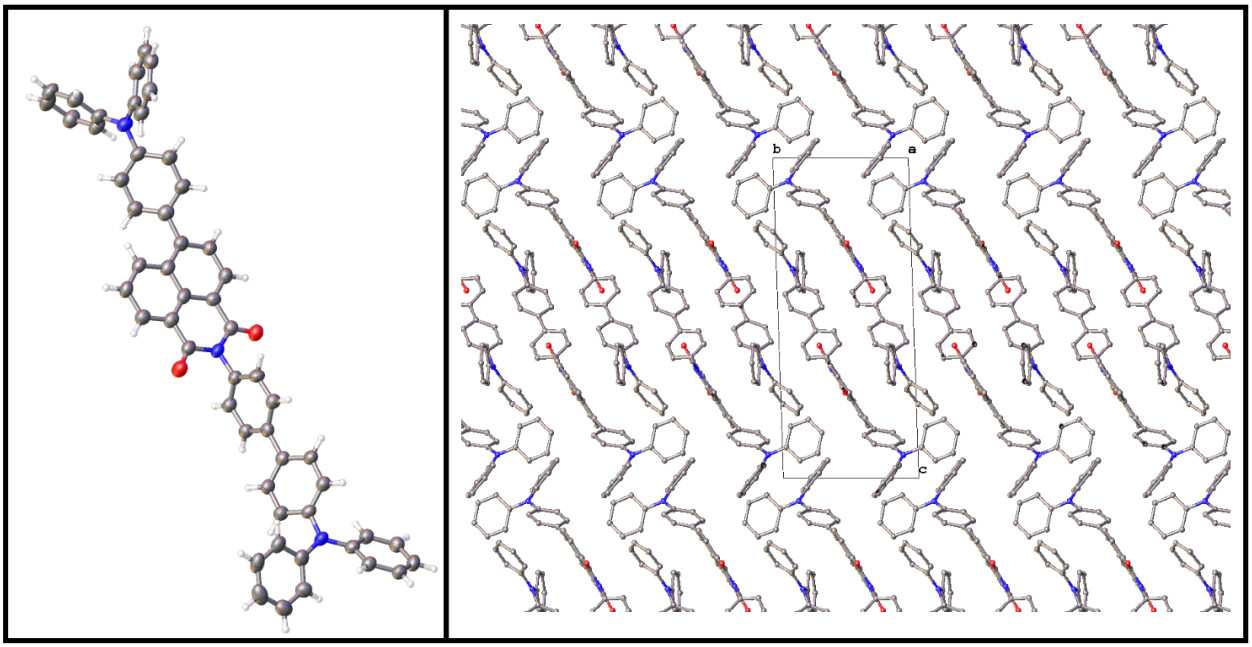

Figure S41: Crystal structure of compound **3** (left) and extended packing (right).

Intermolecular interactions in the structure of **3** primarily consist of C-H···π type interactions between inclined aromatic rings, rather than the parallel face to face π···π interactions more commonly seen in naphthalimide derivatives. This can be conveniently visualised using the Hirshfeld surface, generated with CrystalExplorer version 21.5,[13] represented through a fingerprint plot shown in

Figure S42. C···C contacts comprise only 1.8% of the interactions defining the Hirshfeld surface, compared to 36.8% for C···H contacts.

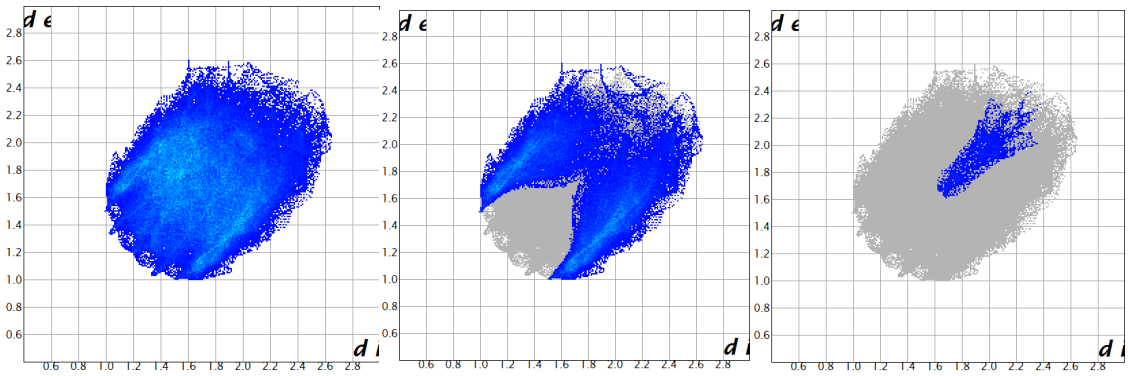

Figure S42. Fingerprint plots for **3** showing (left to right): All contacts; C···H contacts; C···C contacts.

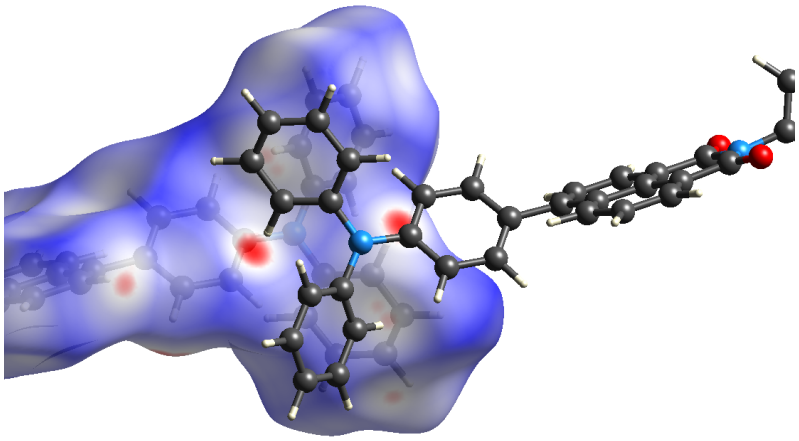

Figure S43. Normalised contact distance mapping of the Hirshfeld surface showing a representative C-H···π contact between the triphenylamine groups

Applying a curvedness mapping to the Hirshfeld surface shows inflections on both sides of the naphthalimide core, consistent with few significant face-to-face π···π stacking type interactions occurring. The most significant π···π contact involving the naphthalimide is the inclined contact with one phenyl ring of a triphenylamine group. The minimum C···π (mean plane) distance for this interaction is 3.30 Å, and the mean planes of the two aromatic systems involved in this interaction are inclined at an angle of 21.7° to one another.

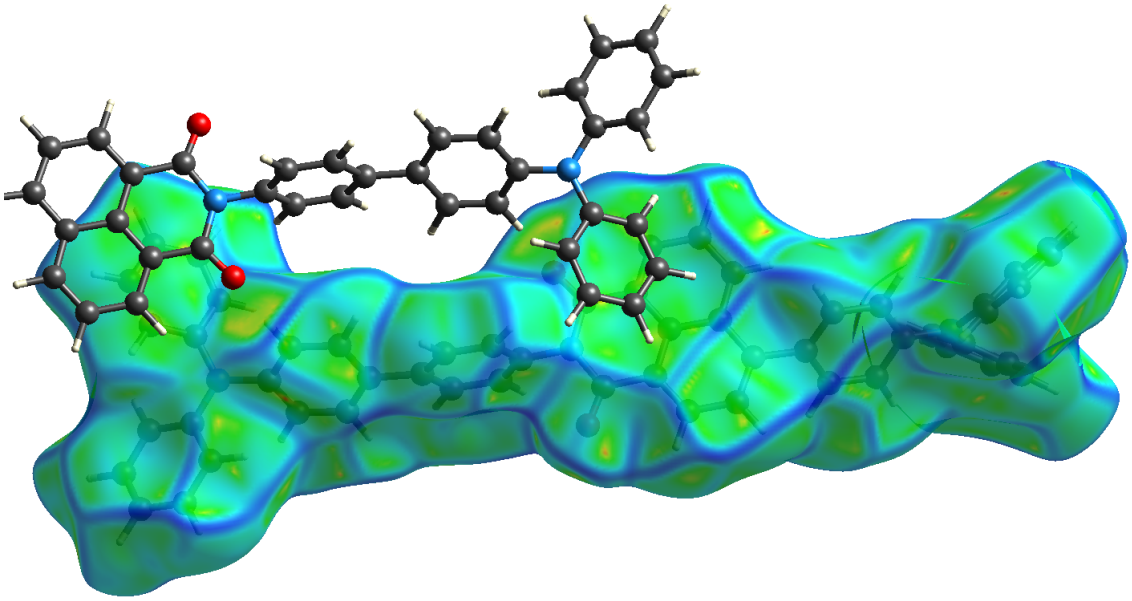

Figure S44. Curvedness mapping of the Hirshfeld surface showing the main π···π contact involving the naphthalimide ring. The curvature (blue lines) across the naphthalimide surface itself is consistent with the lack of substantial overlap between adjacent parallel π systems.

Compound 4

Purple plates of [$C_{62}H_{40}N_4O_4 \cdot CHCl_3$] were grown by slow evaporation of a solution of **4** in $CHCl_3$. The crystal with dimensions of 0.204 × 0.072 × 0.027 mm was coated in NVH immersion oil, mounted on a MicroMount (MiTeGen, USA) and maintained at a constant temperature of 100 K using a Cobra cryostream. Diffraction data were collected on a Bruker APEX-II Duo dual-source instrument using graphite-monochromated Cu Kα (λ = 1.5418 Å) radiation. Datasets were collected using ω and φ scans. The data were reduced and processed using the Bruker APEX-3[4] suite of programs. Multi-scan absorption corrections were applied using SADABS.[5] The diffraction data were solved using SHELXT[6] and refined by full-matrix least squares procedures using SHELXL-2019[7] within the Olex2[8] GUI. All non-hydrogen atoms were refined with anisotropic displacement parameters. All carbon-bound hydrogen atoms were placed in calculated positions and refined with a riding model, with isotropic displacement parameters equal to either 1.2 or 1.5 times the isotropic equivalent of their carrier atoms. The asymmetric unit contains half a molecule of **4**. One phenyl ring of the triphenylamine unit was disordered over two positions with occupancies of approximately 0.5. One molecule of solvent $CHCl_3$ was found in the asymmetric unit and was modelled at half occupancy.

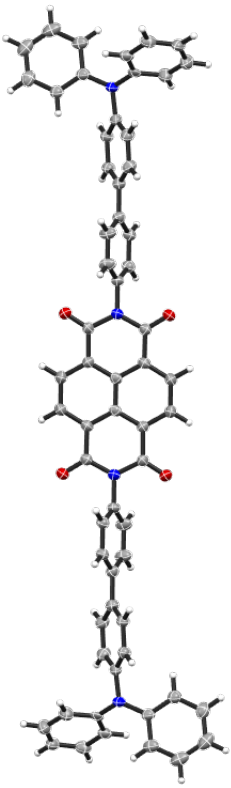

Figure S45. Thermal ellipsoid representation of **4** from the X-ray crystal structure of [**4**·$CHCl_3$]. Positional disorder and solvent molecules are omitted for clarity. Thermal ellipsoids are shown at 50% probability.

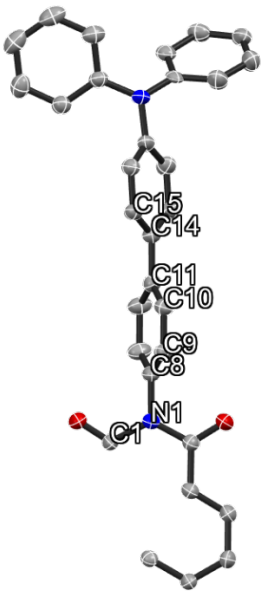

Figure S46. An ORTEP representation the asymmetric unit of the X-ray crystal structure of [**4**·$CHCl_3$]. Positional disorder, solvent molecules and hydrogen atoms are omitted for clarity. Thermal ellipsoids are shown at 50% probability. Torsion angles: C1-N1-C8-C9 114°; C10-C11-C14-C15 20°.

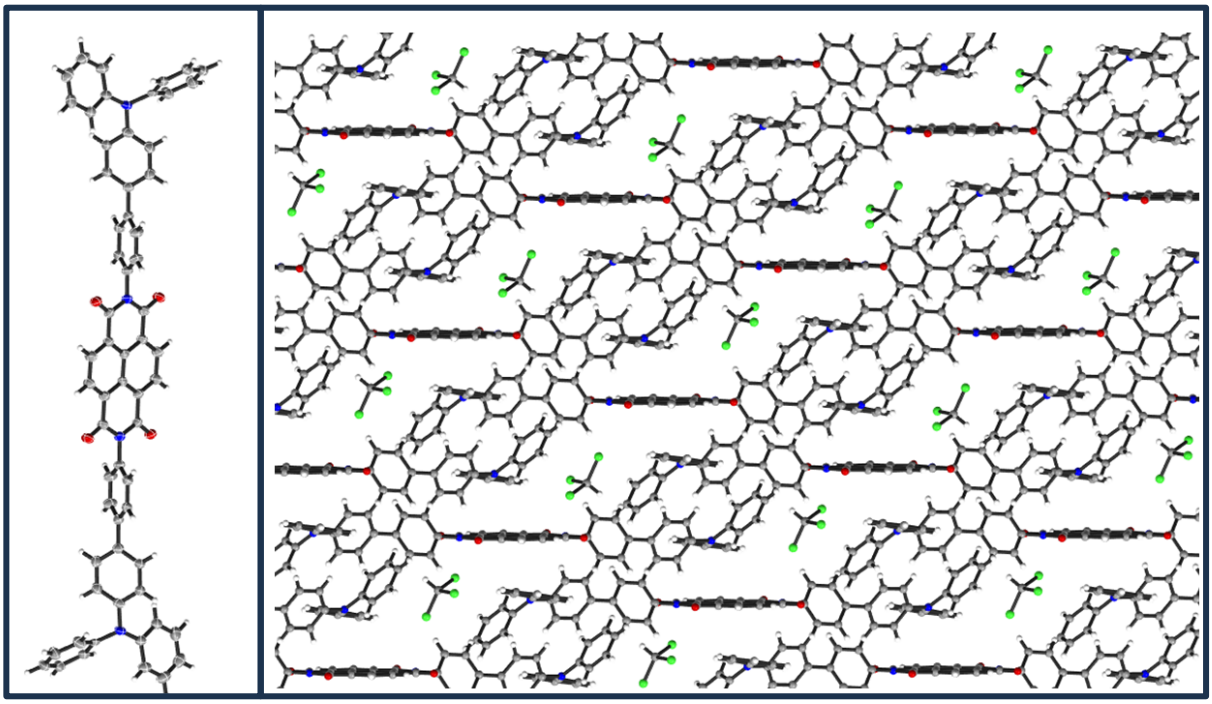

Figure S47: Crystal structure of compound **4** (left) and extended packing (right).

Compound 5

Pink block crystals of [$C_{24}H_{18}N_2O_2$] were grown by slow evaporation of a concentrated diethyl ether solution. The crystal with dimensions 0.41 × 0.244 × 0.155 mm was immersed in NVH immersion oil, mounted on a MicroMount (MiTeGen, USA) and maintained at a constant temperature of 100 K using a Cobra cryostream. Diffraction data were measured using a Bruker APEX-II Duo dual-source instrument using graphite- monochromated Cu Kα (λ = 1.5418 Å) radiation. Datasets were collected using ω and φ scans. The data were reduced and processed using the Bruker APEX-3[4] suite of programs. Multi-scan absorption corrections were applied using SADABS.[5] The diffraction data were solved using SHELXT[6] and refined by full-matrix least squares procedures using SHELXL-2019[7] within the Olex2[8] GUI. All non-hydrogen atoms were refined with anisotropic displacement parameters. All carbon-bound hydrogen atoms were placed in calculated positions and refined with a riding model, with isotropic displacement parameters equal to either 1.2 or 1.5 times the isotropic equivalent of their carrier atoms.

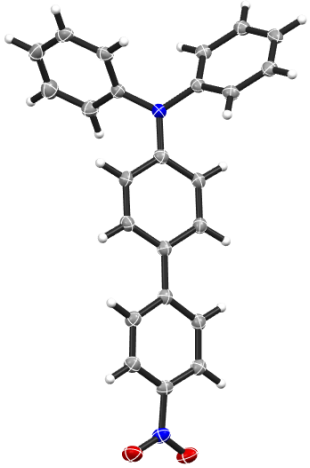

Figure S48. Thermal ellipsoid representation of the X-ray crystal structure of **5**. Thermal ellipsoids are shown at 50% probability.

Compound 6

Yellow plates of [$C_{24}H_{20}N_2$] were grown by slow evaporation of a concentrated diethyl ether solution. The crystal with dimensions of 0.272 × 0.221 × 0.054 mm was coated in NVH immersion oil, mounted on a MicroMount (MiTeGen, USA) and maintained at a constant temperature of 100 K using a Cobra cryostream. Diffraction data were collected on a Bruker APEX-II Duo dual-source instrument using graphite-monochromated Cu Kα (λ = 1.5418 Å) radiation. Datasets were collected using ω and φ scans. The crystal diffracted weakly at high angle and data were collected to a resolution of 0.86 Å. The data were reduced and processed using the Bruker APEX-3[4] suite of programs. Multi-scan absorption corrections were applied using SADABS.[5] The diffraction data were solved using SHELXT[6] and refined by full-matrix least squares procedures using SHELXL-2019[7] within the Olex2[8] GUI. All non-hydrogen atoms were refined with anisotropic displacement parameters. All carbon-bound hydrogen atoms were placed in calculated positions and refined with a riding model, with isotropic displacement parameters equal to either 1.2 or 1.5 times the isotropic equivalent of their carrier atoms.

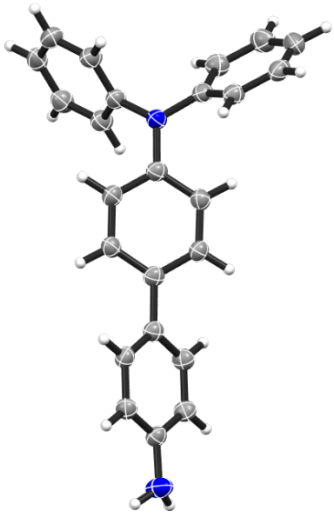

Figure S49. Thermal ellipsoid representation of the X-ray crystal structure of **6**. Thermal ellipsoids are shown at 50% probability.

Table S1. Crystal data and structure refinement for compounds **1**-**6**.

Identification code	**1**	**2**	**3**	**4**	**5**	**6**
Empirical formula	$C_{39.5}H_{27}N_3O_4$	$C_{40}H_{35}N_3O_5$	$C_{54}H_{37}N_3O_2$	$C_{63}H_{41}Cl_3N_4O_4$	$C_{24}H_{18}N_2O_2$	$C_{24}H_{20}N_2$
Formula weight	607.64	637.71	759.86	1024.35	366.40	336.42
Temperature/K	99.99	100(2)	100(2)	100.00	100.00	100.00
Crystal system	triclinic	triclinic	triclinic	triclinic	orthorhombic	monoclinic
Space group	$P\overline{1}$	$P\overline{1}$	$P\overline{1}$	$P\overline{1}$	*Pbca*	$P2_1/c$
a/Å	9.1317(3)	9.7325(3)	9.4126(6)	9.0793(7)	10.3528(3)	13.6209(4)
b/Å	12.3094(4)	11.2122(4)	9.8147(7)	12.3470(8)	15.7578(5)	11.4212(4)
c/Å	14.9218(4)	15.8447(6)	21.2962(15)	12.5800(11)	22.7203(7)	11.9286(4)
α/°	69.2120(10)	75.214(3)	90.736(5)	65.311(6)	90	90
β/°	74.3380(10)	83.986(3)	100.753(4)	83.296(7)	90	102.726(2)
γ/°	75.4100(10)	76.066(3)	97.008(5)	73.552(6)	90	90
Volume/Å^3	1487.01(8)	1620.84(10)	1917.1(2)	1228.90(18)	3706.5(2)	1810.11(10)
Z	2	2	2	1	8	4
ρ_{calc}g/cm^3	1.357	1.307	1.316	1.384	1.313	1.234
μ/mm^{-1}	0.713	0.698	0.627	2.142	0.674	0.556
F(000)	634.0	672	796.0	530.0	1536.0	712.0
Crystal size/mm^3	0.343 × 0.127 × 0.086	0.159 × 0.084 × 0.038	0.15 × 0.08 × 0.02	0.204 × 0.072 × 0.027	0.41 × 0.244 × 0.155	0.272 × 0.221 × 0.054
Radiation	Cu *K*α (λ = 1.54178)	Cu *K*α (λ=1.54178 Å)	CuKα (λ = 1.54178)	Cu *K*α (λ = 1.54178)	Cu *K*α (λ = 1.54178)	Cu *K*α (λ = 1.54178)
2Θ range for data collection/°	6.466 to 140.082	5.774 to 130.59 (0.85 Å)	4.226 to 139.722	7.734 to 140.038	7.782 to 137.386	6.652 to 126.882
Index ranges	-11 ≤ h ≤ 11, -14 ≤ k ≤ 14, -17 ≤ l ≤ 18	−11 ≤ h ≤ 11, −13 ≤ k ≤ 13, −18 ≤ l ≤ 18	-11 ≤ h ≤ 10, -11 ≤ k ≤ 11, -25 ≤ l ≤ 25	-10 ≤ h ≤ 11, -15 ≤ k ≤ 15, -15 ≤ l ≤ 15	-11 ≤ h ≤ 12, -19 ≤ k ≤ 18, -27 ≤ l ≤ 27	-15 ≤ h ≤ 15, -13 ≤ k ≤ 13, -13 ≤ l ≤ 13
Reflections collected	54284	27945	22458	36338	72236	23956
Independent reflections	5582 [R_{int} = 0.0473, R_{sigma} = 0.0224]	5536 [R_{int} = 0.0830, R_{sigma} = 0.0878]	7133 [R_{int} = 0.0895, R_{sigma} = 0.1101]	4588 [R_{int} = 0.0933, R_{sigma} = 0.0534]	3419 [R_{int} = 0.0436, R_{sigma} = 0.0133]	2950 [R_{int} = 0.0530, R_{sigma} = 0.0274]
Data/restraints/parameters	5582/136/452	5536/3/444	7133/0/532	4588/15/401	3419/0/254	2950/0/243
Goodness-of-fit on F^2	1.039	1.067	0.940	1.072	1.049	1.047
Final R indexes [I>=2σ (I)]	R_1 = 0.0541, wR_2 = 0.1550	R_1 = 0.0813, wR_2 = 0.2257	R_1 = 0.0862, wR_2 = 0.2191	R_1 = 0.0699, wR_2 = 0.1925	R_1 = 0.0366, wR_2 = 0.0985	R_1 = 0.0426, wR_2 = 0.1106
Final R indexes [all data]	R_1 = 0.0574, wR_2 = 0.1582	R_1 = 0.1264, wR_2 = 0.2696	R_1 = 0.1638, wR_2 = 0.2750	R_1 = 0.1035, wR_2 = 0.2202	R_1 = 0.0377, wR_2 = 0.0997	R_1 = 0.0522, wR_2 = 0.1170
Largest diff. peak/hole / e Å^{-3}	0.91/−0.48	0.34/−0.39	0.41/-0.32	0.38/−0.45	0.19/−0.20	0.17/−0.16

Photophysical Characterisation

All samples were prepared using high performance liquid chromatography (HPLC) or spectroscopic grade solvents, including tetrahydrofuran (THF), hexane, dimethyl sulfoxide (DMSO), methanol (MeOH), and water, at micromolar (μM) concentrations. UV-vis absorption spectra were measured in an optical path 1 cm quartz cuvette (2.5-3.0 mL) on a Varian CARY 50 spectrophotometer with a wavelength ranges of 200-800 nm and a scan rate of 600 nm min^{-1}, with baseline corrections applied to all spectra.

Steady-state emission spectra were collected at 298 K in 1 cm quartz cuvettes using a Varian Cary Eclipse Fluorimeter with a xenon lamp light source. All samples were excited in an optically dilute regime, where the absorbance at the chosen excitation wavelengths was ≤0.1. Time-resolved measurements were conducted at 298 K using a Horiba Jobin Yvon Fluorolog FL3-22 with a Fluorohub v2.0 single photon controller, utilizing the time-correlated single photon counting (TCSPC) method in reverse mode. Samples were excited at 340 nm with a PDL 800-D pulsed diode laser (NanoLED®). The instrument response function, which is the time distribution of the lamp pulse (<1.0 ns), was recorded separately using a scatter solution of silica nanoparticles (Ludox® from Aldrich) prior to lifetime measurements. The decay curves were analyzed with IBH DAS6 software, fitting the data as a sum of exponentials using nonlinear least-squares error minimization. Photoluminescence quantum yields (Φ_{PL}) were calculated using the optically dilute method, with individual relative quantum yield values derived for each solution and reported as slope values.[14,15] The formula used is as follows: $\Phi_{PL} = \Phi_r(A_r/A_s)(I_s/I_r)(n_s/n_r)^2$, where Φ_r represents the absolute quantum yield of the reference, n is the refractive index of the solvent, A is the absorbance at the excitation wavelength, and I is the integrated area under the corrected emission curve. The subscripts 's' and 'r' denote the sample and reference, respectively. Quinine sulfate in 0.5 M H_2SO_4 (Φ_{pl} = 54.6%) was used as the external reference.[16]

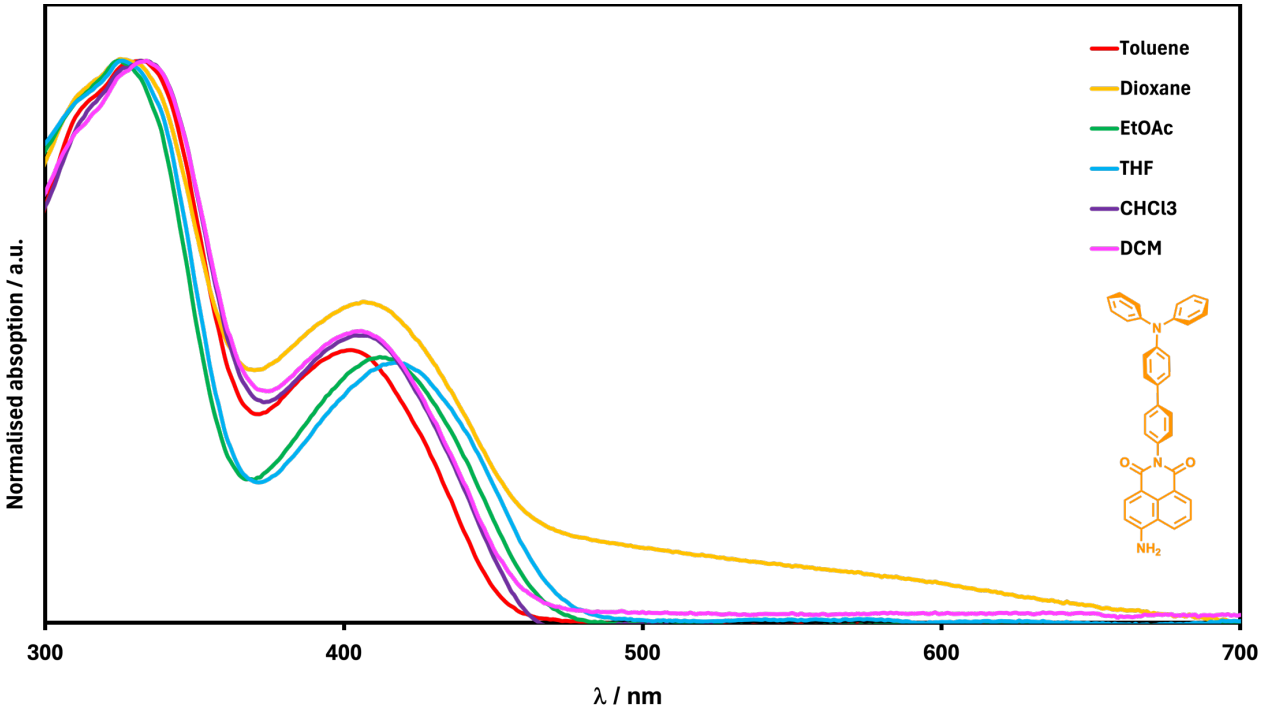

Figure S50. Absorbance spectra for compound **2** in different solvents. Spectra are normalised on the π-π* bands. **2** displayed poor solubility in 1,4-dioxane. As such the broad tail observed from 450-650 nm is ascribed to light scattering by large particulates of **2**.

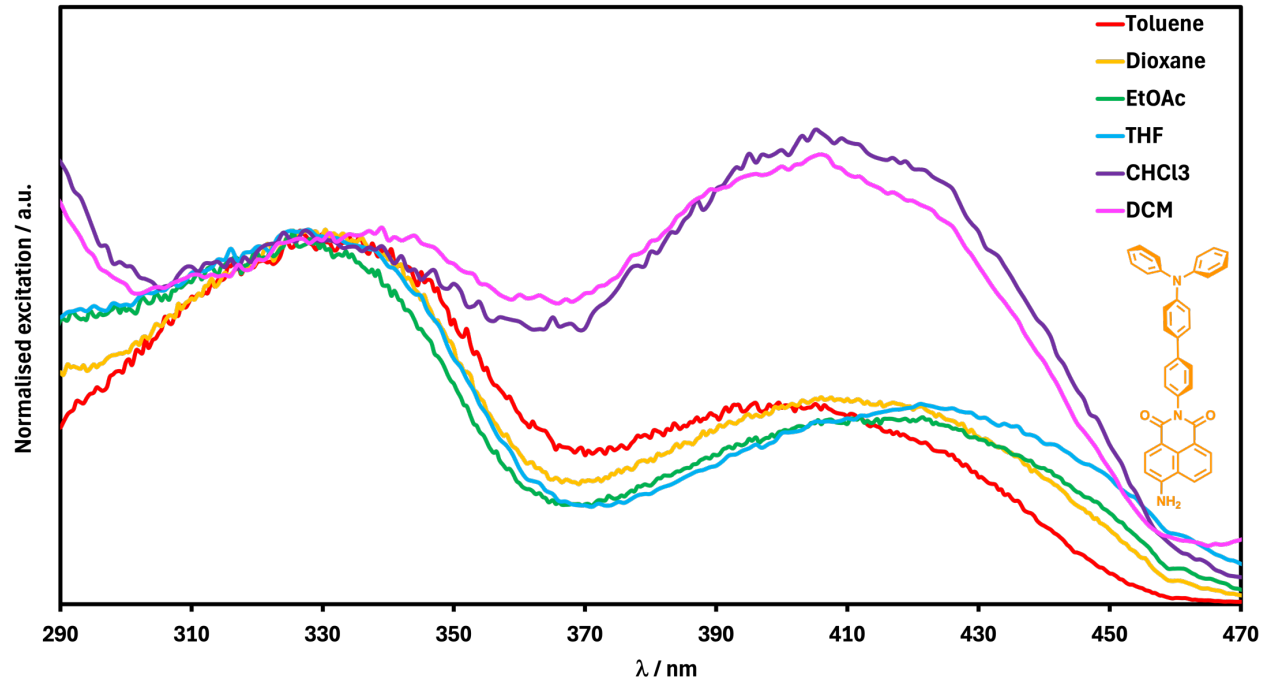

Figure S51. Excitation spectra for compound **2** in different solvents. Spectra are normalised on the π-π* bands and were collected at the corresponding emission maxima (see Figure **S52**).

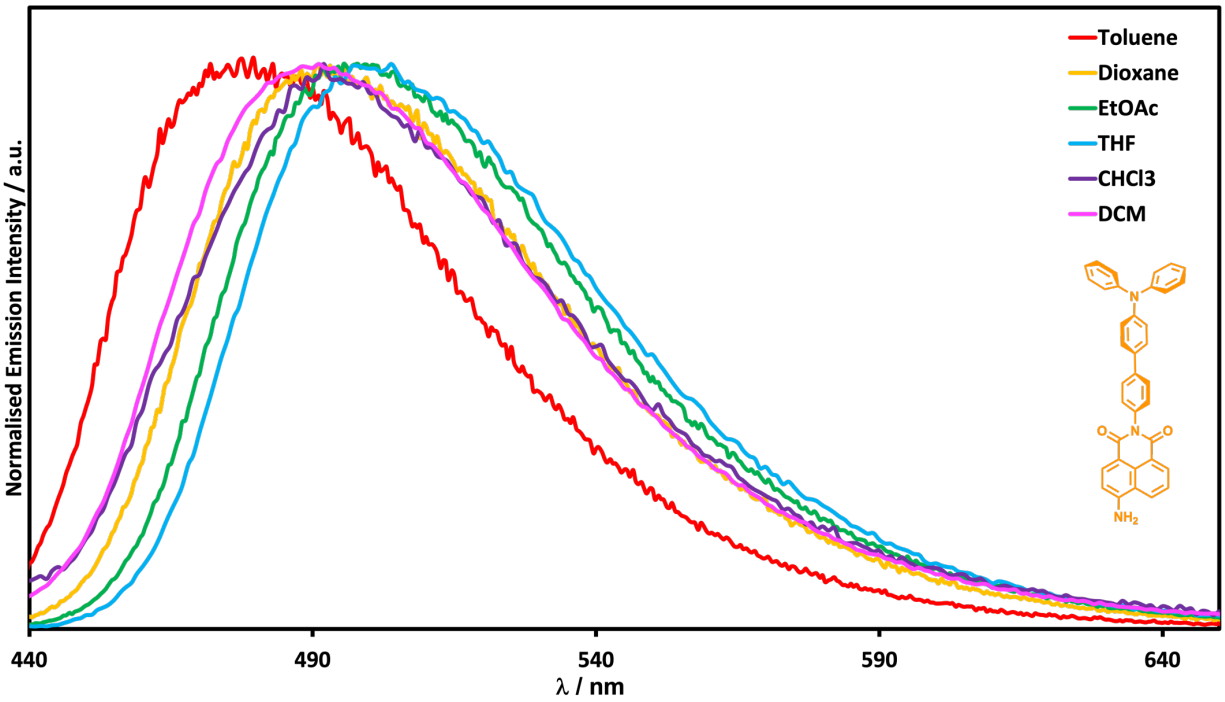

Figure S52. Normalised emission spectra for compound **2** in different solvents. Emission spectra were recorded upon excitation at 400 nm (toluene, DCM, 1,4-dioxane), 405 nm ($CHCl_3$), 414 nm (ethyl acetate), or 415 nm (THF) on samples diluted to 0.1 optical density at the excitation wavelength.

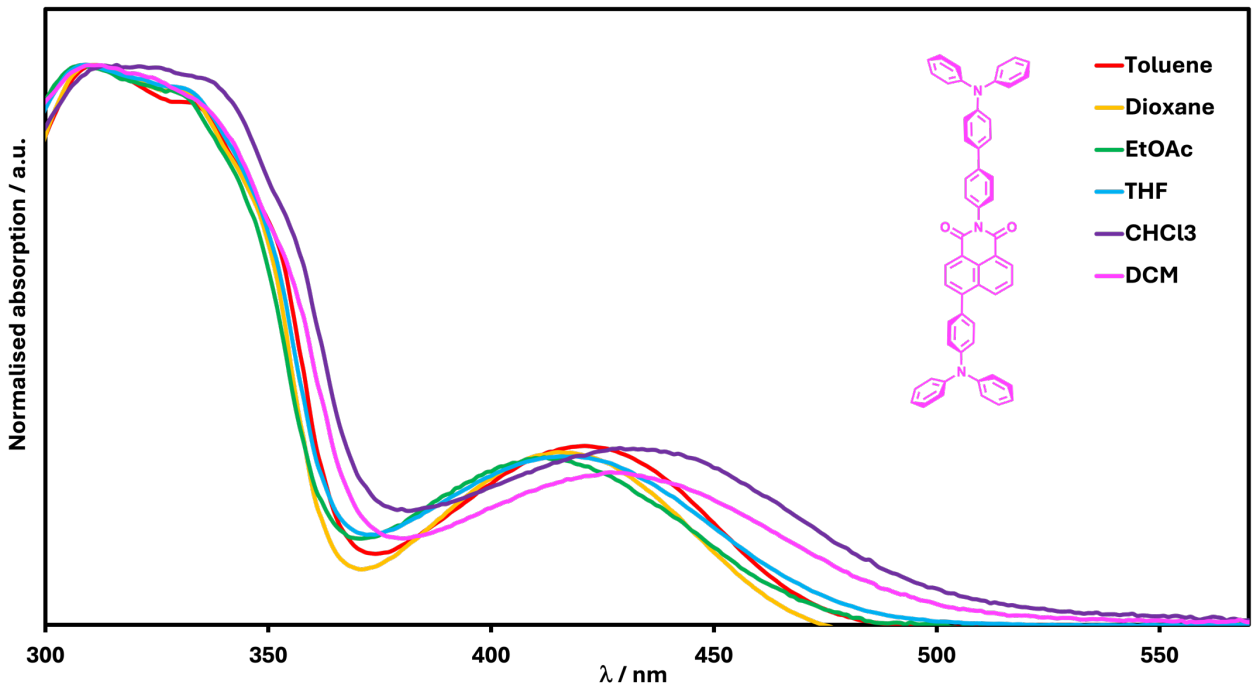

Figure S53. Absorbance spectra for compound **3** in different solvents. Spectra are normalised on the π-π* bands.

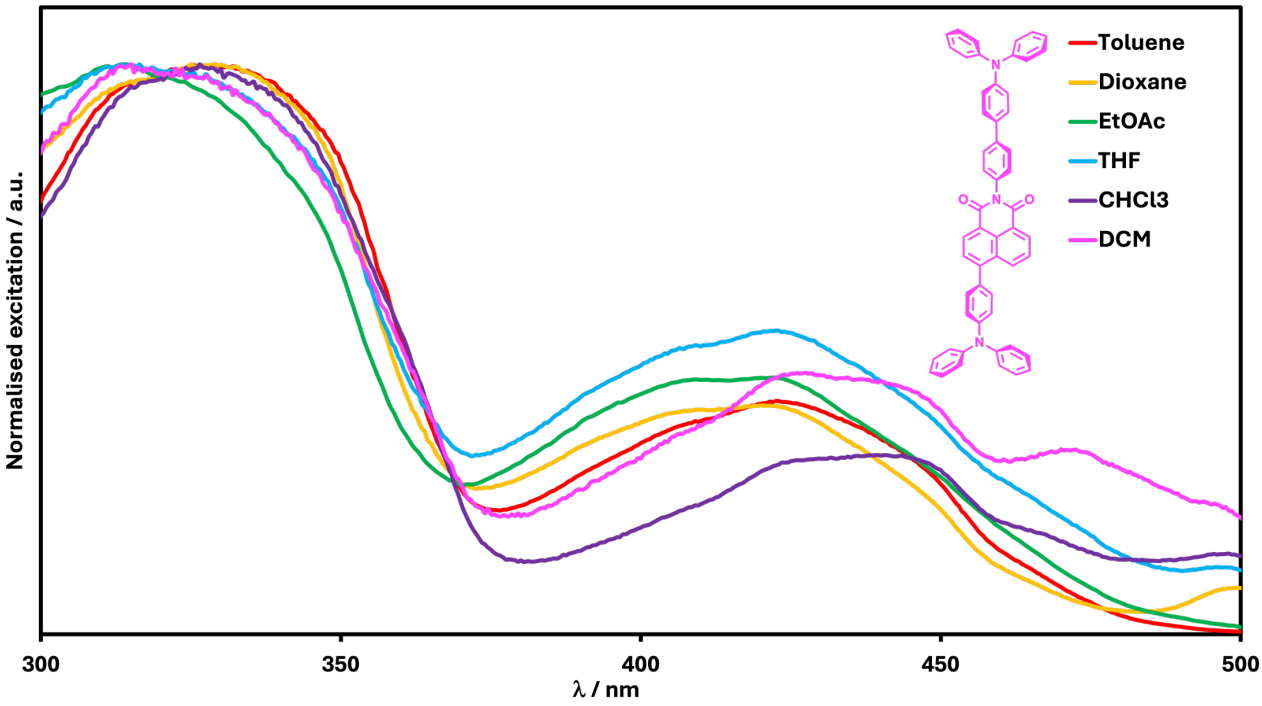

Figure S54. Excitation spectra for compound **3** in different solvents. Spectra are normalised on the π-π* bands and were collected at the corresponding emission maxima (see Figure **S55**).

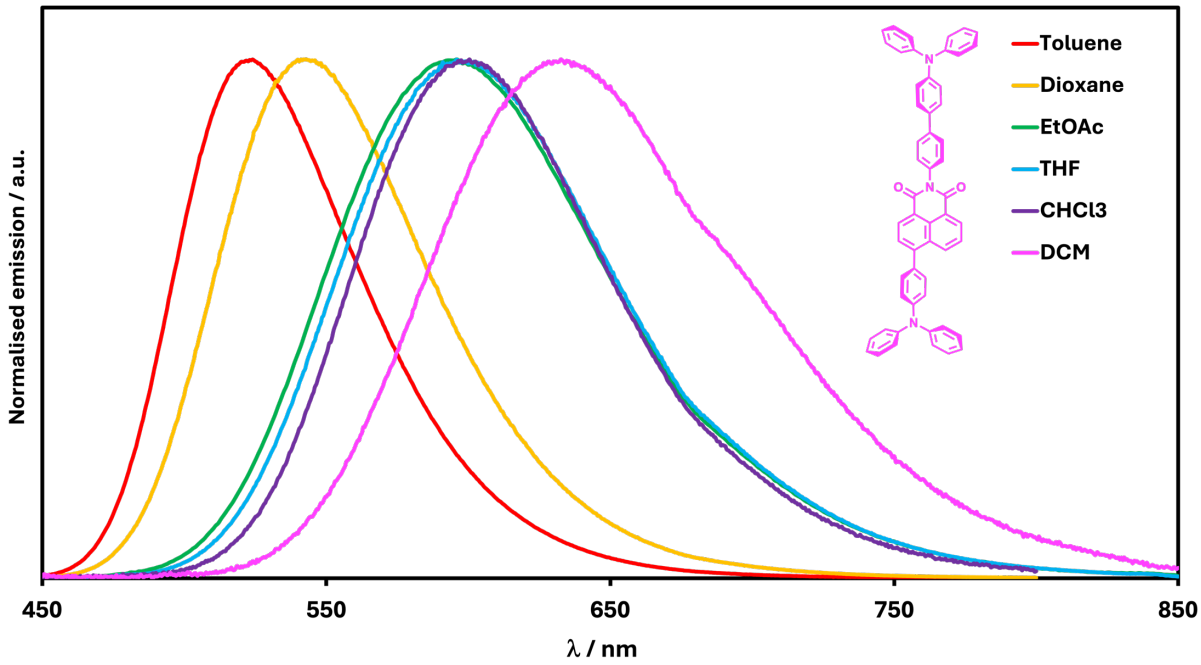

Figure S55. Normalised emission spectra for compound **3** in different solvents. Emission spectra were recorded upon excitation at 420 nm, on samples diluted to 0.1 optical density at the excitation wavelength.

Table S2. Relevant spectroscopic solvent data for compounds **2** and **3**.

Solvent	Orientation Polarizability (Δ*f*)	2			3		
		λ_{abs} (nm)	λ_{em} (nm)	Stokes shift (cm^{-1})	λ_{abs} (nm)	λ_{em} (nm)	Stokes shift (cm^{-1})
Toluene	0.014	441	480	1842	424	526	4573
1,4-Dioxane	0.021	461	495	1490	421	544	5371
EtOAc	0.201	443	498	2493	419	597	7116
THF	0.211	436	502	3015	420	601	7171
$CHCl_3$	0.149	408	463	2912	438	603	6247
DCM	0.218	408	480	3676	429	634	7537

The Lippert-Mataga theory is described by the following equation:

$$\Delta\nu = \bar{\upsilon}_a - \bar{\upsilon}_f = \Delta f \frac{2(\Delta\mu)^2}{hca^3} + constant \ldots (1)$$

$$\text{and: } \bar{\upsilon}_a = \frac{1}{\lambda_{abs}^{max}}, \bar{\upsilon}_f = \frac{1}{\lambda_{abs}^{max}} \text{ and } \Delta f = \left(\frac{\varepsilon-1}{2\varepsilon+1} - \frac{n^2-1}{2n^2+1}\right) \ldots (2)$$

Where: $\Delta\nu$ is the Stokes shift; Δf is the orientation polarizability of the solvent; $\Delta\mu$ is the difference in dipole moments of the fluorophores in their ground (μ_G) and excited (μ_E) states; *h* is Planck's constant; *c* is the speed of light in a vacuum; *a* is the Onsager radius of the cavity in which the fluorophore resides. Plotting $\Delta\nu$ against Δf gives a Lippert-Mataga plot (Figure **4**).

Rearranging *eq. 1* we can solve for Δμ:

$$\Delta\mu = \sqrt{\frac{Shca^3}{2}} \quad \ldots (3)$$

Where *S* is the slope of the linear function.

Table S3. Fitting parameters of Lippert-Mataga plots determined for compounds **2** and **3**. [a] Lippert-Mataga computed values. [b] TD-DFT computed values.

Compound	Intercept (cm^{-1})	*S* (cm^{-1})	a (Å)	Δμ (D)[a]	Δμ (D)[b]
2	1551	11989	6.32	13.7	3.5
3	4710	7526	7.11	20.7	20.4

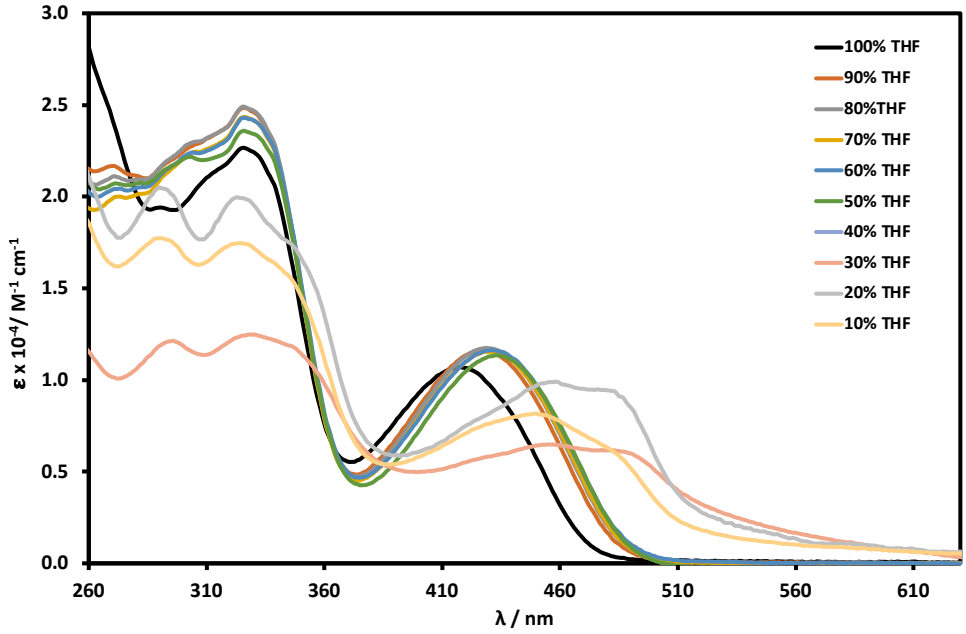

Figure S56. THF/H_2O titration for compound **2**. Spectra show molar absorptivity values of **2** recorded in varying volume ratios of THF and water, from 100% to 10% THF. Each solution had a concentration of 10.8 μM.

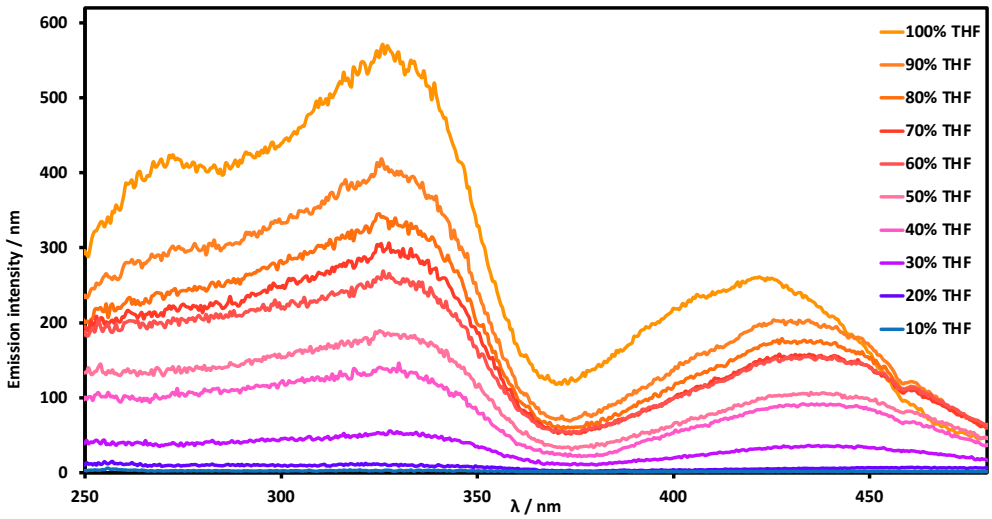

Figure S57. THF/H_2O titration for compound **2**. Spectra show excitation spectra recorded for **2** in varying solvent volume ratios of THF and water, from 100% to 10% THF. Each solution had a concentration of 10.8 μM. Spectra were collected at the emission maximum for each corresponding emission spectrum.

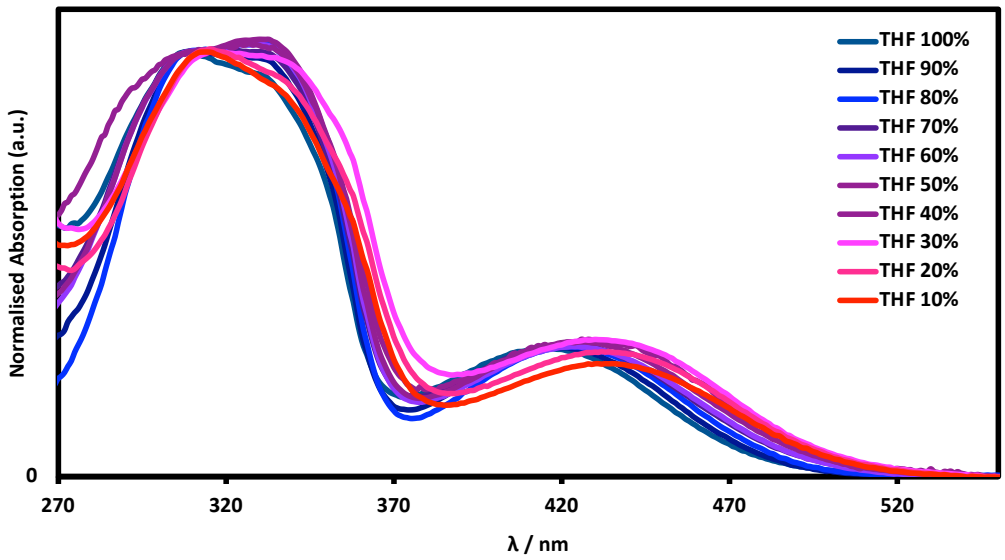

Figure S58. THF/H_2O titration for compound **3**. Spectra show normalised absorbance values of **3** recorded in varying solvent ratios of THF and water, from 100% to 10% THF. Each solution had a concentration of 6.58 μM.

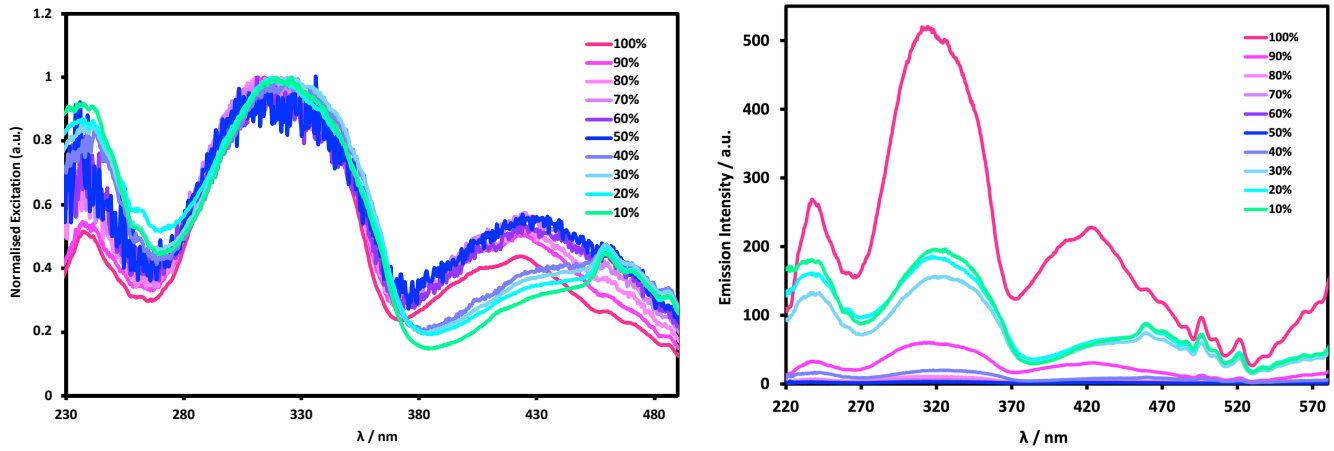

Figure S59. THF/H_2O titration for compound **3**. Spectra show normalised (left) and regular excitation spectra recorded for **3** in varying solvent volume ratios of THF and water, from 100% to 10% THF. Each solution had a concentration of 6.58 μM. Spectra were collected at the emission maximum for each corresponding emission spectrum.

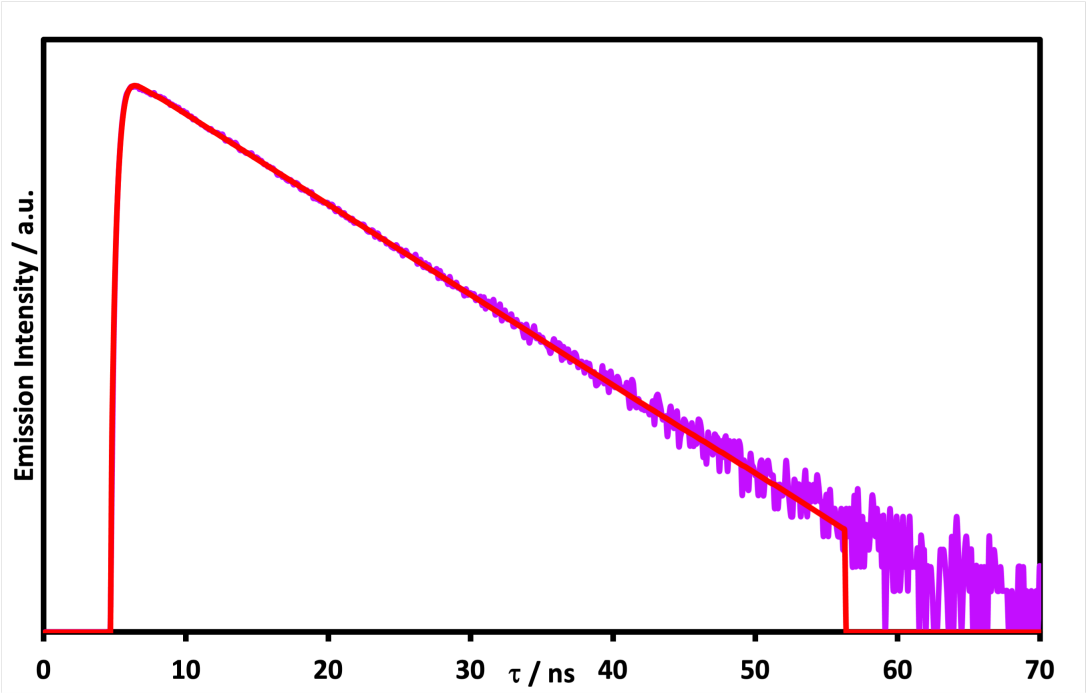

Figure S60. Time-resolved emission decay profile (purple) and fit (red) for **2** (λ_{ex} = 340 nm; emission collected at 500 nm) in 100% THF. Concentration was 15.7 μM. χ^2 = 1.32.

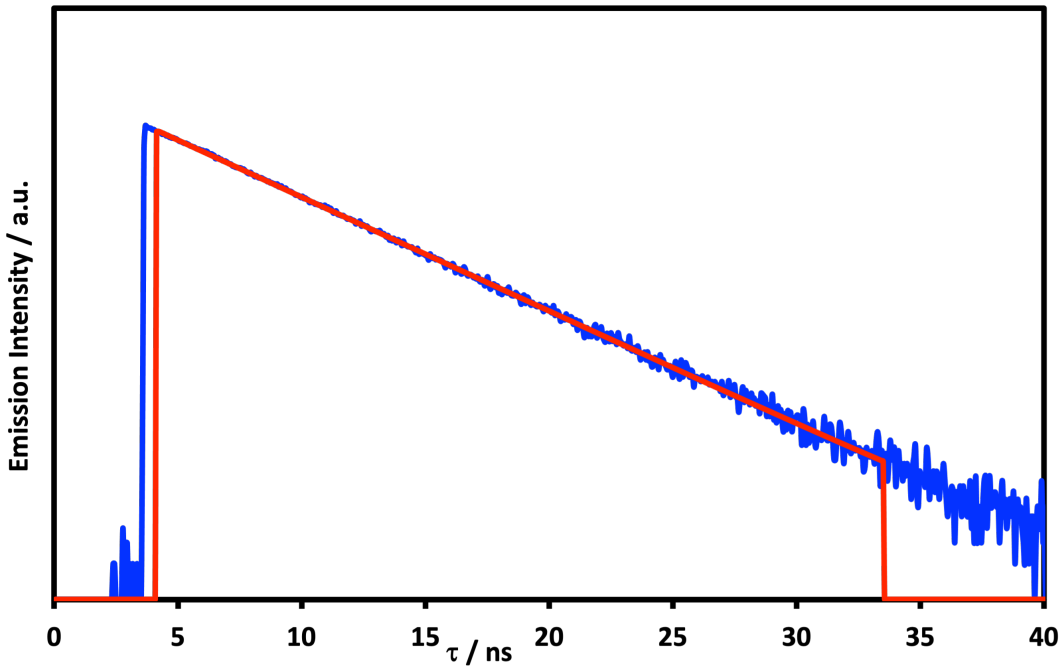

Figure S61. Time-resolved emission decay profile (blue) and fit (red) for **3** (λ_{ex} = 340 nm; emission collected at 601 nm) in 100% THF. Concentration was 6.58 μM. χ^2 = 1.04.

Nanoscale Characterisation

Preparation and characterisation of P188 Particles

All samples were prepared in HPLC or spectroscopic grade solvents (THF and water) with varying concentrations on the order of μM. Dynamic Light Scattering (DLS) measurements were performed at 298 K with a Malvern Instruments Zetasizer Nano ZS provided with a 633 nm He-Ne laser (4 mW) as the light source.

Compound **2** (1.06 mg, 2.00 μmol) or **3** (5.00 mg, 2.00 μmol) were dissolved in THF (20 mL) to give stock concentrations of 0.10 mM. P188 (100 mg, 12.0 μmol) was dissolved in THF (10 mL). An aliquot of stock solution of fluorophore (0.5 mL) was added to the P188 solution and sonicated for 1 min. The solvent was evaporated under reduced pressure, followed by 30 minutes under high vacuum. The mixture was dissolved in deionized water (8 mL), sonicated for 1 min, syringe filtered (0.22 mm MF-millipore membrane filter) into a volumetric flask (10 mL), made up to the mark with deionized water and left for 16 h to equilibrate.

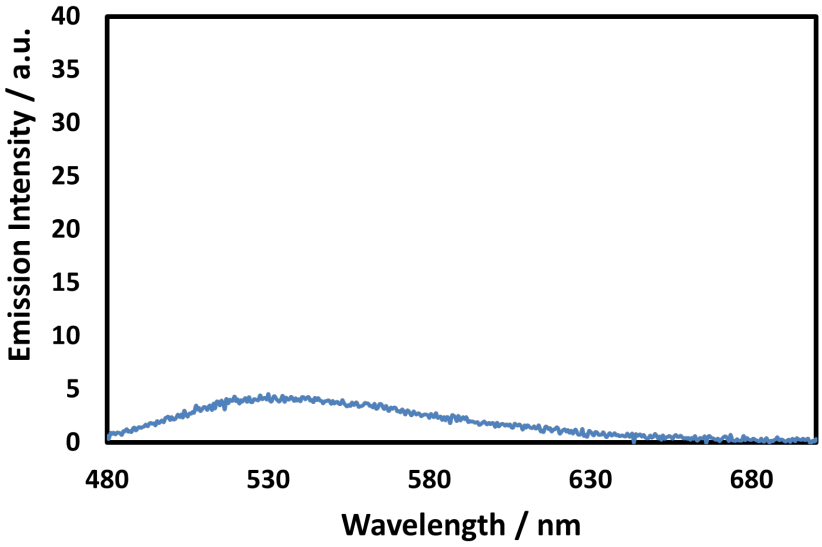

Figure S62. Emission spectrum of P188-**2** nanoparticles after one day.

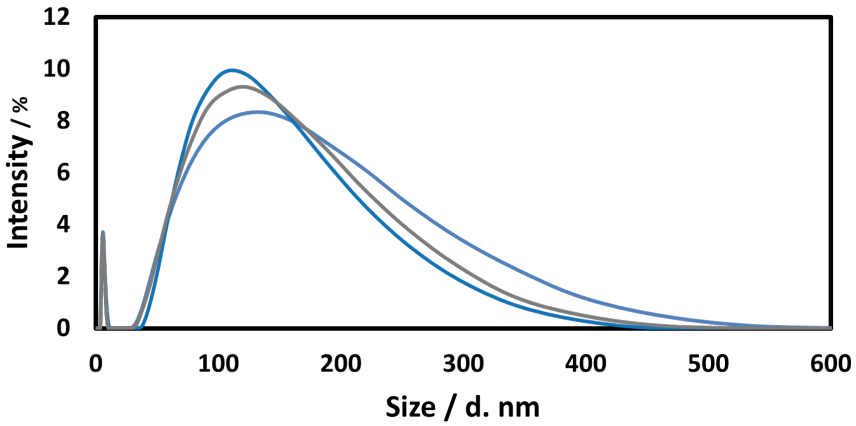

Figure S63. DLS of P188-**2** nanoparticles after one day.

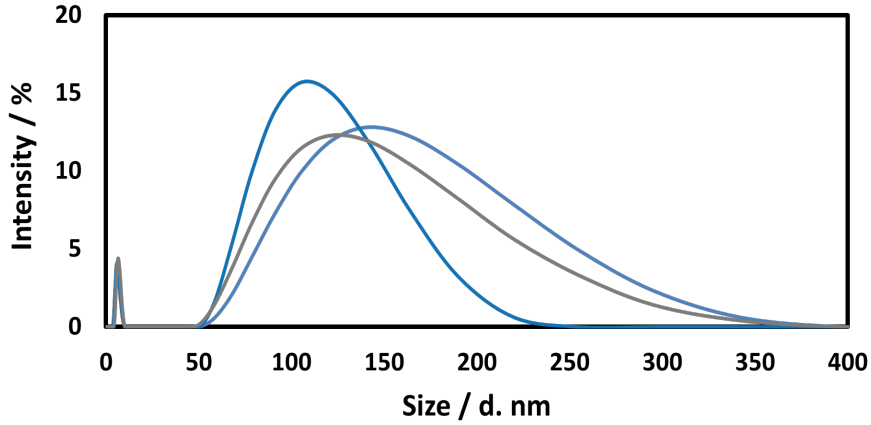

Figure S64. DLS of P188-**2** nanoparticles after seven days.

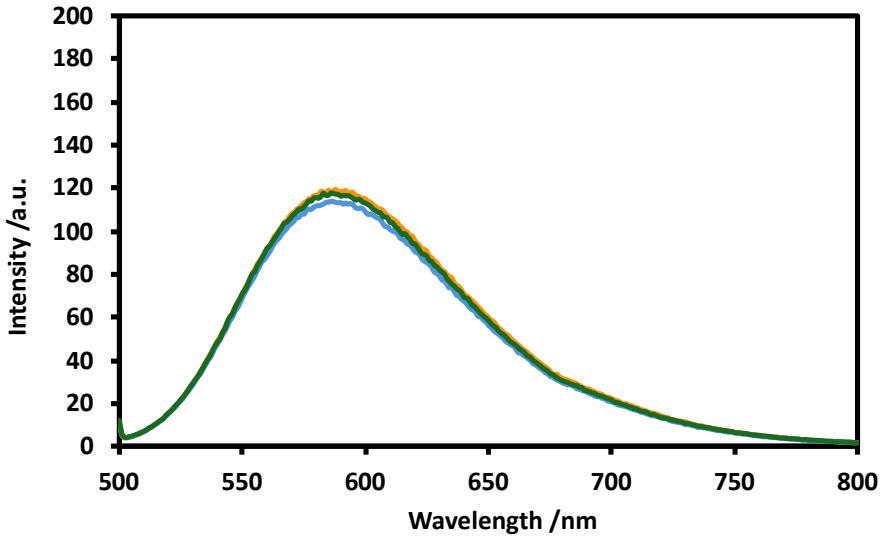

Figure S65. Emission spectra of P188-**3** nanoparticles after: one (orange), seven (blue) and ten (green) days. No changes were observed.

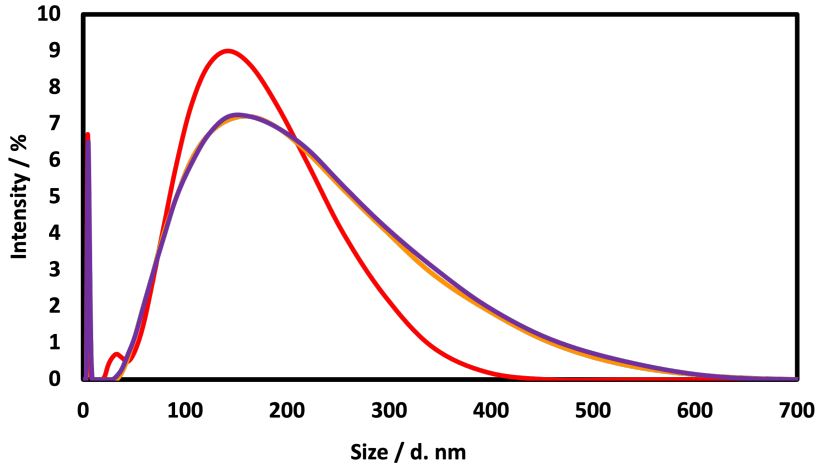

Figure S66. DLS of P188-**3** nanoparticles after one day.

Scanning Electron Microscopy

The aggregation behaviour of compounds **2** and **3** was investigated using Scanning Electron Microscopy (SEM) at the Advanced Microscopy Laboratory (AML) at Trinity College Dublin. Dilute solutions of compounds **2** and **3** (47.1 and 6.58 μM, respectively) were prepared in tetrahydrofuran (THF), with varying volume fractions of antisolvent ranging from 100% THF to 10% THF. 5 μL of each solution was deposited onto clean silicon wafers by drop-casting. The deposited samples were dried under ambient conditions overnight, followed by an additional drying period under high vacuum for a minimum of 24 h. To enhance imaging contrast and reduce static charging effects, the samples were coated with a conductive Pd/Au layer using a Cressington 208Hr high-resolution sputter coater. SEM imaging was performed at low accelerating voltage using a Zeiss ULTRA Plus microscope equipped with an SE2 detector and a 30 μm aperture.

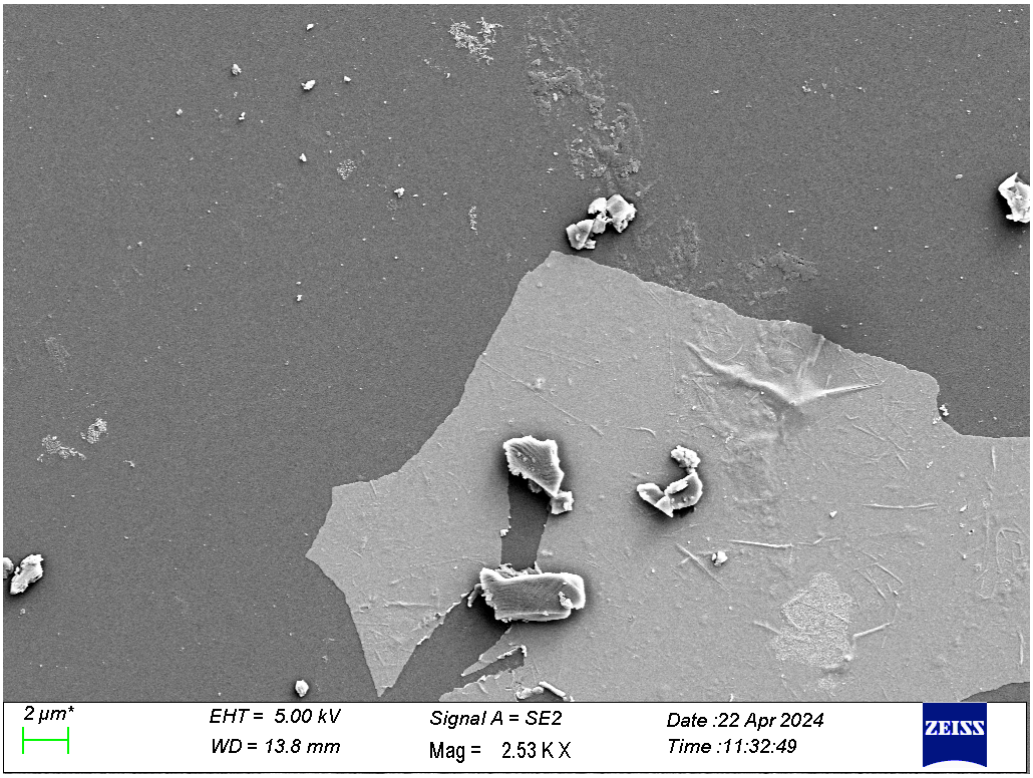

Figure S67: SEM of compound **2** in 100% THF.

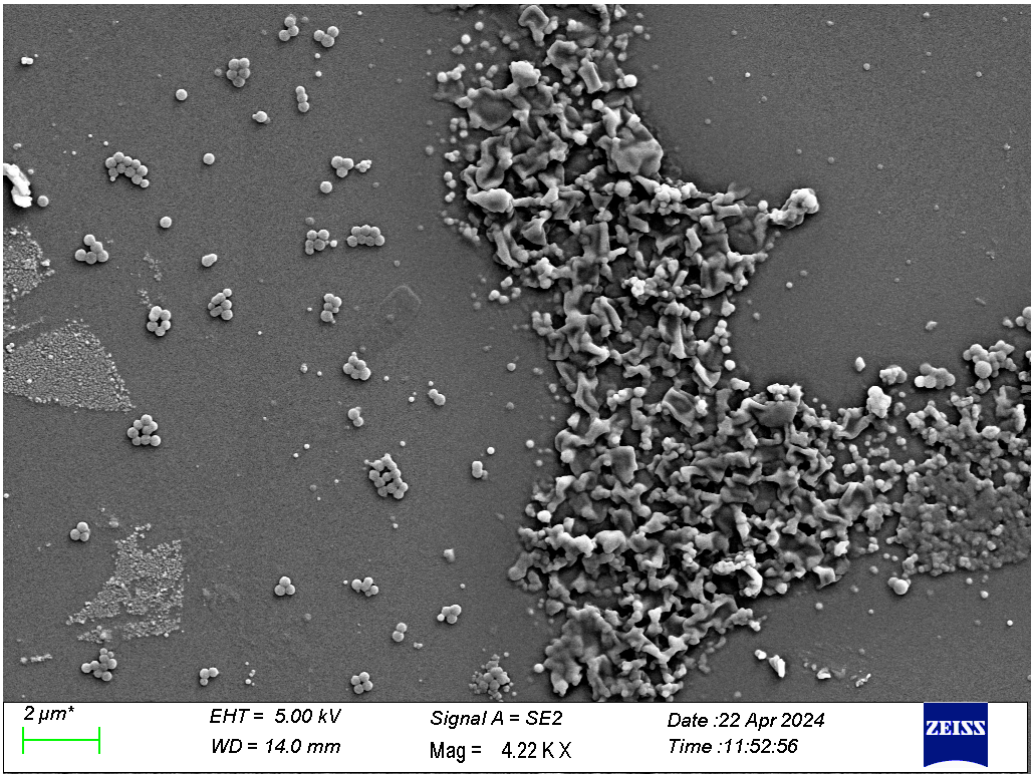

Figure S68: SEM of compound **2** in 90% THF in water.

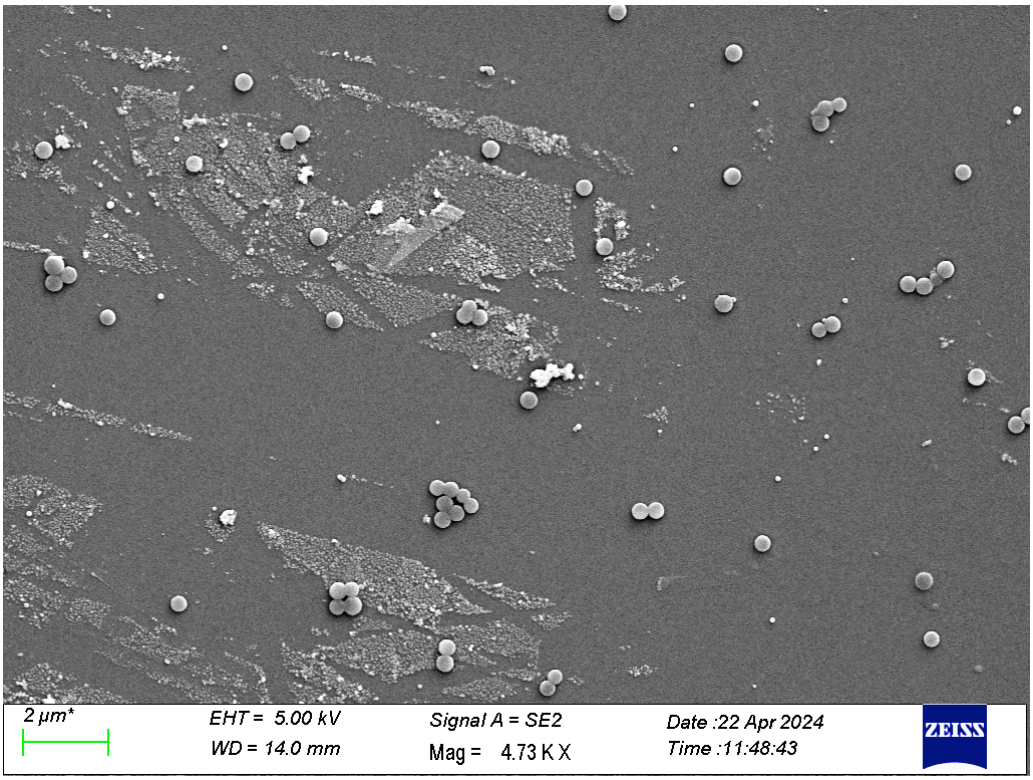

Figure S69: SEM of compound **2** in 90% THF in water.

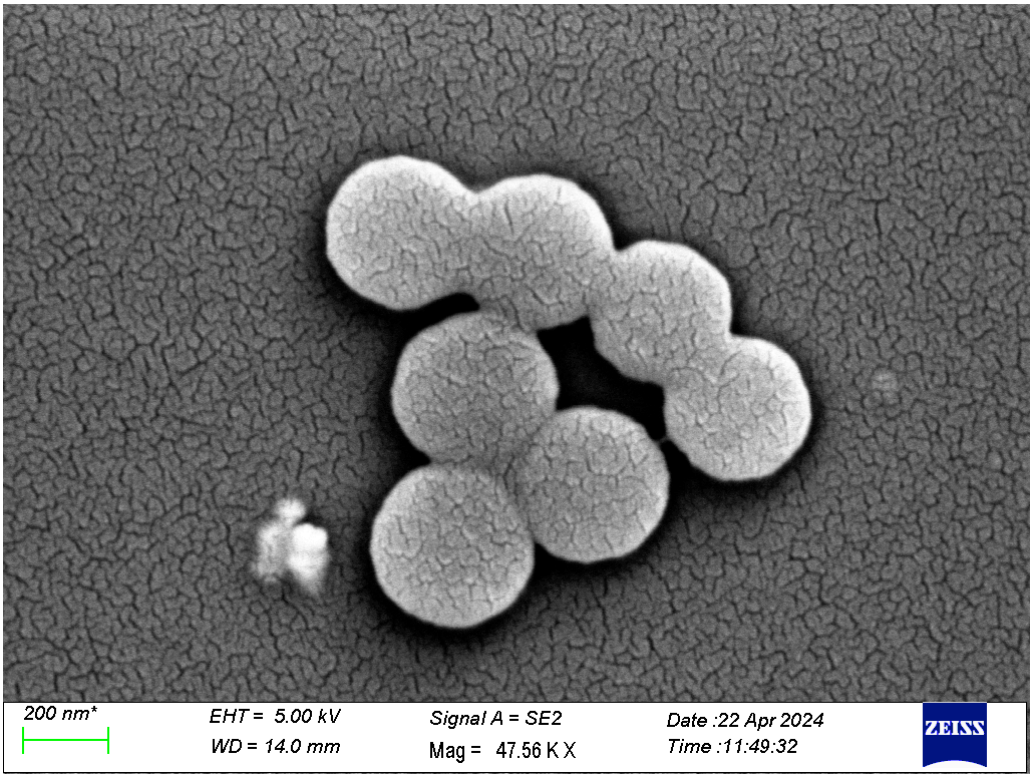

Figure S70: SEM of compound **2** in 90% THF in water.

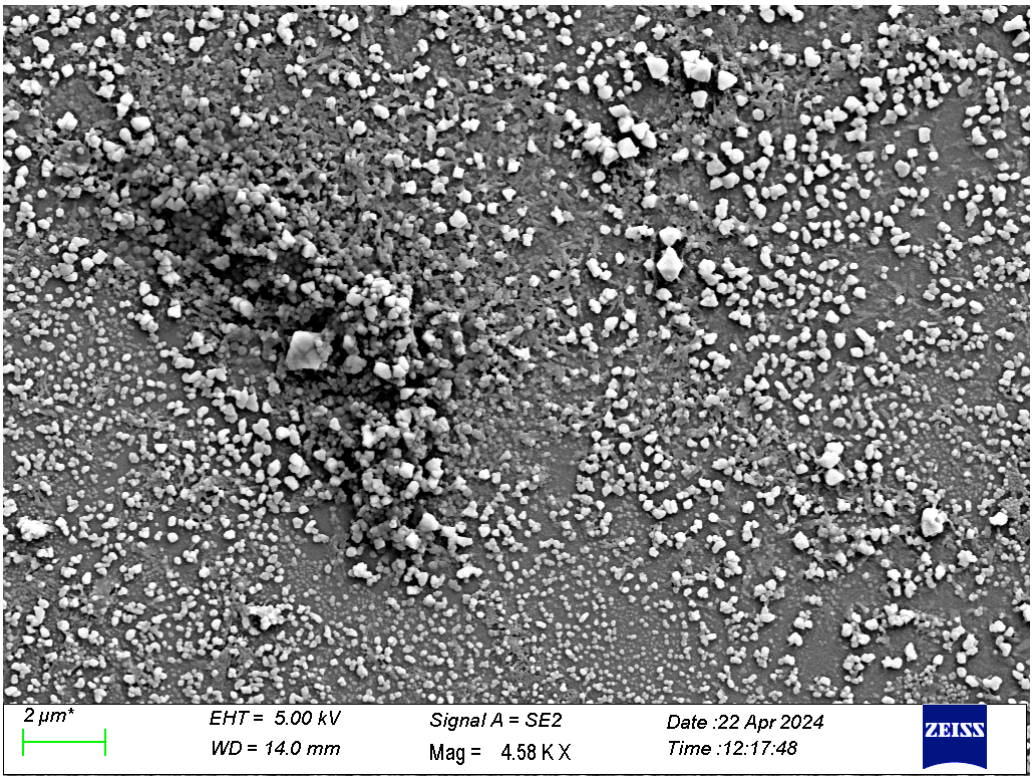

Figure S71: SEM of compound **2** in 50% THF in water.

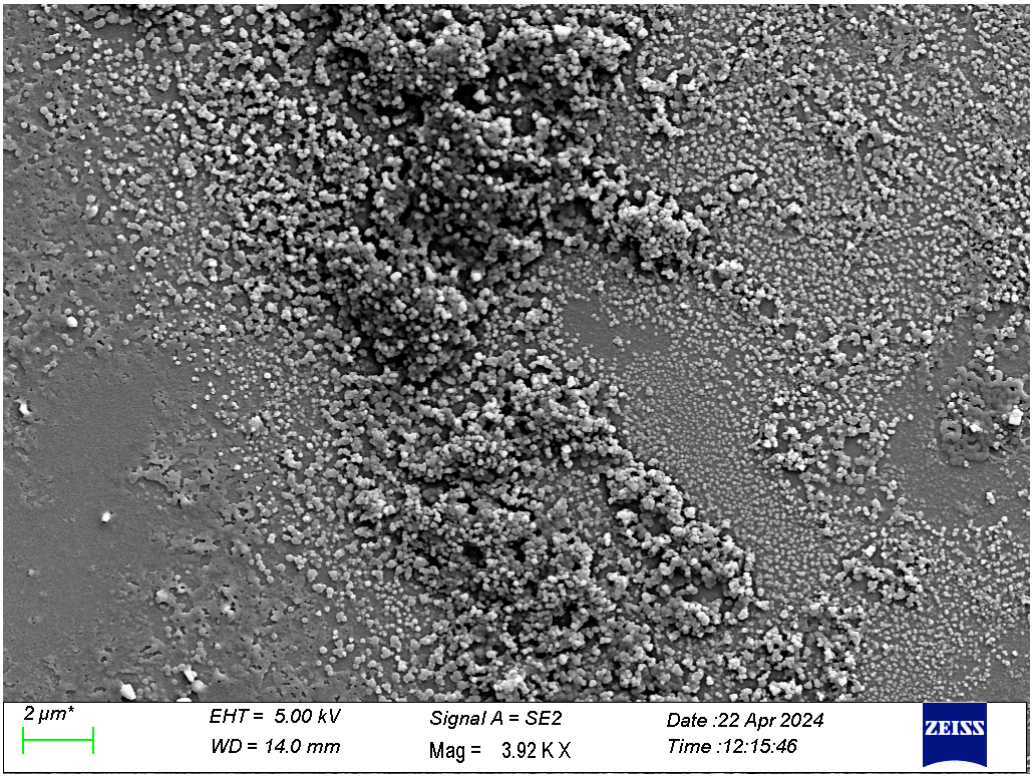

Figure S72: SEM of compound **2** in 50% THF in water.

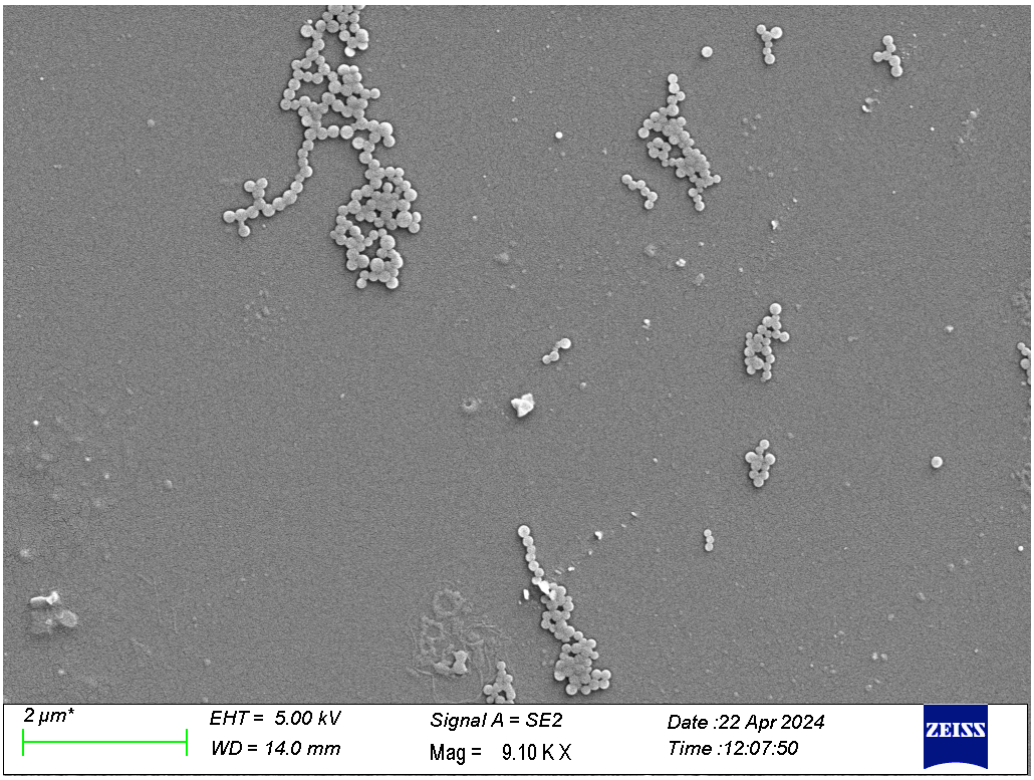

Figure S73: SEM of compound **2** in 50% THF in water.

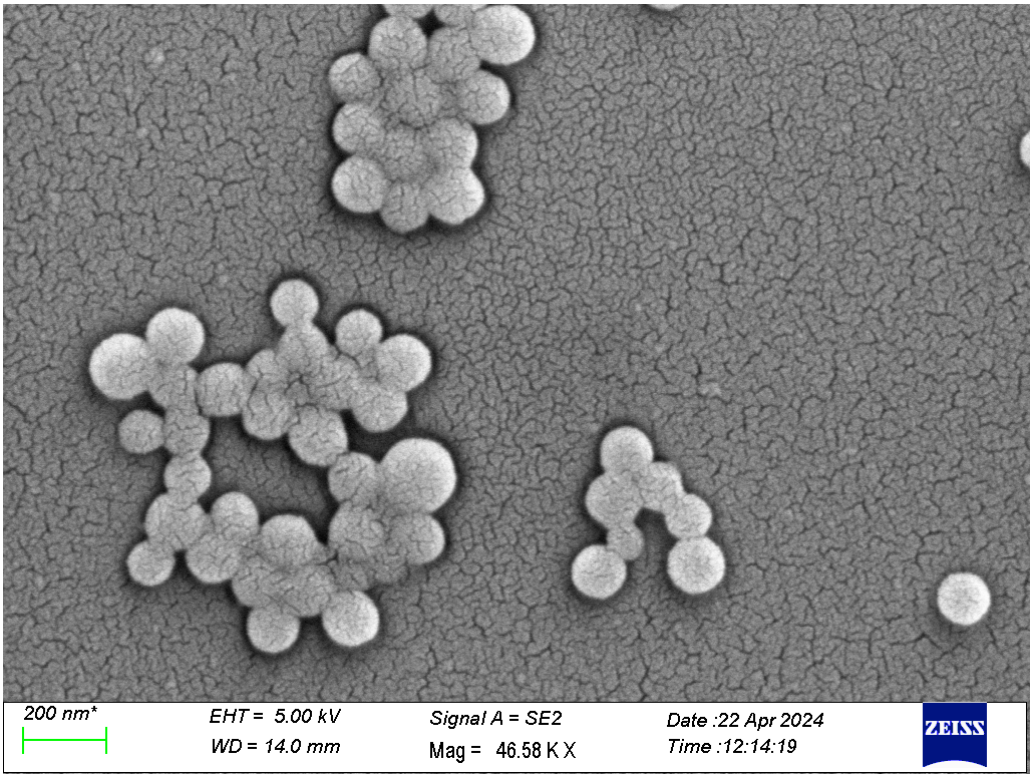

Figure S74: SEM of compound **2** in 50% THF in water.

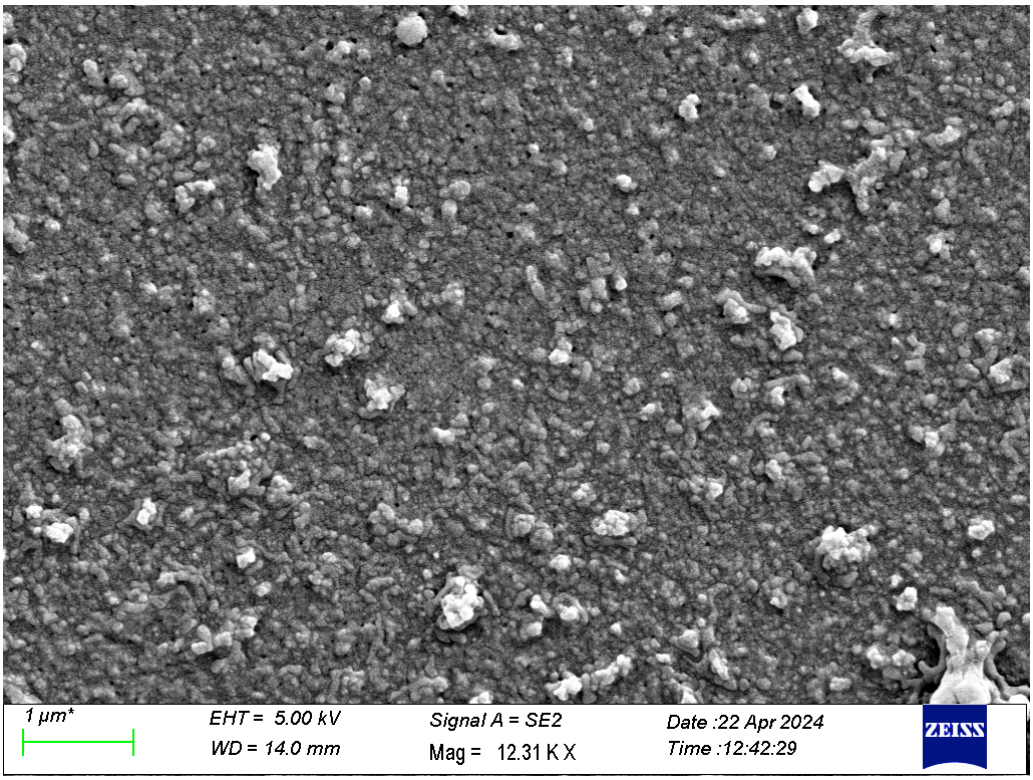

Figure S75: SEM of compound **2** in 10% THF in water.

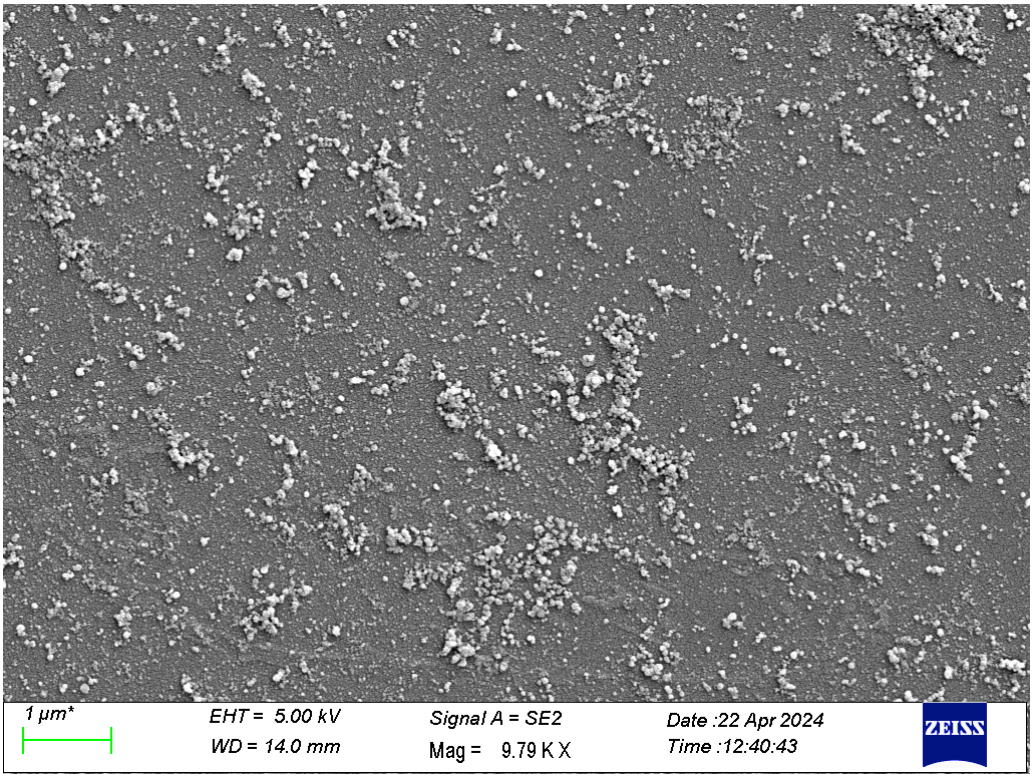

Figure S76: SEM of compound **2** in 10% THF in water.

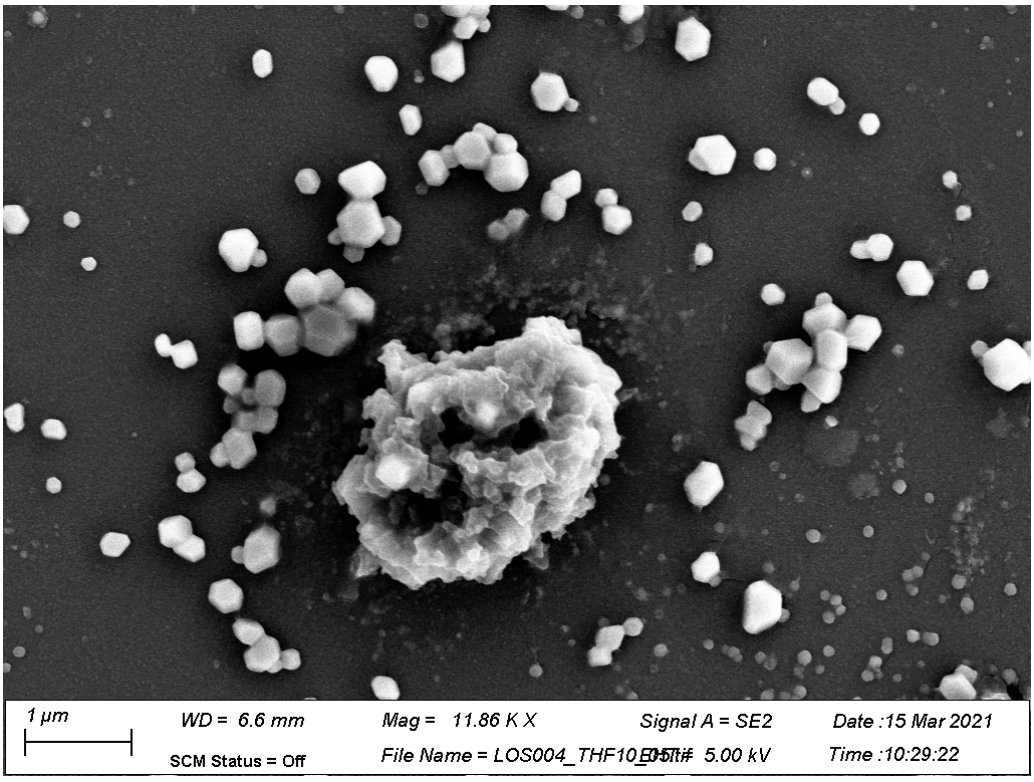

Figure S77: SEM of compound **3** in 10% THF in water.

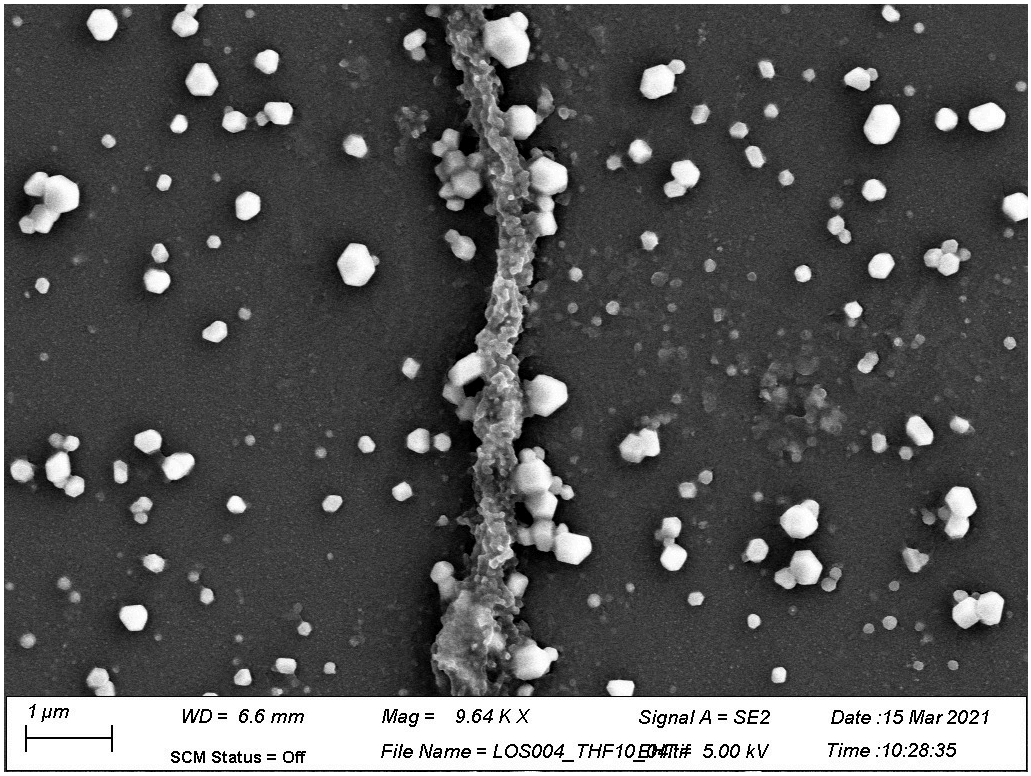

Figure S78: SEM of compound **3** in 10% THF in water.

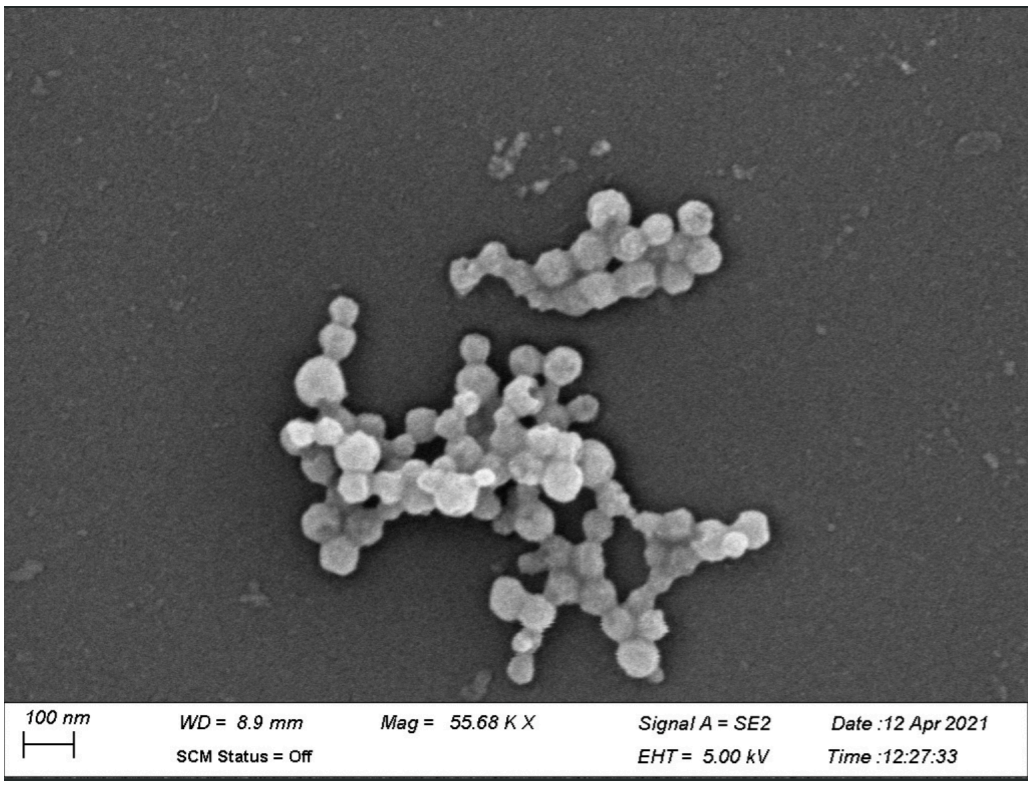

Figure S79: SEM of compound **3** in 10% THF in water.

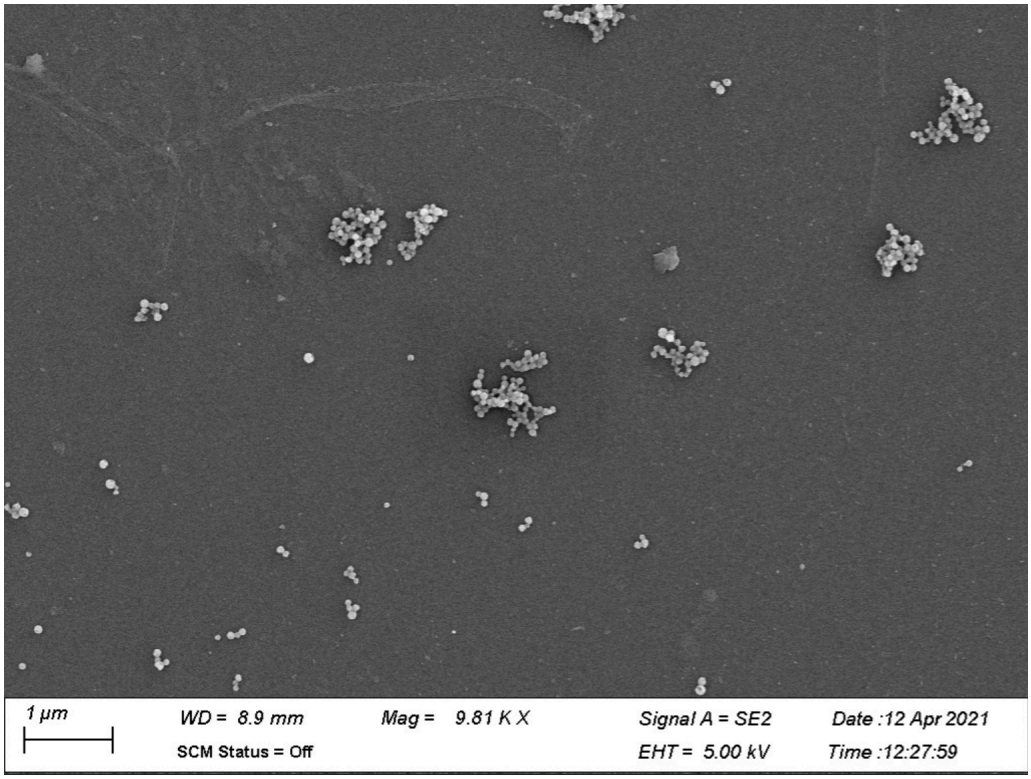

Figure S80: SEM of compound **3** in 10% THF in water.

Theoretical Methods

We have performed the DFT and TD-DFT calculations with Gaussian 16.[17] No simplification was performed. Default Gaussian 16 thresholds and algorithms were used but for an improved optimization threshold (10^{-5} au on average residual forces), a stricter self-consistent field convergence criterion (10^{-10} a.u.) and the systematic use of the *superfine* DFT integration grid, the denser grid available in Gaussian.

Firstly, the S_0 geometries have been optimized with DFT and the vibrational frequencies have been analytically determined, using the CAM-B3LYP range-separated hybrid exchange-correlation functional.[18] These calculations started with the X-Ray structures and were performed with the 6-31G(d) atomic basis set in solution, modelled through PCM[19] using the same solvents as in the experiment. The dispersion effects were accounted for using the D3-BJ model.[20]

Secondly, starting from the optimal ground-state geometries, we have used TD-DFT with the same functional and basis set to optimize the S_1 geometry and compute analytically the vibrational frequencies. All optimized structures correspond to true minima of the potential energy surface. The same level of theory as above was used.

Thirdly, the vertical transition energies were determined with TD-DFT and CAM-B3LYP, but a diffuse-containing basis set, namely 6-31+G(d,p), in gas-phase as well as in solution using the cLR^2 variant of the PCM,[21] in its *non-equilibrium* limit for the TD-DFT part.

Cell Studies

Studies in MDA-MB 231 cells of compounds 2 and 3:

MDA-MB 231 cells were cultured in Dulbecco's Modified Eagle Medium supplemented with 1% penicillin, 1% glutamine and 10% foetal bovine serum. Cells were seeded on eight chamber well slides and left 24 h to proliferate at 5% CO_2 and 37 °C. Cells were then treated with **2** or **3** (diluted 1/10 in cell media to 5 μM) and either imaged live or fixed after 2 h. For cell fixation, the media was removed and the cells were washed with phosphate buffered saline solution (PBS, 2 x 200 μL). To this 4% paraformaldehyde solution (200 μL) was added and the cells left for 20 min, before finally washing with PBS (200 μL). Cells were stored in PBS (200 μL) for imaging. Confocal images acquired using Leica Stellaris 8 (100X/1.49 HC PL APO CS2) with compounds **2** or **3** excited at 405 nm. Control cells checked to ensure no background emission at settings used. Analysis of image files using ImageJ 1.53q

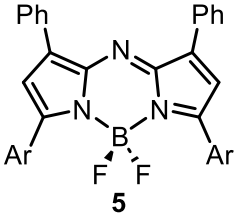

5

Ar = *p*-$MeOC_6H_4$

λ_{max} abs: 694 nm

λ_{max} flu: 716 nm

Figure S82: Structure of BF_2-azadipyrromethene fluorophore **8** used for lipid droplet colocalization experiments.

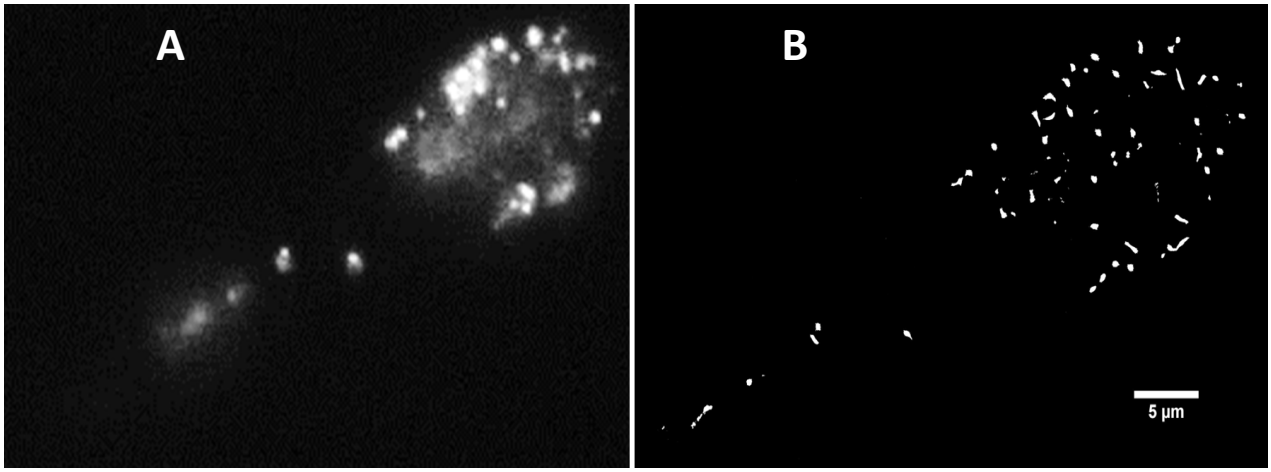

Figure S83: Fluorescence imaging of **3** in MDA-MB 231 cells. (A) Widefield image and (B) corresponding SRFF image following a 2 h incubation. Scale bar 5 μm.

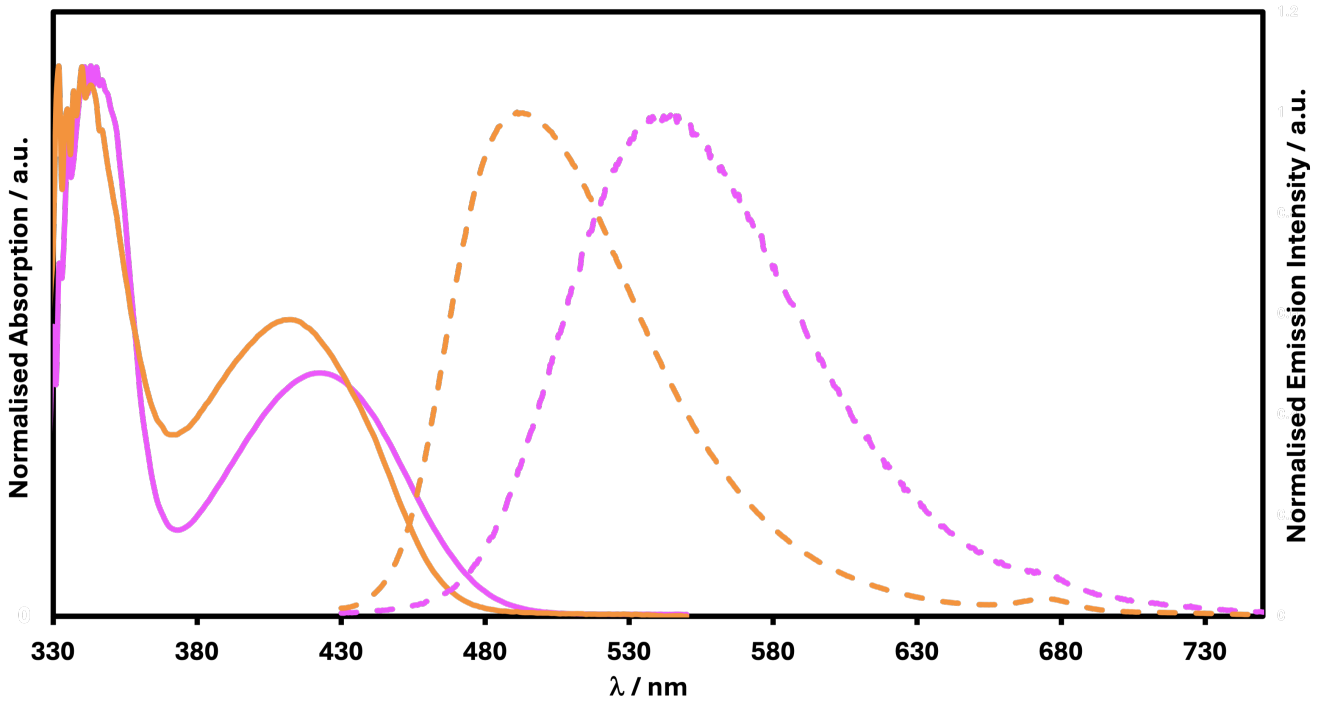

Figure S84: Absorption (solid lines) and emission (dashed lines) spectra of **2** (orange) and **3** (purple) recorded in triolein.

References

1) A. Ionescu, R. Lento, T. F. Mastropietro, I. Aiello, R. Termine, A. Golemme, M. Ghedini, N. Bellec, E. Pini, I. Rimoldi, N. Godbert, *ACS Appl. Mater. Interfaces*, 2015, **7**, 4019.

2) C. Liu, Q. Ni, J. Qiu, *Eur. J. Org. Chem.*, 2011, 3009.

3) C. R. Groom, I. J. Bruno, M. P. Lightfoot, S. C. Ward, *Acta Cryst. B*, 2016, **B72**, 171.

4) Bruker. APEX3. Bruker AXS Inc: Madison, Wisconsin, USA 2016.

5) G. M. Sheldrick, SADABS. University of Göttingen, Germany 1996.

6) G. M. Sheldrick, *Acta Cryst. A,* 2015, **71**, 3.

7) G. M. Sheldrick, *Acta Cryst. C*, 2015, **71**, 3.

8) O. V. Dolomanov, L. J. Bourhis, R. J. Gildea, J. A. K. Howard, H. Puschmann, *J. Appl. Cryst.* 2009, **42**, 339.

9) SAINT. Bruker AXS Inc.: Madison, Wisconsin, USA.

10) D. Kratzert, FinalCif, V131, Freiburg, Germany.

11) U. Anthoni, C. Larsen, P. H. Nielsen and C. Christophersen, *Acta. Chem. Scand.* 1987, **41b**, 216.

12) A. G. Nord and B. Lindberg, *Acta. Chem. Scand.* 1973, **27**, 1175.

13) P. R. Spackman, M. J. Turner, J. J. McKinnon, S. K. Wolff, D. J. Grimwood, D. Jayatilaka and M. A. Spackman, *J. Appl. Cryst.* 2021, **54**, 1006.

14) S. Fery-Forgues, D. Lavabre, *J. Chem. Educ.*, 1999, **76**, 1260.

15) J. N. Demas, G. A. Crosby, *J. Phys. Chem.*, 1971, **75**, 991.

16) W. H. Melhuish, *J. Phys. Chem.*, 1961, **65**, 229.

17) M. J. Frisch, *et al.*, Gaussian 16, revision A.03; Gaussian Inc.: Wallingford, CT, 2016.

18) T. Yanai, D. P. Tew, N. C. Handy, *Chem. Phys. Lett.,* 2004, **393**, 51.

19) J. Tomasi, B. Mennucci, R. Cammi, *Chem. Rev.*, 2005, **105**, 2999.

20) S. Grimme, S. Ehrlich and L. Goerigk, *J. Comp. Chem*. 2011, **32***,* 1456.

21) C. A. Guido, A. Chrayteh, G. Sclamani, B. Mennucci, D. Jacquemin *J. Chem. Theory Comput.,* 2021, 17**,** 5.